The Evolution of Antibiotic Resistance in Bacterial Colonies



Isabel Frost

The Queen's College

University of Oxford

A thesis submitted for the degree of

Doctor of Philosophy

Trinity 2017

Abstract

The continuing rise of antibiotic resistance is threatening a return to the world of pre-antibiotic medicine. Multi-drug resistant pathogens are already claiming lives and causing economic losses in developing and developed countries alike. We need, therefore, to understand what allows resistant strains to spread; what makes them evolutionarily competitive in and amongst other strains and species. The majority of laboratory studies of antibiotic resistance focus on simple growth in liquid culture. By contrast, microbes commonly grow as surface-associated communities, in which interactions between neighbouring cells have strong consequences for competition and evolution.

My first goal was to understand how growth in such environments affects the success of a resistant strain. By competing an antibiotic resistant and susceptible strain of the pathogenic bacterium *Pseudomonas aeruginosa*, I found that growth in dense colonies on agar allowed a resistant strain to protect susceptible strains, to the extent that the susceptible strain may even prevail under antibiotic treatment. This effect was specific to a cooperative mechanism of antibiotic resistance, however; a β-lactamase enzyme that digests the antibiotics surrounding a resistant cell. A further, unexpected reason that susceptible cells could prevail was that they elongate under antibiotic treatment, allowing them to push shorter resistant cells aside in the competition for the growing edge of a colony.

My work suggests that the rise of cooperative resistance mechanisms should be more easily suppressed than for non-social mechanisms. However, one major strategy to overcome antibiotic resistance is the use of antibiotic-adjuvants, drugs which inhibit a mechanism of antibiotic resistance. It is not clear if these adjuvants will tend to suppress or promote cooperative resistance mechanisms. I performed experiments to test the effects of inhibitory adjuvants on cooperative resistance. These revealed that the effects of adjuvants are varied. In liquid culture, an adjuvant inhibited resistance evolution, while, in colony experiments, it promoted resistance evolution by removing the cross protection of susceptible strains.

Given the complexity and importance of antibiotic adjuvants, I developed an eco-evolutionary model to dissect these complexities associated with the combination of interacting microbial and molecular species. As in my experiments, the models identified conditions where an inhibitory adjuvant can increase selection for resistance.

However, the theory also identifies scenarios for which adjuvants will delay resistance evolution by shutting down the associated evolutionary pathway. Broadening the modelling framework to include the stochastic effects of rare mutation, I found that early administration of adjuvant inhibitors can be a powerful way to suppress the emergence of antibiotic resistance.

Microbial interactions are complex and affected by the growth environment. My thesis underlines that the study of antibiotic resistance will benefit from greater consideration of how bacteria interact and, more broadly, how their ecology and evolution determine the rise, or fall, of resistance.

Acknowledgements

I am hugely grateful to my supervisors, Kevin Foster and Craig MacLean, for your patience and support throughout - I have learnt so much from you both! And for taking on a chemist and training her to be a biologist. Thank you to everyone in the Foster lab, and the MacLean lab, past and present. You've encouraged and inspired me and taught me so much. Thank you to Sara Mitri and Alvaro San Millan for being so patient in teaching me microbiology. Thank you to Helen Alexander for opening up the world of modelling.

Thank you so much to my friends and family who have supported me through. I really could not have done it without you, you wonderful people. Thank you first to my family, to Katie, Roger, Sophie, Joe and Molly-dog; you have been incredible. To the Bristol crew; Rachel and Dave, and the Surrey crew; Emily and Bex. To the all the amazing people I've met at the Doctoral Training Centre, especially Anna, Beth, Paul, Ali, Will, and Ronja. You've been with me through every step of this mad journey. Thank you to Alex and Clare for all the dinners and humouring my adventure planning. Thank you to Queen's MCR and all the fantastic people I've had the pleasure to spend the last four years with there.

I am very grateful to the Doctoral Training Centre, funded by the EPSRC, which has been very generous to me. And in particular to my DTC supervisor, Elspeth Garman, who is an inspiration. Further thanks to the DTC for funding my internship at the World Health Organisation and to Liz Tayler, Marc Sprenger and the incredible people of the AMR Secretariat for having me - the experience gave my academic work here a context and meaning. Thank you also to The Queen's College who have been very generous financially and provided me with such an enriching environment to study in.

Contributions

The data Chapters 2, 3 and 4 are collaborative efforts though the majority of the work in each is my own. The contributions of others are summarized here.

- **Chapter 2**: this work has been prepared as a manuscript for submission to a peer reviewed journal. Christopher Thomas kindly provided the plasmids. Kevin R. Foster and R. Craig MacLean conceived the study. Sara Mitri, Alvaro San Millan, R. Craig MacLean, Kevin R. Foster and I designed the experimental framework. I carried out the experiments and microscopy. William P. J. Smith, Yohan Davit, James M. Osborne, Kevin R. Foster and Joe M. Pitt-Francis designed how the system was modelled. William P. J. Smith performed simulations. All authors contributed to the manuscript.
- **Chapter 3**: the majority of this study was my own work, supervised by Kevin R. Foster and R. Craig MacLean. I carried out the experiments, with the exception of the *in vivo* work, which was performed by Rebecca Gabrilska using facilities provided by Kendra Rumbaugh in Texas Tech University Health Sciences Center and who both contributed to the design of the *in vivo* experiments.
- **Chapter 4**: this study was my own work, and was supervised by Kevin R. Foster, Helen Alexander and R. Craig MacLean.

Contents

List of Abbreviations **xiii**

1 Introduction **1**
1.1 Thesis outline 10

2 Cooperation, Competition and Antibiotic Resistance in Bacterial Colonies **15**
2.1 Abstract 16
2.2 Introduction 16
2.3 Results 18
2.3.1 Low antibiotic doses select for resistant strains in liquid cultures 18
2.3.2 Colony growth strongly affects natural selection for resistance 19
2.3.3 Genetic mixing weakens selection for carbenicillin resistance 21
2.3.4 An unexpected benefit to antibiotic susceptibility 24
2.3.5 Cell shape and the increased fitness of susceptible cells . . . 27
2.4 Discussion 30
2.5 Materials and Methods 32
2.6 Acknowledgements 32

3 Antibiotic adjuvants and bacterial competition **33**
3.1 Abstract 33
3.2 Introduction 34
3.3 Methods and Materials 36
3.4 Results 39
3.4.1 The resistant strain outcompetes the susceptible strain during planktonic growth in ticarcillin 39
3.4.2 Addition of an inhibitor during biofilm growth increases selection for resistance 40
3.4.3 Cell elongation shows cross-protection is removed by the adjuvant 41
3.4.4 *In vivo* competition between resistant and susceptible cells . 44
3.5 Discussion 44
3.6 Conclusion 48

4 Antibiotic adjuvants and the evolution of antibiotic resistance 49
4.1 Abstract . . . 49
4.2 Introduction . . . 50
4.3 Methods and Materials . . . 54
4.3.1 The Deterministic Model . . . 54
4.3.2 Non-dimensionalised Equations . . . 57
4.3.3 The Stochastic Model . . . 58
4.4 Results . . . 61
4.4.1 Resistance evolution without inhibitor . . . 61
4.4.2 The inhibitor can suppress antibiotic resistance . . . 61
4.4.3 Modelling partial inhibition . . . 62
4.4.4 Stochastic modelling underlines the power of adjuvants to prevent resistance . . . 66
4.4.5 The later inhibitor is added the more likely double resistance is to emerge . . . 67
4.5 Discussion . . . 70
4.6 Acknowledgements . . . 72

5 Conclusion 73
5.1 Concluding Remarks . . . 78

Appendices

A Appendix to Chapter 2: Cooperation, Competition and Antibiotic Resistance in Bacterial Colonies 81
A.1 Supplementary Materials and Methods . . . 81
A.2 Supplementary Figures . . . 88
A.3 Supplementary Tables . . . 96

B Appendix to Chapter 3: Antibiotic adjuvants and bacterial competition 101

C Appendix to Chapter 4: Antibiotic adjuvants and the evolution of antibiotic resistance. 105
C.1 Parametrization . . . 105
C.1.1 State Variables (Populations) . . . 105
C.1.2 Model Parameters . . . 106
C.1.3 Dimensionless Variables . . . 109
C.1.4 Dimensionless Parameters . . . 110
C.1.5 Default Dimensionless Parameter Settings . . . 112
C.2 Derivation of Dimensionless ODEs . . . 114

C.2.1 Susceptible Growth 114
C.2.2 Resistant Growth 115
C.2.3 Doubly Resistant Growth 116
C.2.4 Antibiotic Dynamics 117
C.2.5 Inhibitor Dynamics 118
C.3 Model Validation 119
C.4 The Stochastic Model shows the same effects of inhibitors for the asocial case. 122

References **123**

List of Abbreviations

AMR . . . . . Antimicrobial Resistance

MSC . . . . . Minimum Selective Concentration

MIC . . . . . Minimum Inhibitory Concentration

HGT . . . . . Horizontal Gene Transfer

YFP . . . . . Yellow Fluorescent Protein

DsRed . . . . . *Discosoma* Red (fluorescent protein)

PBS . . . . . Phosphate Buffered Saline

LB . . . . . Luria-Bertani

IR . . . . . Inhibitor Resistant

GSSA . . . . . Gillespie Stochastic Simulation Algorithm

"It is not difficult to make microbes resistant to penicillin in the laboratory by exposing them to concentrations not sufficient to kill them, and the same thing has occasionally happened in the body."

— Alexander Fleming *Nobel Laureate Lecture*, 1945

1 Introduction

Modern medicine is dependent on antibiotics to perform lifesaving surgery, provide cancer chemotherapy, and for many of the treatments that have defined the past century's revolution in medical care. Not long after the introduction of antibiotics doctors began to notice deadly penicillin-resistant strains of *Staphylococcus aureus* appearing in London hospitals [1]. The 1950s and 70s were a golden age for the discovery of new antimicrobial compounds but as new drugs were introduced resistance rapidly emerged and the pipeline of new antibiotics has all but dried up [2]. In the last 30 years only one new class of antibacterials has been discovered [3]. In Europe alone, infections caused by resistant bacteria kill 25,000 people and cost €1.5 billion annually [4]. This state of affairs has attracted extensive media attention, being described as 'as big a threat as terrorism,' [5] with warnings of an 'apocalyptic' scenario in which 'things as common as a strep throat or a child's scratched knee could once again kill' [2].

The emergence of antibiotic resistant bacteria, as a result of the selection pressure applied by the widespread use of antibiotics, is an evolutionary process which can be understood by applying the principles of microbial competition from ecological and evolutionary theory. There is an extensive body of work looking at antibiotic resistance in this way, in terms of the classical population genetics of well-mixed

populations [6]. Selection for resistance operates at multiple levels [7]; from rates of mutation at a genetic level, through competition between strains at a population level, to the level of transmission between hosts or via the host environment. The key parameters often considered by population geneticists are the rate of *de novo* mutation of novel resistance genes, the rate at which resistance genes are horizontally acquired and the fitness effects of resistance and compensation both during and after antibiotic exposure [8]. However, the importance of these will also depend on the ecological context and the biochemical mechanism of resistance [9]. Bacteria live in an interactive world, where sociality and interactions with other strains have an effect on their ability to outcompete their neighbours for space, resources and survival. Different resistance mechanisms are likely to have different fitness consequences for their bearers and neighbouring strains, leading to disparities in their selection and evolution. Applying the body of existing evolutionary and ecological theory to the problem of antibiotic resistance will shed light on the optimal way of using the drugs we currently have available, to limit the rapid rise in resistance.

Bacterial growth in biofilms has consequences for their evolution

Much of our current understanding of the evolution of resistance to antibiotics has come from experiments on bacteria grown in well-mixed planktonic culture. However, most natural environments do not behave as a chemostat. Bacteria rarely live as isolated entities, they aggregate and form surface-attached communities in colonies and biofilms [10, 11]. These structured bacterial populations are held together by an excreted polymer matrix, containing DNA, polysaccharides and proteins [12]. Furthermore, bacterial tolerance to antibiotics can increase 100 to 1000-fold [13] during this form of growth. The reasons for this are not entirely understood however the slow penetration of the antibiotic into the biofilm, a decrease in growth rate and the presence of persister cells have all been implicated [14].

In this mode of growth, social interactions become important, as neighbouring microbes are forced to interact, and anything secreted by one, is likely to affect the fitness of its neighbours. Social evolution theory has been widely applied to the

interactions of microbes and may offer new insights into the spread of resistance [15]. Both modelling and experimental work have shown spatial structuring, created by growth as a biofilm, is likely to be critical in the evolution of cooperative traits [16, 17].

Public goods and cooperation

Micro-organisms are capable of cooperating with one another to perform a variety of processes including dispersal, nutrient acquisition, biofilm formation and quorum sensing [15]. In this context, and within the study of social evolution more generally, 'cooperation' is defined as a behaviour which is beneficial to another, recipient, cell and is maintained because of this benefit [18]. In the context of microbial evolution cooperative traits may be mediated by the production of 'public goods,' externally secreted products which are costly to produce and provide a benefit to the group, for example iron-scavenging siderophores [15]. Cooperative traits tend to be costly to the cooperating cells and come at the risk that cheating, non-cooperating cells may benefit from the cooperative traits of the collective without paying the associated costs [19]. This effect has been described as the 'tragedy of the commons,' in which, cooperation would be the most efficient use of resources but is unstable in light of the fact that each individual can gain a greater benefit by acting selfishly [15]. One way in which cooperators can combat this instability is to create spatial structure within groups, as if cooperating cells are side by side (for example due to clonal expansion) they are able to benefit from their cooperative trait and exclude cheaters (see Figure 1.1).

Social evolution theory and antibiotic resistance

Mechanisms of antibiotic resistance often involve the production of extracellular enzymes, which detoxify the environment and carry a cost to the producer [20] but may also be beneficial to surrounding individuals. This can therefore be considered a 'public good' and a cooperative trait [15]. One example of this is the production of β-lactamase enzymes, which detoxify the environment allowing the

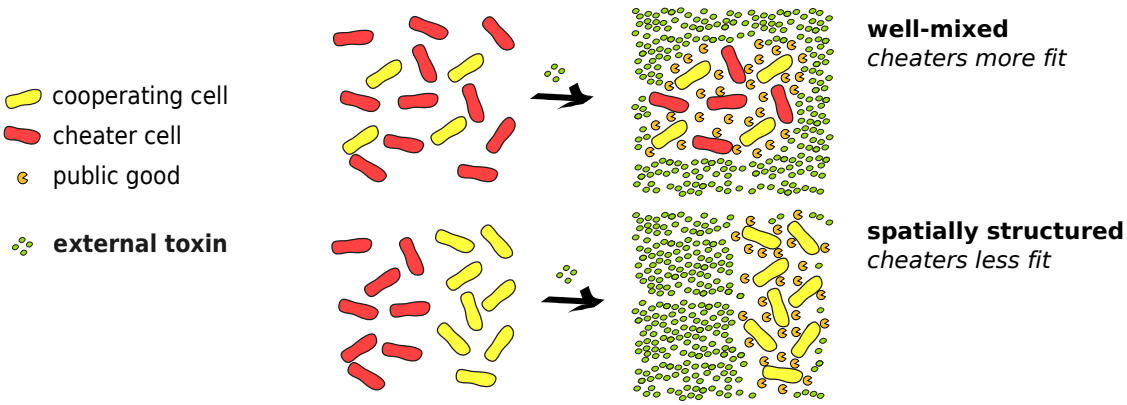


Figure 1.1: Cooperators are selected for when spatial structure prevents cheating non-producing cells from benefiting from the costly production of private goods.

potential for social interactions. Susceptible strains may survive in the presence of resistant strains as cheaters, which do not pay the cost of producing detoxifying β-lactamase enzymes but are cross protected by the breakdown of the β-lactam antibiotic by resistant cells [15] (Figure 1.2). By treating β-lactamase secretion as a social trait, social evolution theory can be used to gain valuable insights into selection for antibiotic resistance [21, 22]. To be called a cooperative trait implies that β-lactamase enzymes have been, at least partially, selected due to their effect outside of the cell. This is difficult to determine for any secreted product and it could be argued that some extracellular leakage is an inevitable by-product. Particularly as the β-lactam antibiotic attacks the cell wall, forcing cells to degrade it externally and expose themselves to potential cheats. However, the experiments presented in this thesis show that these extracellular interactions can have profound consequences for the evolution of both resistant and susceptible strains and in this way social evolutionary classifications of these behaviours are able to provide useful insights into resistance selection.

Mathematical tools, from the field of game theory, have been applied to understand the consequences of the production of antibiotic degradation enzymes for microbial dynamics [23–25]. This type of evolutionary game theoretical analysis is able to unpick the effect of different interactions in different contexts, such as coexistence, cycling and exclusion. However, whether these interactions are so clear

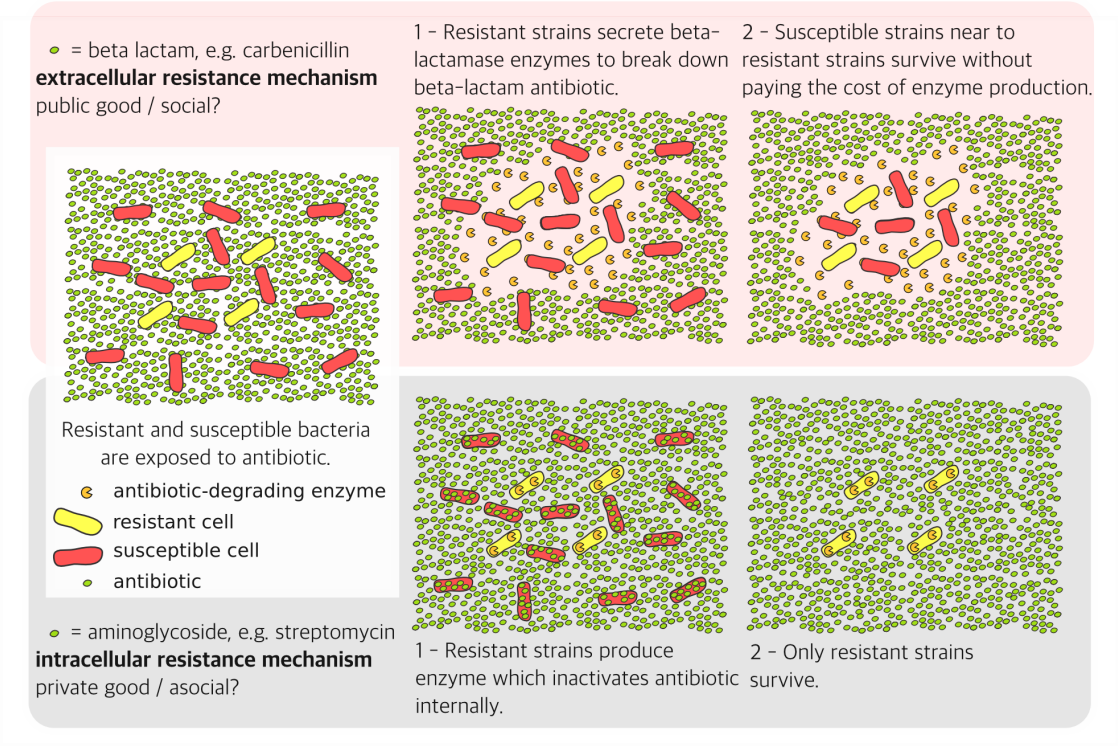


Figure 1.2: Extracellular mechanisms of resistance to antibiotics can have an effect on the fitness of nearby susceptible strains.

cut in reality is still to be discovered. It has been established that such interactions are evident from surveys of antibiotic degradation enzyme producing-resistant and susceptible strains, which had been isolated from natural soil samples [25]. These studies imply that these interactions are not only clinically relevant but more widely applicable to selection for cooperative resistance mechanisms, in microbial communities, in the broader environment.

Resistance to β-lactam antibiotics

β-lactam antibiotics are the most commonly prescribed antibiotics, both in the UK [26] and across Europe [27], due to their low toxicity, cheapness, and availability [28]. Defence against β-lactam antibiotics is often in the form of the production of degradation enzymes [29], called β-lactamases, which hydrolyse the amide bond in the β-lactam ring, making β-lactam antibiotics inactive.

The bacterial cell wall is composed of murein, a peptidoglycan layer that is maintained by transglycosylases, which elongate the strands of peptidoglycan, and

transpeptidases, which crosslink these strands to provide stability against osmotic pressure. β-lactam antibiotics act as a substrate analogue for transpeptidases by binding irreversibly and inactivating the enzyme. This results in changes to cell shape, activation of the stress response and ultimately cell lysis [30] (Figure 1.3). The growth of small satellite colonies around resistant central colonies of bacteria that have been grown on β-lactam containing plates has been widely observed anecdotally, in the lab. Most β-lactam resistant bacteria produce β-lactamase enzymes that cleave the β-lactam ring and render the antibiotic ineffective. For this reason β-lactam antibiotics are now often co-administered with β-lactamase inhibitors, such as the amoxicillin-clavulanate, piperacillin–tazobactam and ampicillin–sulbactam combinations [31, 32]. β-lactamase inhibitors covalently bind to the active site of the β-lactamase enzyme and irreversibly inhibit its ability to degrade β-lactam antibiotics [33].

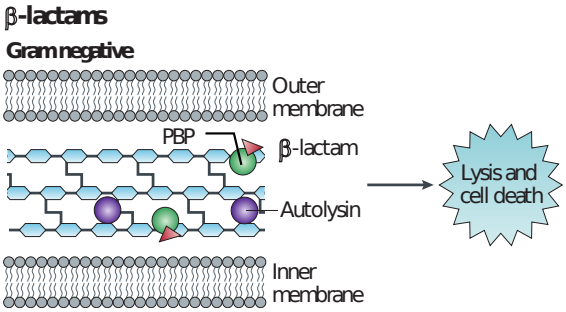


Figure 1.3: Mechanism of action of β-lactam antibiotics. β-lactams bind to penicillin-binding proteins (PBPs) on maturing peptidoglycan strands and hence inhibit transpeptidation. Peptidoglycan synthesis decreases and the increase in autolysins leads to lysis and cell death. Adapted from [30].

β-lactamase enzymes are retained in the periplasm, with some extracellular leakage [34]. There is evidence that β-lactam enzymes are secreted in membrane vesicles [35–37] and high levels of β-lactamase activity have been found in the sputum of Cystic Fibrosis patients undergoing anti-pseudomonal treatment [35]. Furthermore, previous studies on this topic show it is possible for susceptible strains to benefit from the breakdown of β-lactam antibiotics, by resistant strains, and thereby, under certain conditions, outcompete them. I explore these in further detail in the next section.

Resistance to other classes of antibiotic appears to have less activity outside of the cell. This includes resistance to aminoglycosides, which I compare to β-lactamase resistance, in Chapter 2. Aminoglycosides bind to the 16S rRNA component of the 30S ribosomal subunit. This does not immediately prevent translation but causes the ribosome to incorporate the wrong amino acids into the newly synthesized protein. This mistranslation causes proteins to misfold, and their incorporation into the cell envelope compromises its structural integrity, allowing further antibiotic to enter [30] (Figure 1.4). Aminoglycosides are often inactivated intracellularly by an enzyme which attaches a new chemical group.

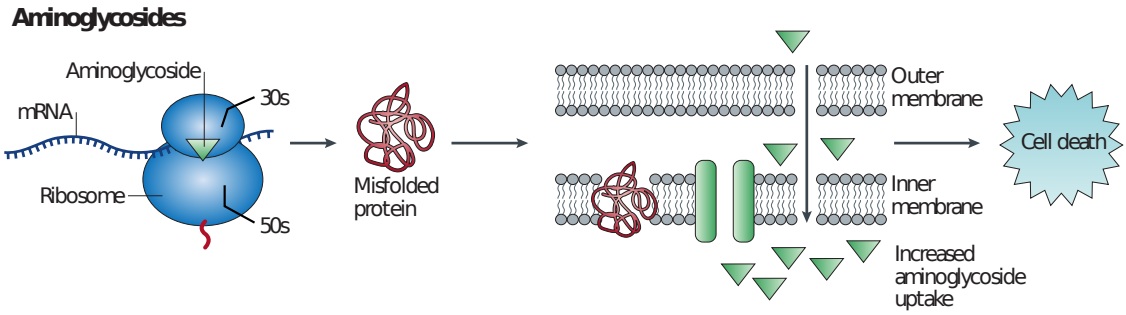


Figure 1.4: Mechanism of action of aminoglycoside antibiotics. When aminoglycosides bind to the 30S subunit of the ribosome they cause misincorporation of amino acids into elongating peptides. These proteins are mistranslated and can misfold. The incorporation of misfolded membrane proteins into the cell envelope leads to increased drug uptake. Combined with the increase in ribosome binding, this process is associated with the death of the affected cell. Adapted from [30].

β-lactamase mediated cross protection

The extracellular effect of β-lactam degradation is likely to have an effect on the fitness of neighbouring cells. This creates the opportunity for social effects through the cross protection of nearby susceptible strains. As early as the 1950s *in vitro* work in rabbits had shown the effect of penicillin on susceptible bacteria was inhibited in the presence of β-lactamase producers [38]. By the 1960s penicillin-susceptible pathogens in clinical infections were found to survive in patients co-infected with β-lactamase producing commensal bacteria. Such isolates were able to withstand concentrations of penicillin 200 times the inhibitory concentration for the susceptible bacteria grown alone [39]. Since then, this association, between the failure of both

penicillins [40] and cephalosporins [31], to eradicate infections, where β-lactamse producers were also present has been reported, both clinically and in animal studies, for a range of bacteria. These include *Bacteriodes, Staphyloccus, Streptococcus* and *Haemophylus* species. This suggests susceptible strains may be protected by resistant strains. However, it is also possible that the failure of treatment in these examples is driven by rapid evolution, either due to horizontal gene transfer (HGT), *de novo* mutation, or the presence of persister cells in a dormant state. Controlled studies of isogenic strains are needed to disentangle these possibilities.

The first such study showed that β-lactamases made by one cell could protect another, albeit using an artificially engineered strain, where β-lactamase export was forced. Specifically, Dugatkin *et al.* [41] found that susceptible *Escherichia coli* were able to survive at relative frequencies of 5-12% in the presence of resistant mutants, genetically engineered to export an inducible β-lactamase enzyme to attach to the outer cellular membrane, at concentrations of ampicillin which were otherwise inhibitory. In a similar experimental setup, to observe these effects, the β-lactamase was allowed to accumulate on one side of a dialysis membrane [42]. In an individual agent based model, partially informed by experiment, Dugatkin *et al.* [43] found as the cost of resistance relative to the benefit increases, susceptible strains are able to survive on the edge of resistant groups. In a more recent study, Bottery *et al.* [44] compared social β-lactamase resistance with selection for selfish, efflux pump-mediated resistance to a tetracycline antibiotic. They found that tetracycline resistance in *E. coli* was selected for at lower effective concentrations of antibiotic than β-lactam resistance due to interactions between resistant and susceptible species. Yurtsev *et al.* [45] found the equilibrium fraction of β-lactamase producing resistant cells, in the presence of susceptible cells, reached 0.25 at 50 times the susceptible minimum inhibitory concentration (MIC).

Another source of evidence that β-lactamases can protect non-producer cells comes from the study of mixed species communities. Perlin *et al.* [46] found resistant *E. coli* protected susceptible *Salmonella enterica* at concentrations of ampicillin that were otherwise lethal. In polymicrobial biofilms, resistant *Moraxella catarrhalis*

have been shown to act as indirect pathogens, which limit the bactericidal activity of β-lactams against susceptible *Streptococus pneumoniae* [47]. Experiments with 3D printing [48], have shown β-lactam susceptible species can benefit from local detoxification of ampicillin, by resistant species, when they are spatially nearby. This gives support to the idea that spatial structure may have a key role in our understanding of these processes.

There is ample evidence that β-lactamases may have social effects, therefore, but this either comes from artificially engineered strains or ecological communities of multiple species. To understand the potential *evolutionary* effects, there is a need for studies on naturally occurring resistance within a species. However, a recent study that looked into the effects of a naturally occurring plasmid, that confers β-lactam resistance, was unable to find evidence of cross protection in co-culture. It could only be seen by growing a protective strain first, to detoxify the environment, before a susceptible strain was then added [49]. This raises the question of the extent and importance of β-lactamase driven cross protection for the evolution of antibiotic resistance. I hypothesised that the reason for the lack of cross protection was that strains were not grown together, in dense communities, like a biofilm, where social interactions are strongest. I therefore set about studying how growth in such conditions affects competition between antibiotic resistant and susceptible strains.

Horizontal Gene Transfer and Antimicrobial Resistance

Horizontal Gene Transfer (HGT) is the transmission of genetic material between a non-parent donor cell and recipient cell [50]. The spread of resistance genes via HGT is an important component of the rapid emergence of resistance to antibacterial therapies [51]. Resistance genes arise, are mobilised onto mobile genetic elements, such as plasmids, phages or the acquisition of naked DNA. Such genes are able to accumulate on multi-drug resistant plasmids and then can be co-selected for by a variety of antibiotics or environmental factors, such as mercury resistance. Such plasmids are initially likely to carry a fitness burden to the recipient cell,

however, over time such costs are often ameliorated [8], making them more difficult to remove via drug cycling or limiting antibiotic use [52].

Pseudomonas aeruginosa as a model organism

P. aeruginosa is a gram-negative opportunistic pathogen, which is often nosocomially acquired. The ability of *P. aeruginosa* to form biofilms is associated with its survival in diverse clinical environments, including medical implants (such as catheters, hip replacements and pace makers), hospital surfaces, and in the airways of chronic lung disease patients [53]. *P. aeruginosa* is the predominant pulmonary pathogen in Cystic Fibrosis, which is the most common inherited lethal disease in Western Europe [54]. In addition, for these patients, 80-95% of deaths are brought on by chronic bacterial infection, causing respiratory failure [55]. *P. aeruginosa* is intrinsically resistant to many antibiotics as it contains a chromosomal β-lactamase (AmpC, which provides protection to a limited range of β-lactam antibiotics) and multi-drug resistant efflux pumps, which it is able to upregulate, in addition to mutating outer membrane porins, to affect drug permeability [56]. These characteristics made it an ideal model organism with which to study the links between social interactions, under biofilm-like growth, and the competitiveness of antibiotic resistant strains.

Specifically, I decided to focus on strains that carry an antibiotic resistant plasmid. Resistance to β-lactam antibiotics is most commonly acquired by HGT of plasmids [57]. The role of plasmids is important clinically because, once selected for, a single plasmid can carry resistance to multiple different antibiotics. The carriage of a plasmid, encoding resistance genes, will often impose a fitness cost on its host [8]. The relevance of plasmid-encoded resistance lead me, in Chapters 2 and 3, to explore selection for resistance, encoded by a non-conjugative, clinical, multi-drug resistance plasmid experimentally. Later, in Chapter 4, I model resistance acquisition by HGT.

1.1 Thesis outline

In this thesis, I ask:

- What is the effect of dense bacterial growth on the evolution of antibiotic resistance?
- How can social evolution theory contribute to our understanding of resistance evolution?
- How does the use of antibiotic adjuvants, compounds which are used to increase the efficacy of antibiotics, affect selection for antibiotic resistance?

In this first chapter, I have outlined the context of this study and the limits of our current knowledge of the social effects of β-lactam antibiotic degrading enzymes.

In the second chapter, I study how growth in colony biofilms impacts resistance evolution in the pathogen *Pseudomonas aeruginosa*. The resistant strain carries a clinical plasmid conferring resistance to streptomycin, which is inactivated intracellularly, and carbenicillin, which is broken down extracellularly and so has more potential for "social" effects, where one cell influences the fitness of another. Resistant and susceptible strains are competed in varying concentrations of one, or the other, antibiotic. Susceptible strains are able to outcompete resistant strains in the presence of antibiotic, but only for carbenicillin, which has extracellular effects. I also show that this effect depends on the different genotypes being mixed. When different strains make single genotype patches within colonies (high genetic relatedness), the resistant strains are always selected. In addition, cell length is found to have an unexpected effect. When exposed to sub-inhibitory concentrations of the β-lactam antibiotic, susceptible cells elongate. Through my own experimental work, alongside collaborating with a modeller, I find this apparent stressed-cell phenotype can enhance the fitness of the susceptible strain. This effect leads to the surprising outcome that resistant strains fare even worse at low doses of antibiotic than none at all. This chapter shows that antibiotic resistance can be a social trait

and that this can lead to the counter-intuitive result that there are conditions where antibiotics will favour susceptible, rather than resistant, genotypes.

The third chapter considers the effect of inhibiting social β-lactamase break down of the β-lactam antibiotic, ticarcillin, using the clinical inhibitor, clavulanic acid. During growth in liquid culture, the addition of the inhibitor, alongside the antibiotic, removes selection for the resistant strain, making it susceptible to the antibiotic. However, during growth as a dense community of cells, addition of an inhibitor has a markedly different effect. I find that the inhibitor prevents the cross-protection of the susceptible strain by the resistant strain. This causes β-lactam resistance to be selected for at a lower effective concentration of antibiotic with the inhibitor than without it. *In vivo* data shows similarities with the results in colonies. This chapter demonstrates the use of an inhibitor can have a variety of effects on selection for resistance, depending on the growth environment. This reveals that the relationship between adjuvant use and the success or failure of resistant strains, to outcompete their neighbours, can be complex. This motivated me to approach the topic using ecolological and evolutionary theory to unpick these effects.

In the fourth chapter I develop a new theory to understand how antibiotic adjuvants affect the evolution of antibiotic resistance, both when resistance is mediated by social and by non-social mechanisms. I begin with a deterministic model, which shows that inhibitors can have a variety of effects on selection for resistance. At intermediate doses of antibiotic, the inhibition of a social resistance mechanism causes resistance to the antibiotic to emerge earlier than antibiotic treatment alone. However, at high doses of antibiotic, the use of an inhibitor, alongside an adjuvant, can suppress the emergence of resistance, in both social and asocial systems. This is because treating a susceptible infection with a combination of inhibitor and antibiotic early, removes selection for the antibiotic resistant strain, and thereby, stalls the emergence of the antibiotic-inhibitor resistant strain. This treatment regime also maintains a susceptible population for a greater duration of the treatment time than prescribing the antibiotic alone. I then validate these findings with a stochastic model, which captures the random nature of rare mutation

events. This model not only recapitulates the results of the deterministic model, but the effect of using an inhibitor prophylactically is strengthened when strains are modelled discretely. Next, I use the stochastic model to consider the effect of delaying dosing with the inhibitor. I find that the later an inhibitor is given during antibiotic therapy, the more often resistance to the combined antibiotic-inhibitor therapy occurs. This is because the antibiotic alone selects for the singly resistant mutant, creating an evolutionary pathway to the doubly resistant strain.

Finally, in the fifth chapter, I summarize the conclusions that can be drawn from the previous chapters and suggest potential areas for future study.

'It is very easy to answer many of these fundamental biological questions; you just look at the thing!'

— Richard Feynman (1918-1988)

2

Cooperation, Competition and Antibiotic Resistance in Bacterial Colonies

Isabel Frost[1], William P. J. Smith[2], Sara Mitri[3], Alvaro San Millan[4], Yohan Davit[5], James M. Osborne[6], Joe M. Pitt-Francis[2], R. Craig MacLean[1], and Kevin R. Foster[1]

1. Department of Zoology, University of Oxford, OX1 3PS, UK.

2. Department of Computer Science, University of Oxford, OX1 3QD, UK.

3. Département de Microbiologie Fondamentale (DMF), Université de Lausanne, CH-1015 Lausanne, Switzerland.

4. Department of Microbiology, Hospital Universitario Ramón y Cajal (IRYCIS). Madrid, Spain.

5. Institut de Mécanique des Fluides de Toulouse (IMFT), Université de Toulouse, CNRS-INPT-UPS, Toulouse France.

6. School of Mathematics and Statistics, University of Melbourne, Victoria 3010, Australia.

2.1 Abstract

Bacteria commonly live in dense and genetically-diverse communities associated with surfaces. In these communities, competition for resources and space is intense, and yet we understand little of how this affects the spread of antibiotic resistant strains. Here we study competition in colonies between a susceptible and a multi-drug resistant strain of the opportunistic pathogen *Pseudomonas aeruginosa*. Colony growth increases inter-strain competition relative to planktonic growth, and this halves the dose needed to select for streptomycin resistance that functions intracellularly. In stark contrast, colony competition increases the selective dose for carbenicillin ten-fold. This is partly explained by cooperative β-lactamase production that protects neighbouring sensitive cells from carbenicillin, by degrading it locally. In addition, we discover a second unexpected effect: the inducible elongation of cells in response to carbenicillin allows sensitive cells to better compete for the rapidly growing colony edge. These combined effects mean one can inhibit bacterial growth while selecting against an antibiotic resistant strain. We argue that the detailed study of bacterial interactions is fundamental to understanding and overcoming antibiotic resistance.

2.2 Introduction

Antibiotic resistance is a major concern that is threatening our ability to treat the most common of bacterial infections [58]. As well as attempting to find new drugs, we need to better understand the processes that promote, or inhibit, the spread of antibiotic resistant strains [13]. There is a large literature on the evolution of antibiotic resistance that has primarily focused on understanding how bacteria respond to antibiotics in liquid culture [9, 59–61]. While tractable, these conditions lie in stark contrast to the way that bacteria often grow. Both in the environment and in infections, bacteria commonly grow in dense communities, which can be genetically-diverse, where competition for space and resources is intense [62–64]. This is particularly important in the context of infection where bacteria can be

100 to 1000 times as resistant to antibiotics during biofilm growth as opposed to planktonic growth [12]. This is due to multiple factors, including presence of persisters, the build up of secreted extracellular products and limited permeability of antibiotics through the biofilm.

Growth of bacteria in these communities, often known as "biofilms" when on a surface [65], is well known to increase the phenotypic ability of bacteria to resist antibiotics [66]. However, these observations are based on single strains and, to understand the rise of resistance, we need to understand how antibiotic-resistant strains compete with different strains under these conditions. Growth in dense and diverse communities generally means that each cell can much more strongly influence the growth and survival of other cells [11, 67]. This effect is known to promote the evolution of competitive phenotypes, including toxin secretion [68], smothering polymers [69] and adhesion [70]. However, growth in dense communities can also lead to spatiogenetic structure and the evolution of cooperative phenotypes, such as enzymes that digest complex molecules outside the cell [62, 71].

The details of how cells are arranged and how they affect each other, therefore, are critical to whether a particular strain will spread within a dense community. We here define a community of cells as a group of multiple interacting microbes in a closely-knit group. How might these effects affect the spread of resistant strains? If the mechanism of resistance only benefits the cell that carries it, this is predicted to lead to purely competitive resistant strains that do not protect their neighbours. In this case, intense competition in colonies is likely to lead to an increase in the strength of selection for resistant strains. By contrast, if the resistance of one cell protects another, antibiotic resistance can become a cooperative trait. In this case, resistant cells may protect sensitive neighbours from antibiotics, reducing the strength of selection for resistance in colonies. Recent work shows that it can be difficult to predict whether a particular mechanism of resistance will have competitive or cooperative effects [72]. However, cooperation appears particularly likely for resistance to β-lactams [41, 45], the most commonly used class of antibiotics, which often arises via the secretion of β-lactamase enzymes that break

down antibiotics, both in the periplasm and extracellularly; β-lactamase enzymes have been found in membrane vesicles, secreted from *P. aeruginosa* cells [35, 73].

It is clear that there can be divergent and complex effects of resistance mechanisms on the ability of bacteria to compete with other strains. Moreover, we lack a systematic understanding of how these effects drive the rise or fall of a particular strain. Here we develop a simple experimental system to understand how competition and cooperation influence the spread of antibiotic resistant strains. Specifically, we compare competitions between a resistant and a susceptible strain of the pathogen *P. aeruginosa* in liquid culture to a colony assay where cells grow at high density. The resistant strain carries a clinical, non-conjugative, multi-drug resistance plasmid (Rms149 [74]). This plasmid, importantly, confers resistance to both the aminoglycoside, streptomycin, which is adenylated in the cytoplasm, and the β-lactam, carbenicillin, which is hydrolysed periplasmically. As we will show, this allows us to directly compare a purely competitive resistance mechanism with one that functions cooperatively. This reveals that how cells compete, whether they cooperate, and how they are arranged are all fundamental to the rise, or fall, of resistant strains.

2.3 Results

2.3.1 Low antibiotic doses select for resistant strains in liquid cultures

We want to understand what allows antibiotic resistant strains to compete effectively in dense and genetically-diverse communities. In order to isolate the effects of antibiotic resistance, we employ competitions between isogenic strains that only differ in whether they carry a clinical antibiotic-resistant plasmid. Plasmid carriage incurs a fitness cost under certain conditions, which we will go on to investigate in more depth.

We first present a typical planktonic assay that competed plasmid-bearing and plasmid-free strains against each other in well-mixed broth (Figures 2.1 and A.1). Plasmid carriage reduced fitness by 3% (s.e. = 0.38%) in the absence of

antibiotics, demonstrating a cost to resistance ($t_{21} = 9.7$, $P < 0.001$). As expected, supplementing culture medium with either an aminoglycoside (streptomycin) or β-lactam (carbenicillin) caused the fitness of the antibiotic sensitive strain to rapidly decrease, because antibiotics suppress the growth rate of the sensitive strain, but not the resistant strain (Figure 2.1).

2.3.2 Colony growth strongly affects natural selection for resistance

We next asked how life in a dense and genetically-diverse community impacts the fate of an antibiotic resistant strain. To do this, we repeated our competition experiments on agar plates (Figures 2.2, A.2 and A.3); known as the "colony biofilm" model [65]. Our first observation was that, without antibiotics, the cost of plasmid carriage is significantly increased to 5.1% ($t_{17.8} = 2.7$, $P = 0.0157$). This increase is consistent with the finding that growth under biofilm conditions increases competition between strains. Specifically, cell division in mature colonies and biofilms only occurs at the very edge [75], and this generates strong natural selection to reach the edge [17, 69, 76–78]. This effect is expected to amplify the fitness benefit of rapid cell division because fast-growing strains have the added benefit of preferentially accessing the growing edge. While expected from a large body of previous work, we were surprised to find that this effect appears to have never been formalised. We, therefore, used an individual-based model of colony growth in order to reconcile our empirical findings with this intuitive effect (Figure A.2 in Appendix A).

How does this increased competition affect the fate of the resistant strain? As for the no-antibiotic case, the basic expectation is that colony growth will amplify any fitness differences between strains. Specifically, the prediction is that selection for antibiotic resistance will be stronger in colonies than in broth cultures. We examined this by assessing the minimal concentration of antibiotic required to generate selection for resistance (Minimum Selective Concentration, MSC), in colonies and broth cultures [79]. We also calculated MSC values relative to the dose required to completely suppress the growth of the sensitive strain (Minimum

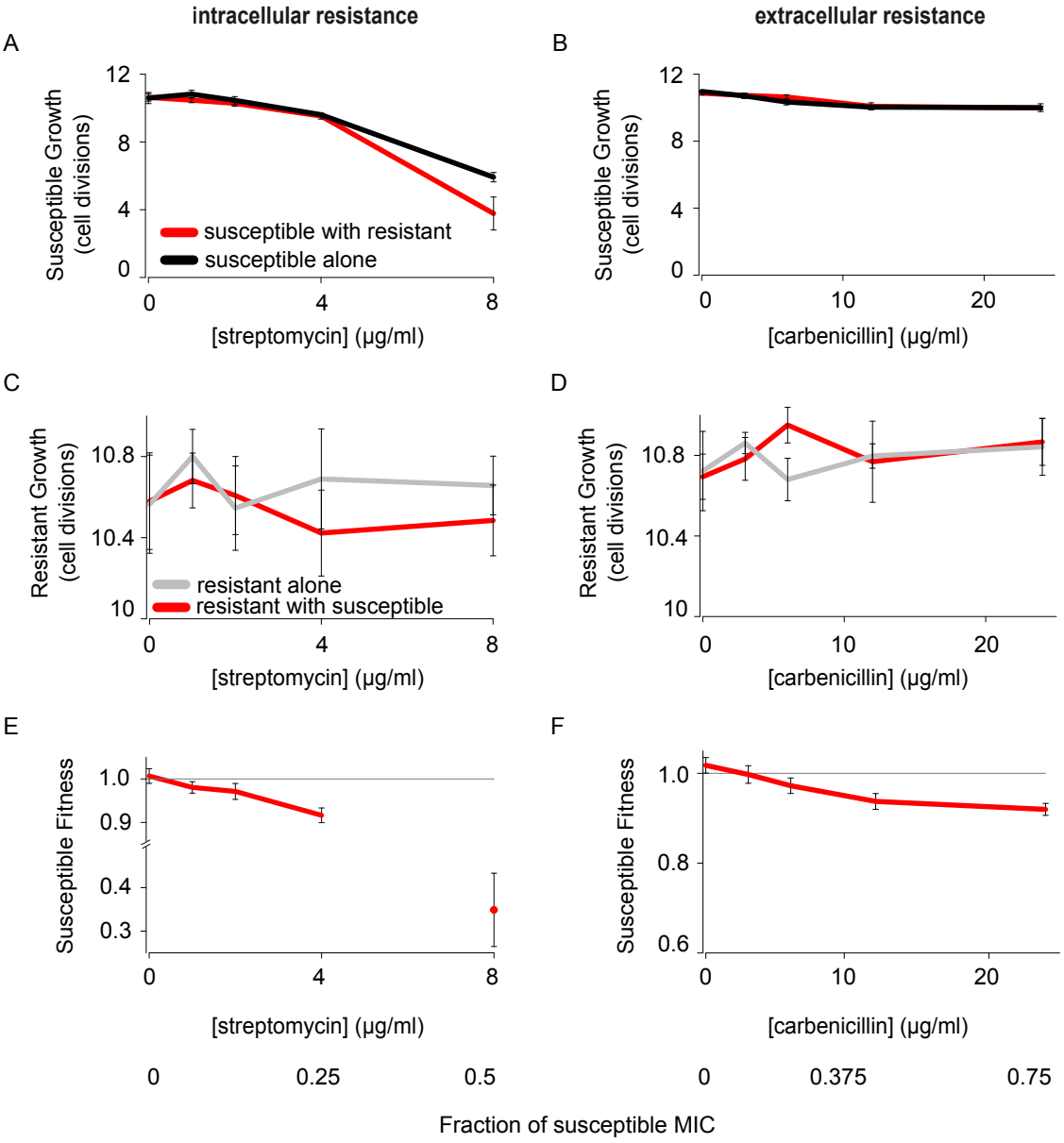


Figure 2.1: Natural selection for antibiotic resistance in liquid culture. Susceptible and resistant strains were competed in liquid culture supplemented with carbenicillin (extracellular resistance) or streptomycin (intracellular resistance). Both streptomycin (A) and carbenicillin (B) suppress the growth rate of the susceptible strain. In contrast, the growth rate of the resistant strain is not altered by antibiotic exposure (C, D). As a result, all antibiotic concentrations select for the resistant strain (E, F). The mean and standard error of two experiments, each with n = 6 for co-cultures and n = 3 for monocultures, are shown. See also Figure A.1 in Appendix A.

Inhibitory Concentration, MIC) (Tables S1 and S2). This latter measure controls for any phenotypic differences in antibiotic resistance between colonies and liquid (including the effects of antibiotic tolerance). Consistent with our prediction, colony growth decreases the MSC for streptomycin from 1.6 µg/ml (9.7% MIC; Figure 2.1) to 0.78 µg/ml (2.4% MIC; Figure 2.2). However, the shift from liquid to colony growth greatly increases the MSC for carbenicillin from 2.3 µg/ml (7% MIC; Figure 2.1) in liquid to 20 µg/ml (62% MIC; Figure 2.2) in colonies.

Why does colony growth dramatically weaken selection for β-lactamase secretion? Previous work suggests that the simplest explanation for weakened selection is that secreted β-lactamases may provide cross-protection to the antibiotic sensitive strain [41, 44, 45]. Consistent with this explanation, the growth rate of the susceptible strain is dramatically increased by the presence of the resistant strain (Figure 2.2). Further evidence of cross-protection comes from comparing the morphology of susceptible cells grown in the presence and absence of resistant cells. Carbenicillin is known to cause cell elongation and filamentation due to induction of the SOS response [80, 81] and inhibition of cell wall synthesis [30]. Cell elongation occurs in susceptible cells both when they grow alone and when they are grown in combination with resistant cells. However, the presence of resistant cells markedly reduces the filamentation of susceptible cells, providing evidence of cross-protection at the single-cell level (Figure 2.3A, B).

2.3.3 Genetic mixing weakens selection for carbenicillin resistance

Theoretical work predicts that the spatial organisation of genotypes is fundamental for the evolution of cell-cell interactions in biofilms [17, 76–78, 82, 83]. Specifically, it predicts that the formation of clonal patches within colonies will limit cross-protection, which will favour resistant cells over susceptible cells. We next tested the importance of spatial structure for the competitiveness of our antibiotic resistant strain. We inoculated colonies with a varying number of cells, at a concentration of carbenicillin that selected against antibiotic resistance in our earlier experiments

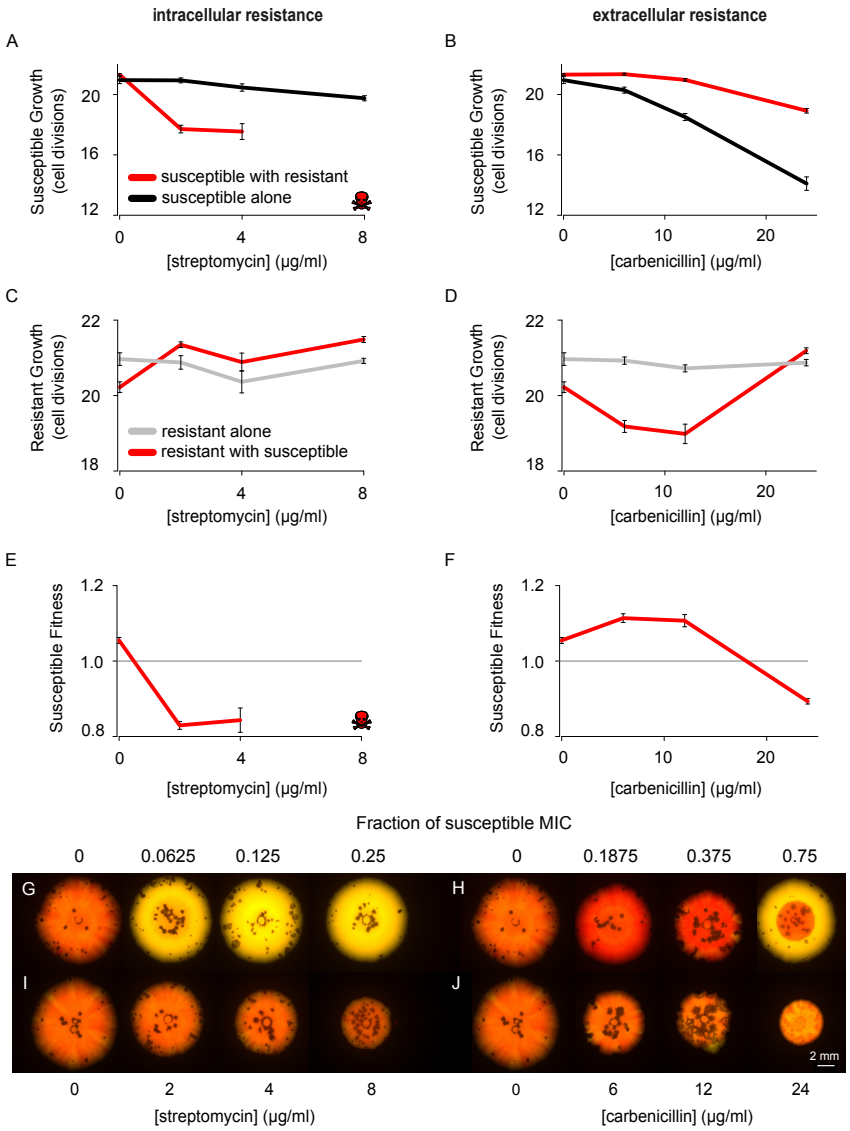


Figure 2.2: Natural selection for resistance in bacterial colonies. Susceptible and resistant strains were competed over seven days on solid agar with either streptomycin (intracellular resistance) or carbenicillin (extracellular resistance). On streptomycin, resistant strains outcompete susceptible strains at all concentrations of antibiotic (A), where skulls denote that no colony forming units were observed. However, the resistant strain increased the growth rate of the sensitive strain in the presence of carbenicillin, demonstrating cross-protection (B). Resistant growth increases in the presence of streptomycin when the susceptible strain is present (C) but is suppressed by the presence of the susceptible strain on carbenicillin (D). Streptomycin always selects for resistance (E) whereas low doses of carbenicillin select for the sensitive strain (F). Representative images of the colonies in which yellow resistant and red susceptible strains are competed over 6 days, also demonstrate this result (G, H) while control colonies, in which both colours are susceptible, show the effect of these concentrations of antibiotic on non-resistant cells (I, J). The mean and standard error of two experiments, each with n = 6 for co-cultures and n = 3 for monocultures, are shown. See also Figures A.2 and A.3 in Appendix A.

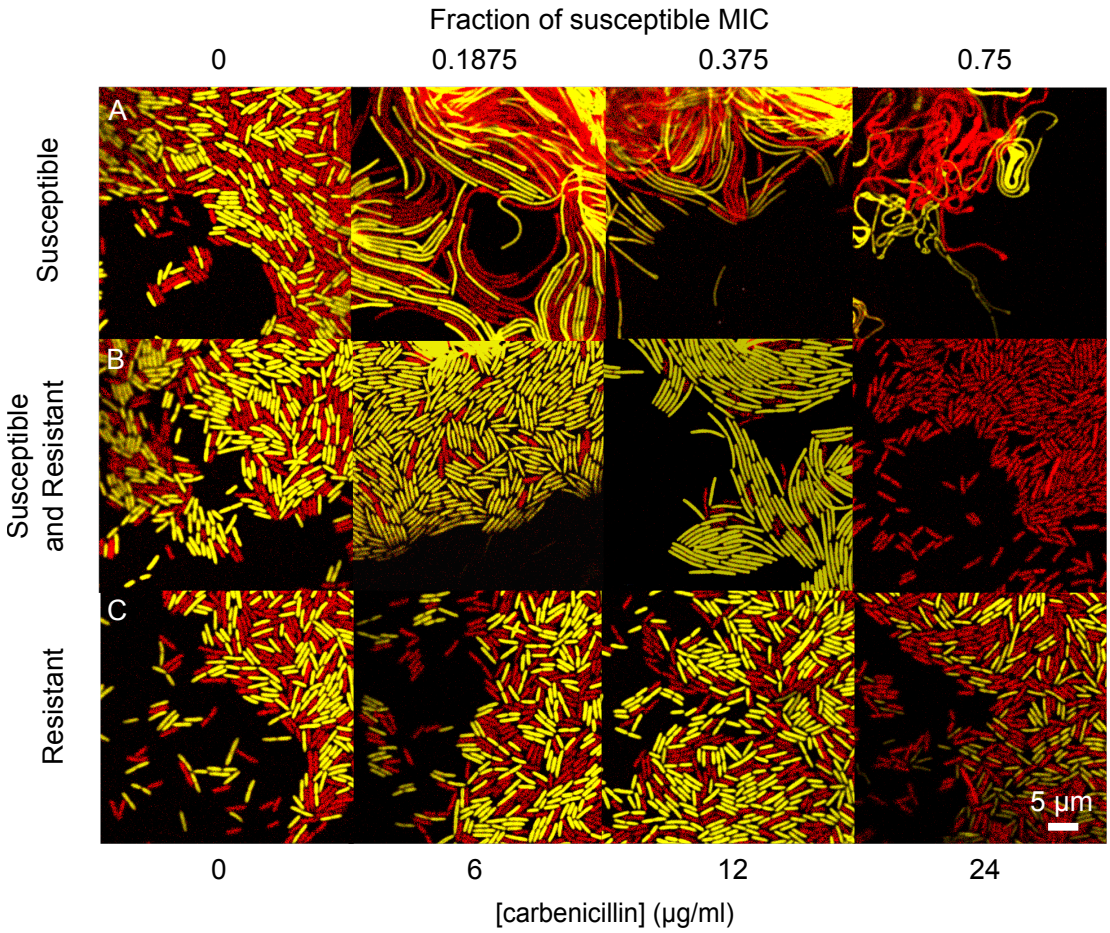


Figure 2.3: Confocal images showing filamentation of bacterial colonies affected by antibiotic stress. Confocal images of the colony edge after two days show carbenicillin causes susceptible cells grown alone on increasing concentrations of antibiotic, moving horizontally across the first row, to filament (A). In the second row, susceptible cells, in yellow, filament less when in the presence of resistant strains, in red, (B) than when grown alone in the row above (A). Furthermore, at intermediate concentrations of antibiotic there is enrichment of the susceptible strain (B). When the resistant cells are grown alone on the antibiotic (C) they do not filament at these concentrations of carbenicillin. The MIC (minimum inhibitory concentration) is the lowest concentration of antibiotic that completely inhibits growth of susceptible cells (here measured in a colony) (Table A.1, Appendix A). From left to right, susceptible only, resistant only, red resistant and yellow susceptible and yello resistant and red susceptible are shown growing on antibiotic free media

(Figure 2.2). Inoculating with fewer cells leads to a greater degree of spatial structure in the form of larger clonal patches (Figures 2.4 and A.5) [84]. In line with our prediction, the fate of the resistant cells was reversed under conditions of low inoculation density and they were able to outcompete the susceptible cells (two-way ANOVA, F1, 15 = 10.9, P = 0.005), (left hand data point, Figure 2.4E). By contrast, at higher inoculation densities, we observe that susceptible cells can outcompete resistant cells, replicating our earlier results. Moreover, the effect of density on competition is not seen until after two days of growth, once the communities are fully confluent (Figure A.5). This suggests it is spatiogenetic structure within the colonies that is key to the observed effects, not simply the fact susceptible cells are physically isolated for longer at a low inoculation density (Figure 2.4).

If spatial structure within colonies is capable of causing resistant strains to outcompete susceptible strains, then removing spatial structure should remove the competitive advantage of resistant strains. In order to test this prediction, we mixed one set of colonies daily using an inoculation loop [69]. When there was no antibiotic present, this mixing had no effect on susceptible fitness (three-way ANOVA, $F_{1,31} = 0.978$, P = 0.33). However, as predicted, mixing the low density treatment reversed the outcome of the competition such that the resistant strain was no longer able to outcompete the susceptible strain (three-way ANOVA, $F_{1,28}$ = 5.2, P = 0.03), (Figure 2.4E, G). Simply disordering a bacterial colony, therefore, can remove the competitive advantage of an antibiotic resistant strain. In sum, our data show that spatial structure in bacterial communities can be critical for the spread of antibiotic resistance.

2.3.4 An unexpected benefit to antibiotic susceptibility

Our experiments demonstrate that density and spatial structure can be fundamentally important for the rise of resistance to β-lactam antibiotics. Moreover, our data generally support a simple model where resistant cells experience a growth rate cost from carrying a plasmid, and will cross-protect susceptible cells when they are nearby

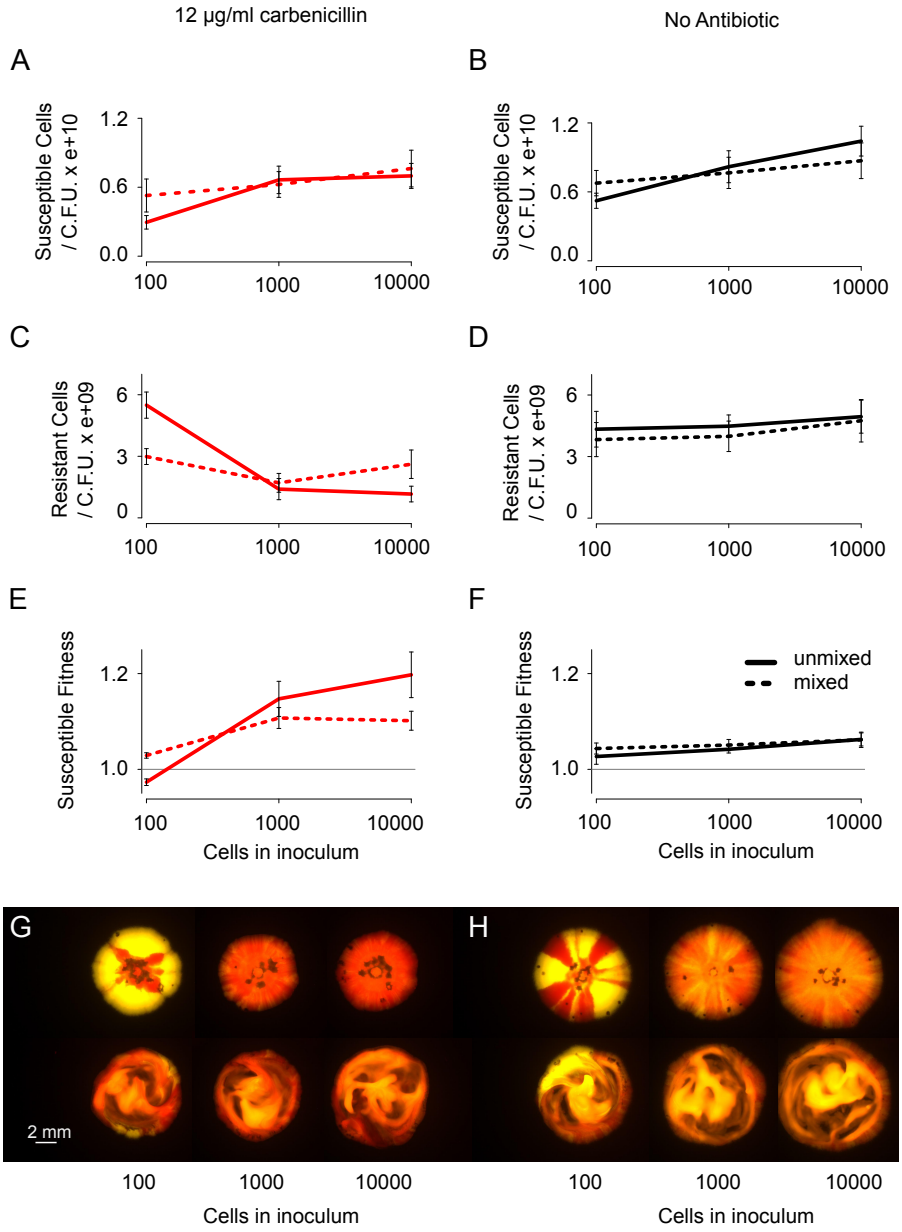


Figure 2.4: Spatiogenetic structure and the evolution of antibiotic resistance. Susceptible (red) and resistant (yellow) strains were co-inoculated onto plates containing either no antibiotic (black line) or 12 µg/ml carbenicillin (red line) (A - D). Final cell counts are shown here, as opposed to cell divisions (Figures 2.1 and 2.2), because the use of different densities itself changes the number of cell divisions that occur (low cell density treatments experienced reduced nutrient competition and increased cell division). The final cell count removes this effect and is an easier metric to interpret. The growth data is shown in the Supplementary Information (Figure A.5). From this data the relative susceptible fitness was calculated (E, F). The extent of separation between susceptible and resistant strains in a colony can be varied with the number of inoculating cells, as can be seen in images taken after 6 days (G, H). Mixing (dotted line) decreases the fitness of the resistant strain in colonies with a low initial density (colonies in LHS row in Figure 2.4G go redder upon mixing) and increases fitness in colonies with a high initial density (colonies in middle and RHS row go yellower upon mixing). The mean and standard error of two experiments, each with n = 3, are shown. See also Figure A.5.

(high density and low spatiogenetic structure). However, there are a number of intriguing patterns in our data, which all suggest that this simple view is insufficient.

The first observation is that low doses of carbenicillin can actually benefit the sensitive strain. Specifically, the fitness advantage of the susceptible strain doubles from 5.5% to 11% upon the addition of low doses of carbenicillin (t_{16} = -2.9, P = 0.01). One explanation for this strong effect could be that carbenicillin promotes the growth of susceptible cells. However, we see no evidence for growth promotion in pure cultures (Figures 2.1B, 2.2B) and, more importantly, the increase in fitness in mixed culture is due to a decrease in the growth rate of resistant cells, not an increase in the susceptible cells (red line in Figure 2.2B and D). This effect on resistant cells is also not a direct effect of the antibiotic, as this depression of growth rate is not seen in pure resistant cultures (grey line in Figure 2.2D). Instead, the antibiotic is somehow shifting the balance of competition in mixed culture toward the susceptible strain and allowing it to suppress the growth of the resistant strain.

Competition within colonies is intense and a large body of theoretical and empirical work has shown that the effects of natural selection occur primarily at the growing edges [69, 85–87]. In particular, this shows that it is the lateral growing edge - forming the circumference of a colony - that is most critical (upwards growth is much more limited than lateral growth). This led us to hypothesise that susceptible cells were somehow able to obtain better access to the lateral growing edge, allowing them to grow outwards and inhibit the growth of resistant cells. All of our frequency data so far has been from measurements of the whole colony (Figures 2.1, 2.2, 2.4). Focussing in on the growing edges of colonies does indeed reveal that the edge becomes increasingly dominated by susceptible cells over time (Figure 2.3B, middle row). However, this might happen simply because susceptible cells divide faster (above, Figure A.4) and does not demonstrate an additional mechanism that allows them to dominate at the edge. To assess the importance of positioning, we need to experimentally test whether susceptible cells do better with antibiotic because they can influence spatial structure.

This test was inadvertently performed in the experiment in Figure 2.4, which examines whether increases or decreases in genetic mixing affect cross-protection. As discussed above, mixing up the colonies enabled cross-protection and benefited susceptible cells in the low density treatment. However, there was a second and unexpected effect of mixing. In high density inoculations, where cells start off well-mixed, physically mixing colonies reduces susceptible fitness (Figure 2.4E right hand points). Moreover, this effect is caused by increasing the resistant cell abundance (Figure 2.4C). Disrupting spatial structure in colonies where susceptible cells are already winning, therefore, reduces susceptible fitness. This is exactly what is predicted from a model where antibiotic treatment somehow helps susceptible cells to obtain a better position in the colony. This model also predicts that the effect of mixing is not seen in the absence of antibiotics, which is also the case (Figure 2.4F).

2.3.5 Cell shape and the increased fitness of susceptible cells

How does antibiotic exposure allow susceptible cells to find more favourable positions in the colony? Inspection of the colony edge gave a clear candidate: susceptible cells in mixed colonies change shape upon the addition of antibiotics (Figure 2.3). If shape is important, then a key prediction is that changes in cell shape should proceed any increase in the frequency of susceptible cells. To test this prediction we tracked the aspect ratio of cells during competitions and compared this with the frequency of susceptible and resistant cells at each time point. Consistent with the shape-drives-fitness model, the elongation of susceptible cells precedes their competitive gains against resistant cells (Figure 2.5).

Time-lapse imaging of the colony edge highlighted a candidate mechanism for the advantage of elongated cells. We see sets of elongated cells that align orthogonally to the edge of the colony and push themselves outwards. This enables cells to grow ahead of the resistant strain and cut it off from the growing edge (Figure 2.6A). The clearest support for the effect of cell shape would come from manipulating the shape of susceptible cells to ask how shape affects the ability to

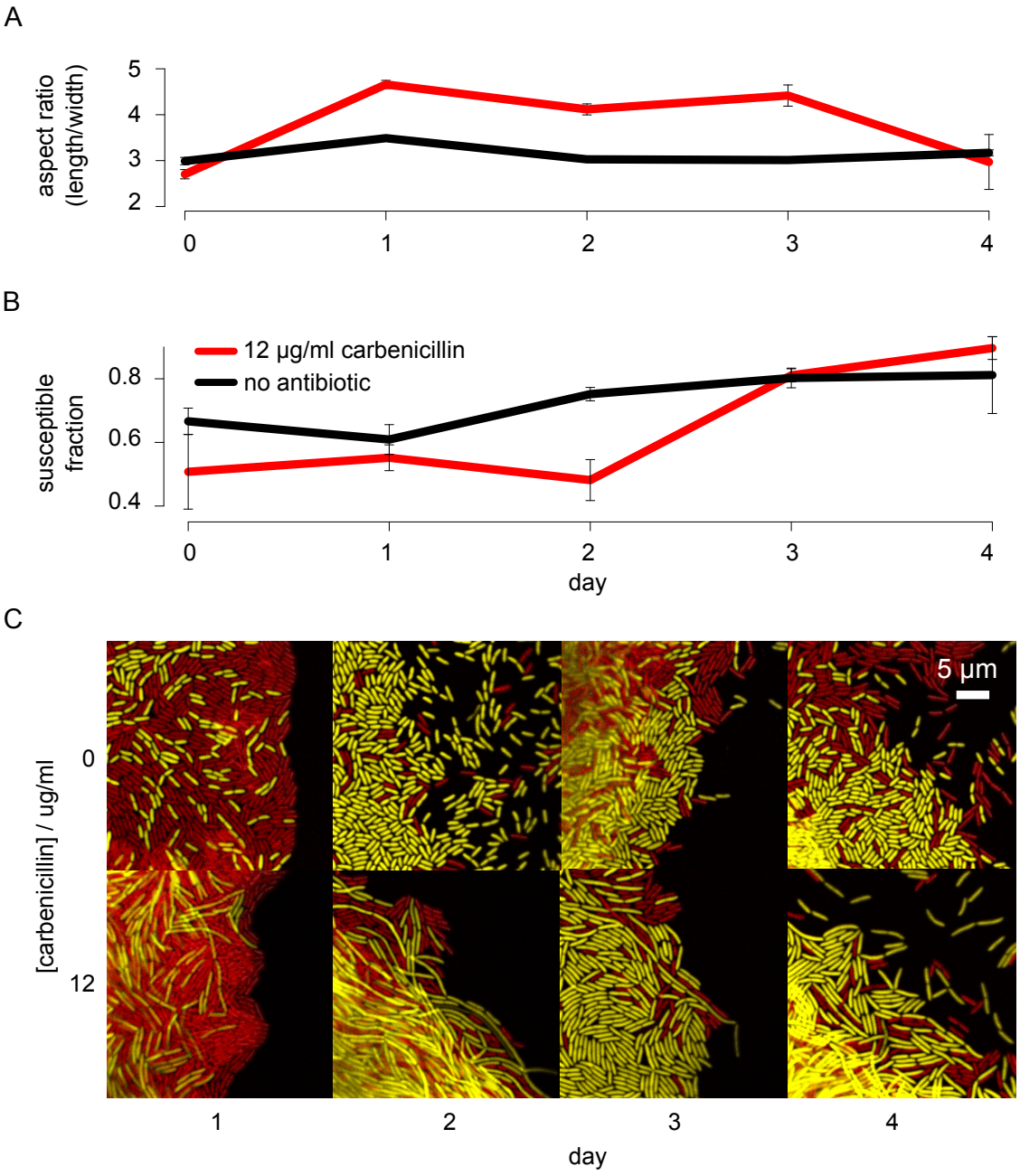


Figure 2.5: Susceptible cells increase in aspect ratio before outcompeting resistant cells in carbenicillin treated colonies. Yellow susceptible and red resistant cells were competed on either 12 µg/ml carbenicillin (red) or no antibiotic (black). The edge of these colonies was then imaged during growth to measure cell length and relative cell numbers (A, B). The bottom images are micrographs of the colony edge under the different conditions showing the shifts in aspect ratio in susceptible cells, in the presence of resistant cells, during carbenicillin treatment (C). The mean and standard error of two experiments, each with n = 3, are shown.

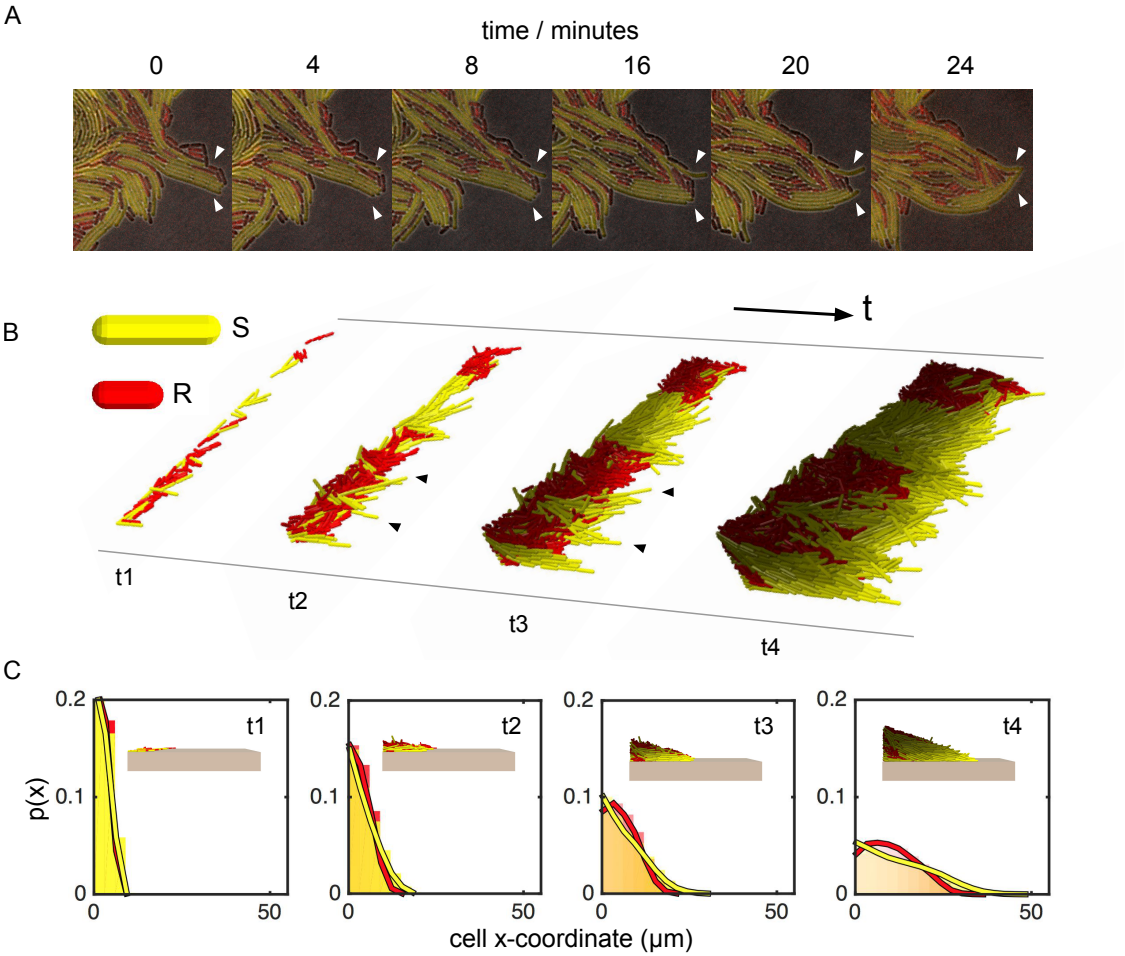


Figure 2.6: Cell shape is important for competition at the edge of colonies. Micrographs show longer susceptible cells (yellow) extending from the colony edge and occluding shorter resistant cells (red). This is shown in time-lapse images of growth at the edge of a representative colony after 10 hours, growing on 12 µg/ml carbenicillin (A). These images differ in quality from earlier images (e.g. Figure 2.5) because we had to use a lower fluorescence intensity to avoid bleaching during time-lapse imaging. An individual-based model shows the same effect (B). In the model, we can alter cell shape alone and follow its effects on cell sorting. Starting from a random configuration of Susceptible (S) and Resistant (R) cells in a 1:1 mixture, at t1, we observe that long cells extend from the colony edge (t2, black arrows). This improves their resource access and, as in our experiments, allows them to occlude the shorter cells from the edge. This, in turn stimulates further growth (t3, black arrows). By t4, S cells have become enriched at the colony edge through positive feedback. Histograms of cell x-coordinates track the growth of the colony edge and quantify the shape-driven enrichment process in the individual-based model, taken at the same 4 time points as in B (C). p(x) shows the probability of finding a given strain at a given point in the colony. Data merged from a sample of 20 simulations; times t1-t4 correspond to 12, 24, 36 and 56h of growth respectively. The colour brightness intensity of each cell corresponds to its growth rate, with brighter cells indicating faster growth. See also Figure A.6.

spatially organise and compete. We do not know of any route to prevent susceptible cells from elongating under antibiotic treatment without strong pleiotropic effects on growth rate and other phenotypes. However, recent theoretical work – based upon individual-based modelling – also suggests that cell shape can be important for positioning in bacterial biofilms [88].

We, therefore, extended these simulation models in order to study the effect of cell shape on positioning at the edge of a colony (Figure 2.6 and A.6). We focused on the growing edge because this is the critical area of competition in an expanding colony and the region where we see strong enrichment for elongated susceptible cells. As we observe in the time-lapse imaging (Figure 2.6A and Movie S1), the individual based model shows how long cells can align themselves orthogonally to the colony edge and push outwards occluding shorter cells from the edge. This gives them a competitive advantage as they can spread outwards, allowing them to align with the direction of growth ahead of resistant strains and hence to dominate the growing edge (Figures 2.6B and A.6).

To summarise, the combination of competition data, imaging and our individual based simulations all support a model where carbenicillin drives cell elongation and this provides an unexpected, but strong, fitness advantage to susceptible cells during biofilm growth. In combination with the effects of cross-protection, this means that sub-MIC doses of carbenicillin can inhibit bacterial growth while selecting against an antibiotic resistant strain.

2.4 Discussion

Understanding the spread of antibiotic resistant strains is a major goal for both science and society. Our work underlines how much there is still to understand. We find that simply moving from a typical liquid culture assay to a dense colony community has major impacts on the fitness of resistant strains (Figures 2.1 and 2.2). Consistent with theory ([17, 69, 76–78], Figure A.4), for a competitive resistance mechanism, we see that growth in colonies greatly increases natural selection for resistance. Also consistent with theory [15, 89], we see the opposite effect for a

cooperative resistance mechanism, such that treatment can even favour susceptible strains in colonies and the loss of resistance. Mechanistically, this occurs because β-lactamase production protects the sensitive strain, allowing it to outcompete and outnumber the resistant strain in the colony (Figures 2.3 and 2.4). Furthermore, by focussing on the growing edge, where natural selection is at its most powerful [17, 90], we discovered a second unexpected effect. Our data and theory suggest that exposure to low levels of carbenicillin leads to cell elongation, which allows susceptible bacteria to preferentially access the growing edge of treated colonies (Figures 2.5 and 2.6). The combined effect of these two factors increases the dose of carbenicillin required to generate selection for resistance by an order of magnitude.

Alexander Fleming warned 'if you use penicillin use enough,' in the belief that low doses of antibiotic would promote the *de novo* emergence of resistance. Clinical practice tends to use the highest dose of antibiotic achievable without toxicity, however if this rapidly selects for resistant strains it will not be effective for long. The work presented here, alongside modelling work from others [91], suggests an intermediate dose may reduce the total burden of infection, under certain conditions, whilst maintaining competition between susceptible and resistant strains. This may give the immune system the opportunity to clear the infection. In support of this, *in vivo* work has shown such an intermediate dosing strategy in some cancers can slow down the rate at which resistance evolves and thereby prolong the effective life of a drug by maintaining competition between susceptible and resistant cancer lines within a tumour [135].

In this work we compare the selection for resistant strains growing on different antibiotic in either liquid culture or as a colony biofilm. Biofilms in different infections, from the Cystic Fibrosis lung to a burn wound infection, can differ dramatically. This biofilm model is perhaps more representative of a short term infection, such as a burn wound, as there are space and resources for colony expansion. During chronic infection, as in the case of an infected Cystic Fibrosis lung, bacteria are likely to be densely packed and opportunities for range expansion may be more limited.

Our work cautions against the focus on liquid culture assays for understanding antibiotic resistance evolution. Few pathogenic bacteria live like this and we have shown that competitive outcomes in dense and diverse communities can be very different. Encouragingly, this shift in perspective may help to identify exposure regimes that suppress the growth of sensitive strains without favouring resistant strains [91–93].

2.5 Materials and Methods

In our experiments we compete susceptible and resistant strains of *P. aeruginosa* on LB media, either in the form of broth culture or on agar plates. Resistant strains are isogenic with susceptible strains with the exception that they have been transformed with a clinical, multi-drug resistant plasmid, Rms149 [74]. We recognise that *P. aeruginosa* also carries a chromosomal β-lactamase, however we found this was not active against carbenicillin, as can be seen from the MIC determination shown in the Appendix. Further details of the experimental methods and the models used in this paper are provided in the Supplementary Materials and Methods (A.1).

2.6 Acknowledgements

Thanks to Christopher Thomas for kindly providing plasmids. I.F. and W.P.J.S. received funding from the Systems Biology Doctoral Training Centre, funded by the EPSRC (grant number EP/G03706X/1). A.S.M. is supported by a Miguel Servet fellowship from the Instituto de Salud Carlos III (MS15/00012) co-financed by the European Social Fund and The European Development Regional Fund "A way to achieve Europe" (ERDF). K.R.F. is supported by European Research Council Grant 242670 and a grant from the Calleva Research Centre for Evolution and Human Science (Magdalen College, Oxford). R.C.M was funded by the Royal Society, European Research Council grant 281591, and Wellcome Trust Grant 106918/Z/15/Z. The authors declare no competing financial interests.

'Nature! ...We obey her laws even when we rebel against them; we work with her even when we desire to work against her.'

— Johann Wolfgang von Goethe (1749-1832), translated by T. H. Huxley

3

Antibiotic adjuvants and bacterial competition

Isabel Frost[1], Rebecca Gabrilska[2], Kendra Rumbaugh[2], R. Craig MacLean[1], and Kevin R. Foster[1]

1. Department of Zoology, University of Oxford, OX1 3PS, UK.

2. Department of Surgery, Texas Tech University Health Sciences Center, 3601 4th Street, Lubbock, Texas, 79430, USA.

3.1 Abstract

The rise of antibiotic resistance is leading to increasing interest into ways to inhibit bacterial mechanisms of resistance. β-lactamase inhibitors have long been used to limit resistance to β-lactam antibiotics, but the way that β-lactamases function – by detoxifying the environment - suggests that inhibition may lead to counter-intuitive effects. Here, we investigate how the inhibition of β-lactamases impacts natural selection for antibiotic resistance, carried on a multi-drug resistant plasmid. We compete susceptible and resistant strains of *Pseudomonas aeruginosa* in liquid and in colonies under antibiotic treatment (ticarcillin), with and without the β-lactamase inhibitor, clavulanic acid. We find the effect of inhibition can vary

dramatically depending on the growth environment. During liquid growth the inhibitor removes the advantage of resistant strains. This effect equalises the relative fitness of susceptible and resistant strains during exposure to ticarcillin, in combination with the clavulanic acid. In contrast, in populations of bacteria growing as closely-knit, colony-biofilms, the primary effect of inhibition is to limit the cross-protection that susceptible cells receive from resistant cells. This causes clavulanic acid to amplify natural selection for antibiotic resistance. Our results show that β-lactamase inhibition has a role to play in the success or demise of resistant strains. However, this role is complex and requires an understanding of microbial interactions in different growth environments.

3.2 Introduction

Antibiotic resistant infections threaten the hard-won advances made in medicine over the past century, and portend a time in which we are 'cast back into the dark ages of medicine' [94]. By 2050 the death toll could be one person every 3 seconds [95]. The economic consequences of untreatable infections, for both developed and developing economies, have been predicted as a global potential GDP loss of $100.2 trillion by 2015 [95]. The World Health Organization Global Action Plan on Antimicrobial Resistance stresses it is imperative that research addresses this burgeoning tidal wave [96]. One way we can do this is by applying knowledge of evolutionary theory, amassed since Darwin's original work, to the forces of selection at work in the complex evolutionary systems of infection and microbial interactions [91].

With few new antibiotics in the pipeline, prolonging the useful life of current antibiotics, offers a promising way, to bridge the gap, between current therapies and the diminishing supply of new drugs. One avenue of research, has been to find molecules that can act as adjuvant drugs alongside antibiotics. Antibiotic adjuvants, are compounds, without antibacterial properties, which enhance the activity of an antibiotic, often by blocking the most common mechanism of resistance [97]. In the literature, it is often assumed, the inhibition of a resistance mechanism will suppress the emergence of antibiotic resistance [98], however, an evolutionary approach is

required for a thorough understanding of the effect inhibiting resistance will have on resistance selection. Not least because bacteria grow in diverse environments, some of which involve surface-associated growth, in dense communities. In such environments, the enzymes secreted by one bacterium, as a resistance mechanism, will have an effect on neighbouring cells. Inhibition of such mechanisms is likely to disrupt these microbial interactions and may lead to complex effects.

Antibiotic adjuvants are a growing area of research and some adjuvants are already in clinical use. Specifically, the β-lactamase inhibitors, sulbactam, tazobactam and clavulanic acid, which are often prescribed alongside β-lactam antibiotics, such as amoxicillin, piperacillin and ticarcillin. β-lactamase resistance most commonly occurs through the production of β-lactamase enzymes [60]. β-lactamase inhibitors covalently bind into the active site of the β-lactamase enzyme, irreversibly inhibiting its ability to hydrolyze β-lactam antibiotics [33].

Over the last four decades [99], β-lactam-inhibitor combinations have become increasingly common in clinical treatment, due to the realisation that they can increase the effectiveness of antibiotics in the presence of resistant bacteria. However, their effect on the spread of resistant strains, itself, has received little attention. A position commonly expressed, is that the use of inhibitors will be good for both treatment and resistance evolution [97]. By contrast, one recent study [45], based on an engineered resistance plasmid, suggested that the addition of inhibitors can promote resistance evolution. However, the use of an artificial construct, and liquid culture, makes it difficult to know if this result will be typical. We, therefore, decided to study the effects of antibiotic adjuvants, in a study system based upon a clinically-derived resistance plasmid, under different growth conditions.

We followed competitions between resistant cells, carrying a clinical plasmid, and genetically identical cells, that do not carry this plasmid, in *Pseudomonas aeruginosa*, in order to study the effects of adding an adjuvant. The plasmid provides bearers with resistance to the β-lactam, ticarcillin, which is hydrolysed extracellularly, and we add the adjuvant β-lactamase inhibitor, clavulanic acid. The reason for selecting this particular combination was both because this a clinically

used combination of inhibitor and adjuvant and as a validation of previous results with a different antibiotic (Chapter 2). We then compete these two strains, both during growth in liquid culture and during dense growth on agar, to study how adjuvant treatment affects the competitiveness of resistant strains. Finally, we study the effects in an *in vivo* mouse model. Our work suggests, that the potential for social effects, in antibiotic resistance, can be fundamental to understanding how antibiotic adjuvants can affect the spread of resistant strains.

3.3 Methods and Materials

Bacterial strains

We used YFP and DsRed labelled strains of *P. aeruginosa* strain PA01 with plasmid Rms149. Minimum inhibitory concentration (MIC) assays show the relative susceptibility to antibiotic of the different strains and were performed in triplicate both by broth and agar dilution [100] (Table 3.1).

Table 3.1: MIC values for bacterial strains used in this study. Colour is not included as this did not affect the MIC.

	MIC in Ticarcillin (μg/ml)		MIC in Ticarcillin with 2 μg/ml Clavulanic Acid (μg/ml)	
	Broth	Agar	Broth	Agar
PAO1	32	32	32	16
PAO1 Rms149	>1024	>512	64	16

Liquid competitions

Pre-cultures of the strains were incubated overnight at 37 °C with 250 RPM shaking overnight in 3 ml of LB broth (Fisher Scientific, NJ, USA). These were then diluted in 3 ml of fresh LB broth to an OD_{600} of 0.05 and incubated under the same conditions for 2 hours. Cultures of these strains were then mixed at a ratio of 1:1 in phosphate buffered saline (PBS) with an OD_{600} of 0.3. This was diluted 10-fold in PBS and 1 μl was added per well in a 96 well plate, in triplicate. Wells contained a final total volume of 200 μl LB Lennox broth (Fisher) with the following antibiotic concentrations: ticarcillin; 0, 4, 8, 16, 32 μg/ml and with or without

2 μg/ml clavulanic acid. The antibiotic concentrations, used for the liquid and biofilm cultures, are different, as we wished to achieve the same level of susceptible inhibition, over the experimental time frame. Competitions were run for 20 hours at room temperature (22 °C) at 250 RPM. Competitions were diluted 10^5-fold and 50 μl of each was added to a plate using glass beads to count colony forming units (C.F.U.). We used the fluorescence lamp from an Axio Zoom.V16 microscope (Zeiss) to differentiate cells labelled with YFP. The number of cells in the starting inoculum was measured in the same way.

Competitions on agar

We wished to investigate the conditions required for the protection of the susceptible strain, by a β-lactamase producing strain, and whether this was inhibited by the presence of a β-lactamase inhibitor. To do this, we performed the same competitions on solid agar plates. These were set up in the same way as liquid competitions. The resulting 1:1 mixtures were diluted by a tenth in PBS. 1 μl of this mixture was added per agar plate in a single central drop. Plates contained 25 ml LB Miller agar (tryptone 10 g / l; yeast extract 5 g / l; sodium chloride 10 g / l; agar 15 g / l) and 2, 4, 8 μg/ml ticarcillin, which were chosen as sub-MIC values in addition to a no antibiotic control for every competition. Initial ratios were calculated by plating 50 μl of a 10^{-6} dilution of the inocula on LB agar plates. These were incubated overnight at 37 °C so C.F.U. could be counted. Competition plates were left at 20 °C and imaged on a stereoscope daily for 6 days. On day 7 the colonies were scraped from the agar and suspended in 1 ml PBS, diluted 10^6 and 10^5-fold and plated out to count C.F.U, using fluorescence to differentiate cells labelled with YFP.

The fitness was determined using the following formula [101]:

$$\text{susceptible fitness} = \frac{ln\left(\frac{N_{\text{suceptible,final}}}{N_{\text{susceptible,initial}}}\right)}{ln\left(\frac{N_{\text{resistant,final}}}{N_{\text{resistant,initial}}}\right)} \tag{3.1}$$

Where $N_{\text{suceptible,initial}}$ and $N_{\text{suceptible,final}}$ are the numbers of susceptible cells before and after the competition and $N_{\text{resistant,initial}}$ and $N_{\text{resistant,final}}$ are the numbers of resistant cells before and after the competition.

Microscopy

The Axio Zoom.V16 microscope (Zeiss) under the PlanApo Z 0.5X objective and the associated Zen Blue software was used to carry out fluorescence microscopy imaging. These colonies were imaged while still growing on the agar plate and these images were taken at 3.5X. Three colonies were imaged for each condition and multiple images were taken of individual colonies. For confocal imaging colonies were cut out of the agar plate and placed on a slide on the second day of growth. Confocal laser scanning microscopy (CLSM) imaging was carried out with the LSM 700 laser-scanning microscope (Zeiss) under the 50X objective using Zen Black software.

In vivo Mouse Experiments

PAO1-DsRed and PAO1-YFP-Rms were grown in LB overnight, then subcultures of each were grown in fresh LB for the infection. The experiment was performed twice, first with 11 week old Swiss Febster females and then with 12 week old mice. The treatment groups contained 3 mice each, though in some treatments mice were excluded if they did not survive until the end of the experiment. Concentrations of 0, 2, 8 and 32 μg/ml ticarcillin with and without 2 μg/ml clavulanic acid were tested. Clavulanic acid was prepared fresh daily. Prior to infecting the wound bed with bacteria, the first treatment was applied onto the sterile wound. Then, shortly after, the wound was infected with a 1:1 ratio of PAO1-DsRed and PAO1-YFP-Rms149, which were mixed immediately before infection. The mice were then treated every 24 hours thereafter, by injecting the dosage under the bandage and topically onto the infected tissue. After the seventh treatment, on the seventh day, the mice were euthanized and the infected wound tissue was collected. The tissue was homogenized with 2.4 mm metal beads in 1 X PBS and serially diluted in PBS. 100 μl pf this suspension was plated on on *Pseudomonas* isolation agar, *Pseudomonas* isolation agar with 30 μg/ml ticarcillin, and LB agar. YFP and DsRed-labelled colonies were counted using fluorescence from a GE Typhoon FLA 9000. In addition, colony PCR (Lightcycler 480 with SYBR green) was used to detect presence of the Rms149 plasmid (including control colonies), for a sub-sample of colonies. This was to ensure

the plating method was correctly identifying plasmid-bearing resistant strains and no unexpected plasmid transfer or *de novo* resistance was found.

Statistical Analysis

Statistical analyses were carried out in RStudio [102]. An ANOVA or t test was used unless otherwise stated; please see the Appendix for further details. Error bars show standard error. Solid and liquid competition experiments were performed using all colour combinations to allow for different costs associated with the colour markers. For these experiments (Figures 3.1 and 3.2) the mean and standard error of two experiments, each with n = 6 for co-cultures and n = 3 for monocultures, are shown.

3.4 Results

3.4.1 The resistant strain outcompetes the susceptible strain during planktonic growth in ticarcillin

First, we characterise the behaviour of the resistant and susceptible strains, in the simplest way possible; in well-mixed, liquid culture, in the same vein as the majority of bacterial experiments (Figure 3.1). In Chapter 2 it was shown that, when no antibiotics are present, carriage of the clinical plasmid reduced fitness by 3%, in the absence of antibiotics, demonstrating a cost to resistance. These results show that there is never selection for the susceptible strain in competition with the resistant strain when growing in ticarcillin (Figure 3.1D). The presence of the β-lactamase inhibitor reduces the strength of selection for the resistant strain (three-way ANOVA, $F_{4,49} = 7.094$, $P = 0.01$) but the susceptible strain is never able to outcompete the resistant strain. This is because ticarcillin, without the inhibitor, suppresses the susceptible stain (two-way ANOVA, $F_{2,27} = 5.652$, $P = 0.025$) but not the resistant strain (two-way ANOVA, $F_{3,26} = 1.048$, $P = 0.32$) (Figure 3.1A and B). In the presence of the β-lactamase inhibitor the resistant strain is suppressed by ticarcillin, but not to the same extent as the susceptible strain initially (Figure 3.1C). These results are inline with the insight behind current dosing strategies; addition of the β-lactamase inhibitor restores the inhibitory capacity of the antibiotic, while

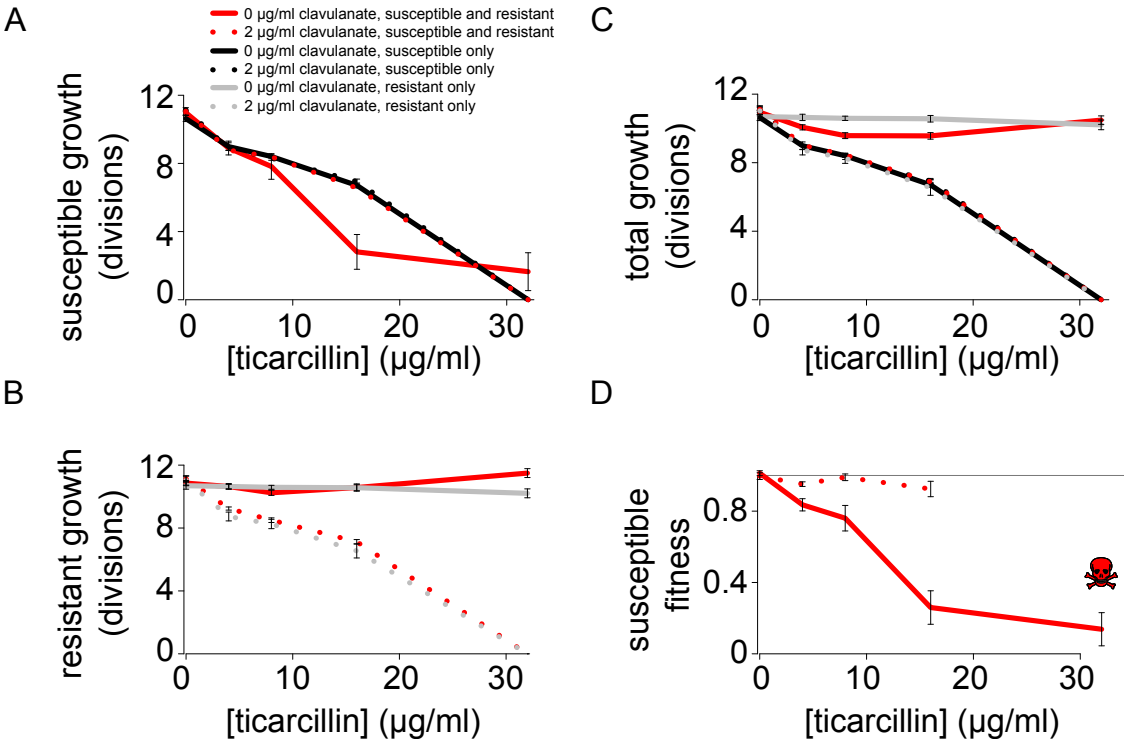


Figure 3.1: Selection for antibiotic resistance in liquid culture. Susceptible and resistant strains were competed in liquid culture supplemented with ticarcillin (solid line) or ticarcillin with a β-lactamase inhibitor, 2 μg/ml clavulanic acid (dotted line). Both conditions suppress the growth of the susceptible strain (A). In contrast, the growth of the resistant strain is only suppressed by ticarcillin in the presence of the β-lactamase inhibitor (B). As a result selection for the resistant strain is weaker in the presence of the β-lactamase. However, there is never selection for the susceptible strain under any condition with antibiotic (D). The skull denotes none of either strain was counted. The mean and standard error of two experiments, each with n = 6 for co-cultures and n = 3 for monocultures, are shown. See also Figure B.1 in Appendix B.

decreasing natural selection for antibiotic resistance. Notably, our results also differ from previous work. Yurtsev *et al.* [45] found β-lactamase producing resistant strains of *Eschericia Coli* were outcompeted by susceptible non-producing strains, at concentrations of the β-lactam, ampicillin, 50-fold larger than their MIC.

3.4.2 Addition of an inhibitor during biofilm growth increases selection for resistance

We next investigated the effect of adjuvants during colony growth. Our previous work (Chapter 2) showed susceptible cells were only able to benefit from local carbenicillin breakdown by resistant cells during this mode of growth. To test

this in the presence of ticarcillin, we grew an equal mixture of susceptible and resistant strains on agar plates containing antibiotic over 7 days, in a 'colony biofilm' model [65] (Figure 3.2). In the absence of the β-lactamase inhibitor, susceptible strains grew better in the presence of the resistant strain than alone, at 2 μg/ml ticarcillin ($t_{15.431}$ = -4.474, $P < 0.001$). This demonstrates the cross-protective effect of β-lactamase production (Figure 3.2B). At this dose of ticarcillin, resistant strains fared worse in the presence of the susceptible strain than alone ($t_{15.895}$ = 6.8018, $P < 0.001$) (Figure 3.2C). This caused selection for the susceptible strain growing at these low doses of antibiotic (t_{11} = 9.7022, $P < 0.001$) (Figure 3.2D). This is even more evident when we look at the colonies (Figure 3.2E, top row), in which the red susceptible strain dominated the colony, even in the presence of the yellow resistant strain, at 2 μg/ml ticarcillin. This effect was reversed with the addition of the β-lactamase inhibitor. In the presence of clavulanic acid, the β-lactamase was inhibited and there was no longer a cross-protective effect, causing the inhibition of the susceptible strain ($t_{17.94}$ = -5.9422, $P < 0.001$). The resistant strain was also inhibited but less so than the susceptible strain and hence the selection for the susceptible strain was reversed and there was selection for resistance at a lower effective concentration ($t_{16.521}$ = -5.0201, $P < 0.001$) (Figure 3.2D). Again, this effect is visually very striking in the images of colonies (Figure 3.2E, bottom row), in which, in contrast to the colony growing in the absence of inhibitor, there is now clear selection for the yellow resistant strain at the colony edge.

3.4.3 Cell elongation shows cross-protection is removed by the adjuvant

Images of the growing colony edge after 2 days provide further insights (Figure 3.3). 2 µg/ml ticarcillin caused enrichment of the susceptible yellow strain at the growing edge (Figure 3.3B), and when the β-lactamase inhibitor was added this was no longer the case (Figure 3.3C). Furthermore, susceptible cells elongate in the presence of the antibiotic [80, 81]. Confocal images show that resistant cells, in the presence of the antibiotic, only filamented when the β-lactamase inhibitor was present (Figure

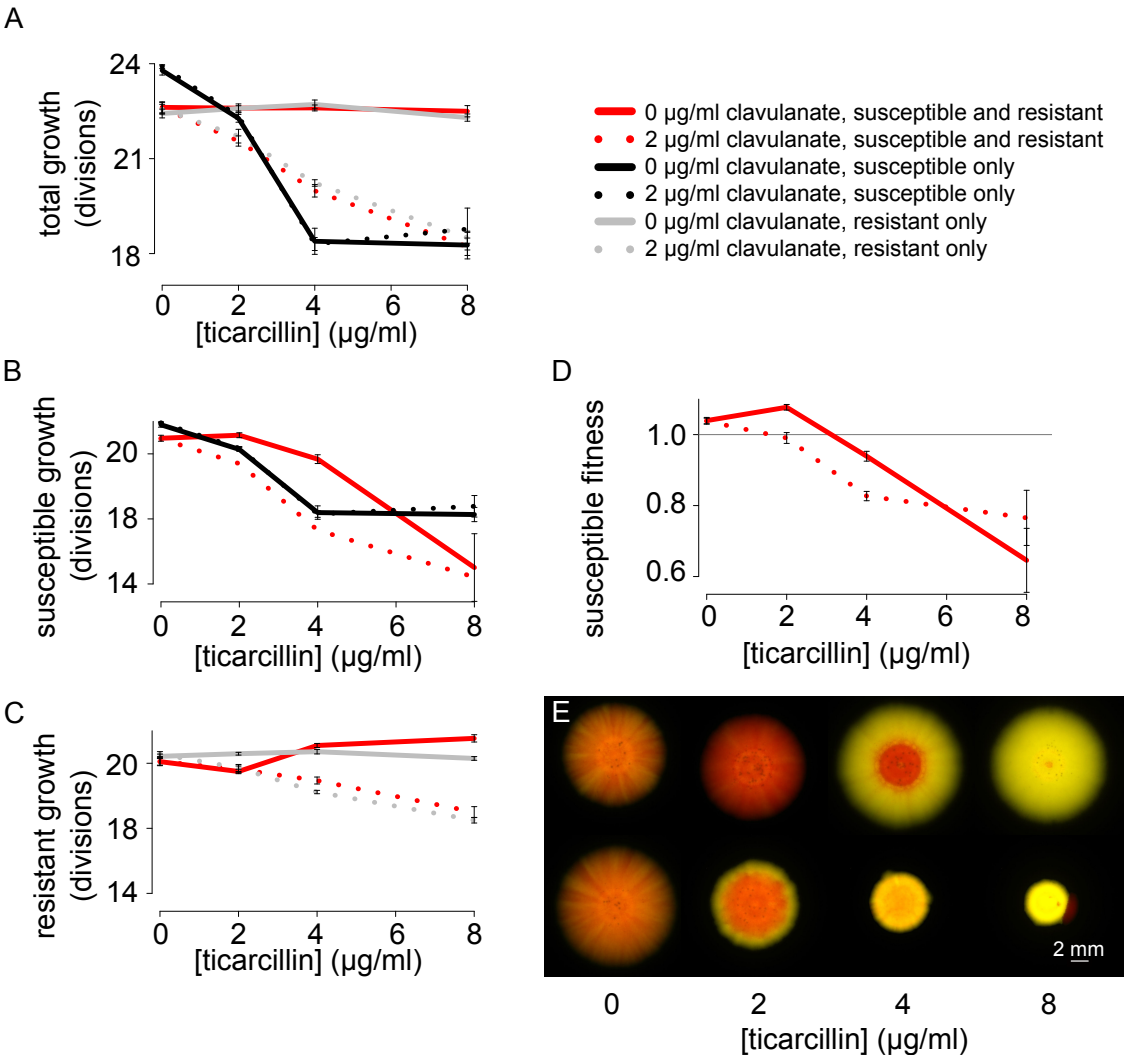


Figure 3.2: Natural selection for resistance in bacterial colonies. Susceptible and resistant strains were competed on increasing concentrations of ticarcillin, with and without the β-lactamase inhibitor, clavulanic acid (2 μg/ml). Total growth of susceptible colonies was repressed by the antibiotic with and without the inhibitor, however, the growth of the colonies containing a resistant strain are only repressed in the presence of an inhibitor (A). Without the inhibitor, growth of the susceptible strain was less suppressed in the presence of the resistant strain than alone, suggesting the resistant strain had a cross protective effect (B). Resistant growth was only affected by the antibiotic when the inhibitor was present (C). At sub-inhibitory concentrations, ticarcillin selected for the susceptible strain, however, this effect was reversed with the addition of the β-lactamase inhibitor (D). Representative images of these colonies after 6 days, in which the susceptible strain is red and the resistant strain is yellow, are also shown (E). The top row of images were grown without clavulanic acid and the bottom row were grown in the presence of 2 μg/ml clavulanic acid. The mean and standard error of two experiments, each with n = 6 for co-cultures and n = 3 for monocultures, are shown. See also Figure B.2 in the Appendix B.

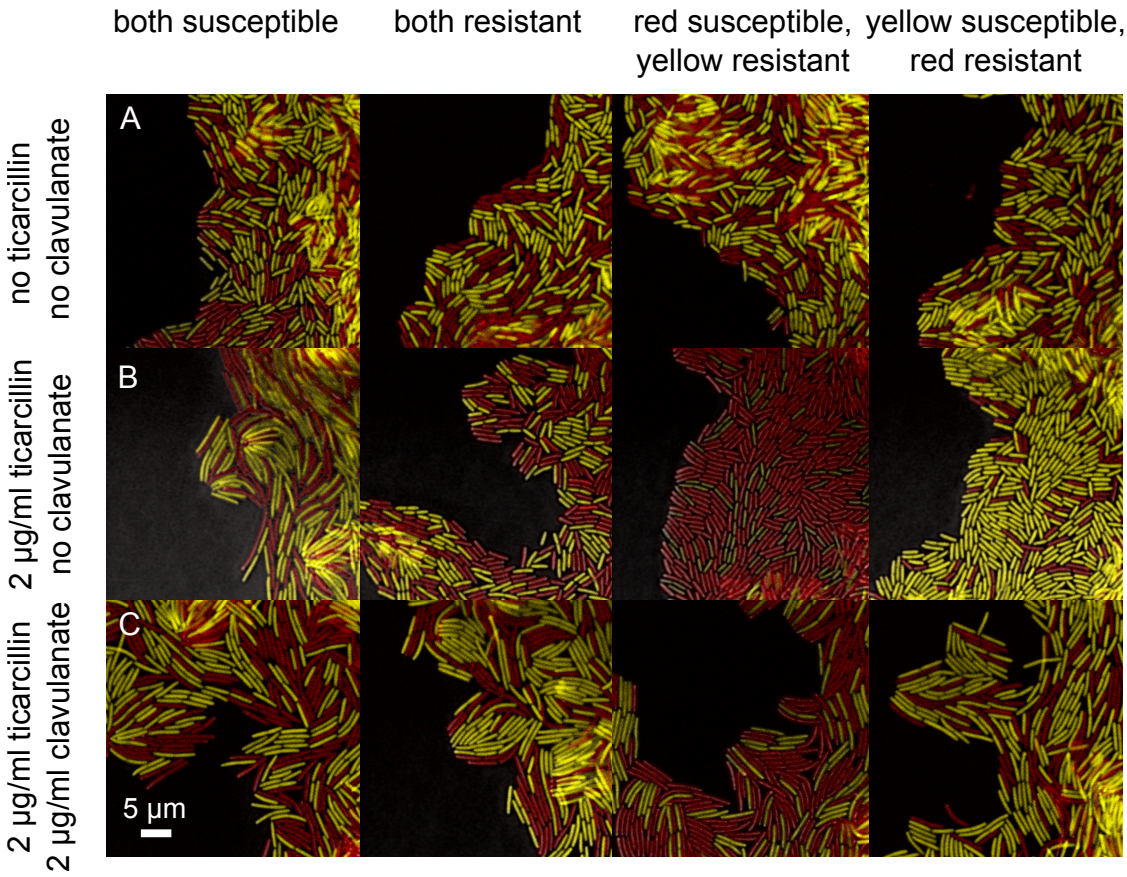


Figure 3.3: Confocal images showing filamentation of bacterial colonies affected by antibiotic stress. Resistant cells are no longer able to protect susceptible cells from filamentation on ticarcillin in the presence of the β-lactamase inhibitor. Colonies were imaged confocally after two days of growth. From left to right, susceptible only, resistant only, red resistant and yellow susceptible, and yellow resistant and red susceptible are shown growing on antibiotic free media (A), and ticarcillin with (B) and without (C) the β-lactamase inhibitor, clavulanic acid.

3.3C). In addition, susceptible strains in the presence of resistant strains filamented less on the antibiotic than when grown alone, though they returned to filamenting when the inhibitor was present, even in the presence of the resistant strain. Previous experimental work, supported by modeling in Chapter 2, has shown that there is a surprising further contributor to the increase in susceptible cell fitness on low doses of β-lactam antibiotics (Figure 3.2D); cell shape. Susceptible cells elongate in response to the antibiotic (Figure 3.3) and this gives them a competitive advantage at the colony edge. This advantage is lost when both cells elongate.

3.4.4 *In vivo* competition between resistant and susceptible cells

We have shown here, and in Chapter 2, that β-lactamase producing strains protect their sensitive neighbours, by locally detoxifying the environment of antibiotic. However, to understand the role of social β-lactamase production, in the more complex setting of a host, an *in vivo* model is essential. We therefore investigated competition between susceptible and resistant strains in a burn-wound mouse model (Figure 3.4). In these experiments, we see again evidence of cross-protection at low doses of antibiotics, though these results were not significant. Growth on 2 μg/ml ticarcillin, causes an increase in the susceptible growth rate ($t_{5.123}$ = 0.7882, P = 0.47) (Figure 3.4A). Simultaneously the resistant growth is suppressed ($t_{6.703}$ = -1.4763, P = 0.19) (Figure 3.4B) and this leads to an increase in the susceptible fitness ($t_{6.952}$ = 1.57, P = 0.16) (Figure 3.4D). This is same effect seen in Chapter 2 (Figure 2.2) and in Figure 3.2D, which we found to be driven by the elongation of susceptible cells in the presence of antibiotic in Chapter 2 and showed here to be suppressed by the presence of an inhibitor. We also see a trend towards the ability of an adjuvant to suppress cross-protection and accelerate resistance, although the data were not significant. The increase in fitness on 2 μg/ml ticarcillin is reduced in the presence of 2 μg/ml clavulanic acid ($t_{8.926}$ = 0.8246, P = 0.43) (Figure 3.4D), as the resistant strain is less suppressed ($t_{8.272}$ = -0.5964, P = 0.57) (Figure 3.4B). In sum, the experiments suggest that social interactions between competing resistant and susceptible strains may have a role to play in clinical infections. The *in vivo* results of this chapter are not significant and indicate that a larger experiment would be needed to observe the effects we have seen *in vitro*.

3.5 Discussion

We have shown that the mode of bacterial growth, in dense communities of cells, as opposed to free swimming bacteria in planktonic culture, can have very different effects on selection for resistance. The results here extend those in Chapter 2,

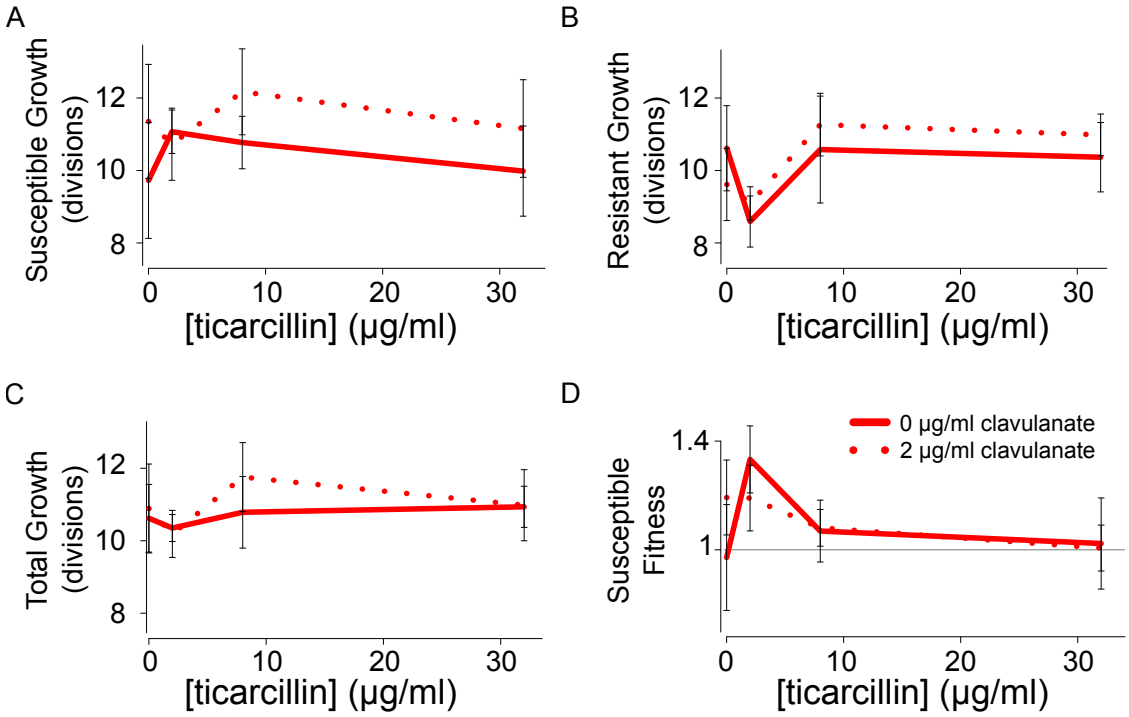


Figure 3.4: *In vivo* effects of using a β-lactam inhibitor. Susceptible and resistant strains were competed in a mouse wound model supplemented with ticarcillin (solid line) or ticarcillin with a β-lactamase inhibitor, 2 μg/ml clavulanic acid (dotted line). The susceptible strain experiences a slight increase in growth in the presence of the antibiotic (A). In contrast, the growth of the resistant strain is initially suppressed by ticarcillin (B). Total growth of both strains is not highly affected by the antibiotic in this model at these concentrations (C). Selection for the resistant strain is partially weaker in the presence of the β-lactamase (D). The mouse model is a complex environment, however, the key markers we expect are present, though not significant. The mean and standard error of two experiments, each with n = 3, unless one of the mice did not survive, are shown. See also Figure B.3 in Appendix B.

by showing that susceptible strains can experience a cross-protective effect, from resistant strains, on both ticarcillin and carbenicillin. During liquid growth, the addition of an adjuvant restores the efficacy of the antibiotic against both strains and renders them of equal fitness (Figure 3.1D). This is the view commonly held in the chemical adjuvant literature [97] and is in accordance with the clinical efficacy of β-lactamase inhibitors [99]. However, during dense colony growth the addition of an inhibitor can increase selection for the resistant strain (2 μg/ml and 4 μg/ml, Figure 3.2D and E). This effect is suggested by the *in vivo* data and has been seen by others in the evolution literature [45]. This counter-intuitive result, that inhibiting

a resistance mechanism can increase selection for it, can be explained in light of the fact that the majority of β-lactamase is in the periplasm of gram-negative cells [103]. This periplasmic β-lactamase will be less accessible to the inhibitor and any β-lactamase enzyme, external to the cell, will be inhibited first.

The experiments in this Chapter focus on sub-inhibitory concentrations of antibiotic. Several pieces of evidence indicate we may expect to find differences in the level of β-lactamase inhibition at concentrations of antibiotic-inhibitor combinations relevant during clinical antibiotic use. Amoxicillin clavulanic acid, is often administered twice daily in the form of Augmentin and achieves a time above the MIC of 30 to 40% [104]. Different inhibitors show different levels of clearance from the body, stability to hydrolysis and permeability into the cell. Clavulanic acid is superior to other clinically approved inhibitors at entering the cell [105], however, it is vulnerable to degradation in aqueous solution [106] and is removed from the body more quickly than ticarcillin (half life of 56 to 392 min for ticarcillin and 26 to 266 min for clavulanic acid) [107], with which it is commonly administered. Hence, there are various processes, through which, a within-patient bacterial infection, may be exposed to sub-inhibitory concentrations of both antibiotic and inhibitor, and it is important to understand resistance selection at these concentrations [79].

A conceptual model

The cross-protective action of β-lactamase strains towards susceptible strains increases the window of selection, during which susceptible strains outcompete resistant strains on antibiotic, as they maintain a higher growth rate. Inhibition of a social resistance mechanism, such as β-lactamase secretion, then is likely to initially reduce this selective window and cause selection for the resistant strain at lower antibiotic concentrations. This is because the external β-lactam degradation, that benefits the susceptible strain, is likely to be inhibited first. These effects are discussed further in Figure 3.5. Our results, during dense community growth, show the addition of an inhibitor can reduce the window of selection for the susceptible strain and thereby promote resistance.

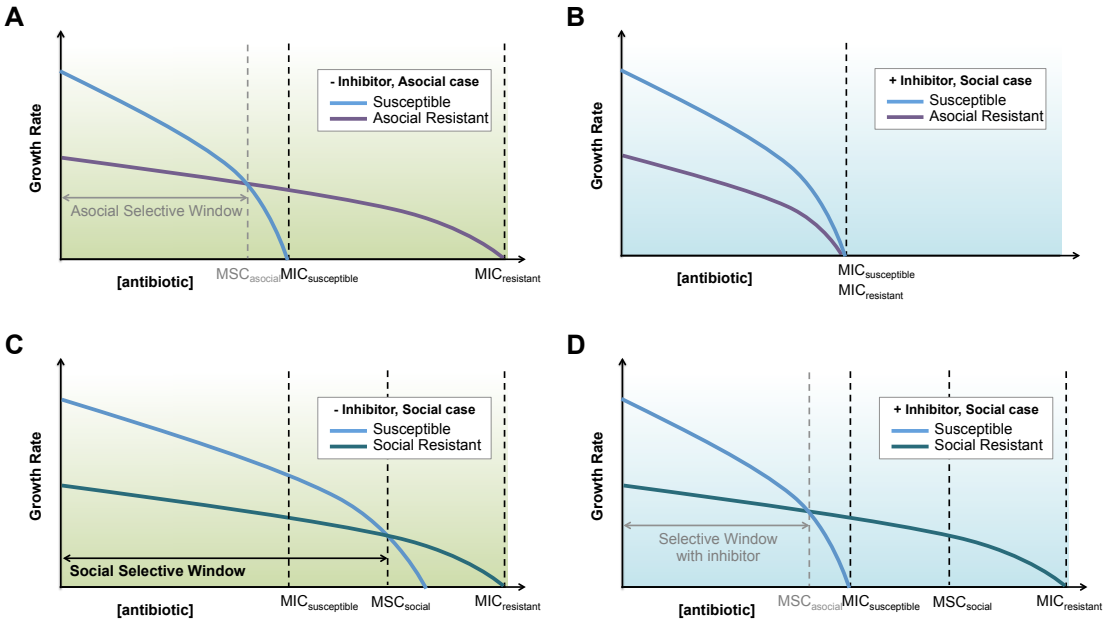


Figure 3.5: The effect of β-lactamase inhibition on selection for β-lactam resistance. In the most basic case, (**A**) susceptible and resistant strains are grown together on an increasing dose of antibiotic and the resistance mechanism of the resistant strain has no social effect or interaction with the susceptible strain. Theory suggests initially the resistant strain will grow more slowly due to the fitness cost imposed by being resistant. However, once the minimum selective concentration (MSC) [108–110] of antibiotic is reached the resistant strain is able to outcompete the susceptible strain and the fitness cost of being resistant is outweighed by the conferred benefit to surviving antibiotic assault. In the presence of an inhibitor of the asocial resistance mechanism (**B**), there will no longer be a benefit incurred by carriage of the costly resistance mechanism and if the resistant strain is fully inhibited there will never be selection for resistance to the antibiotic in the presence of the inhibitor. The possibility not included in this simplistic diagram, is that the resistant strain may be only partially inhibited. In this case there will still be selection for the resistant strain at the MSC. In contrast, if the resistance mechanism of the resistant strain interacts with the susceptible strain, for example by detoxifying the environment of antibiotic, the MSC will be shifted to a higher concentration of antibiotic and the resistant strain will be selected for at a higher effective antibiotic concentration (**C**). If the antibiotic is used alongside an inhibitor in this system two outcomes are possible and these are concentration dependent. If the resistant strain is fully inhibited and the external resistance mechanism also, the outcome will be as in the inhibition of the asocial (**B**). However, if the resistance mechanism is only partially inhibited, social effects external to the cell are likely to be affected first. This removes the social effect and the MIC of the susceptible strain is reduced. This causes the MSC to be reduced and for resistance to be selected for at a lower effective dose of the antibiotic in the presence of the inhibitor (**D**).

3.6 Conclusion

Antibiotic adjuvants are a promising route forward given the current crisis in untreatable, antibiotic resistant infections. These results provide evidence that adjuvants can inhibit both resistance and resistance evolution. However, their effects can also depend strongly on the nature of social interactions between cells. In particular, under conditions of resilient infections, where cells interact closely, as is the case in biofilms, which can be relatively impermeable to antibiotics [10] and making it difficult to achieve high doses. In these environments, adjuvants can have the opposite effect intended, and increase selection for resistance. This suggests the role of adjuvants is complex and that understanding how cells interact may provide valuable insights into selection for resistance.

'Some experts say we are moving back to the pre-antibiotic era. No. This will be a post-antibiotic era. In terms of new replacement antibiotics, the pipeline is virtually dry. A post-antibiotic era means, in effect, an end to modern medicine as we know it. Things as common as strep throat or a child's scratched knee could once again kill.'

— Margaret Chan, Director General of the World Health Organisation [2]

4

Antibiotic adjuvants and the evolution of antibiotic resistance

Isabel Frost[1], Helen Alexander[1], R. Craig MacLean[1] and Kevin R. Foster[1]

1. Department of Zoology, University of Oxford, OX1 3PS, UK.

4.1 Abstract

The threat posed by antibiotic resistance is becoming increasingly urgent. One proposed solution is the use of antibiotic adjuvants: drugs that increase the effectiveness of antibiotics, for example, by inhibiting common mechanisms of resistance. However, the potentially complex effects of these drugs on the spread of antibiotic resistance has received surprisingly little attention. Here we use evolutionary modelling to study how adjuvants impact resistance evolution. We begin with a deterministic model, that shows how adjuvants can promote or inhibit resistant strains, depending on how they are used in combination. In particular, the model predicts that prophylactic administration of an adjuvant, alongside a high dose of antibiotic, can block the rise of singly and doubly resistant strains. We then use a more realistic stochastic model, that can allow for mutation, to show that, for certain conditions, even in this more complex model, the same

predictions hold. This model shows that the earlier an adjuvant is added, the less likely it is that resistant strains will emerge. We argue that policy involving adjuvant use needs to pay attention, not just to treatment outcome, but also to the potential impact on antibiotic resistance.

4.2 Introduction

A recent UK government report estimated that, without policies to stop the spread of antimicrobial resistance (AMR), the annual death rate from AMR infections would increase from 700,000 deaths to 10 million by 2050 [95]. With this looming catastrophe, academics and industry are looking to novel methods of combating antibiotic resistance. Combination antibiotic therapies, as are already the treatment norm in Tuberculosis, have been considered and models of the synergistic and antagonistic interactions, between different antibiotics, is an area of growing interest in the literature [59]. Another avenue of research has been to prescribe antibiotics alongside adjuvants, drugs which have few antibacterial properties, in their own right, but are able to make antibiotics more effective, through various routes, including blocking bacterial mechanisms of resistance [97]. In principle, small-molecule inhibitors can act as adjuvants against many mechanisms of resistance ([98]) and the most successful, the β-lactamase inhibitors, have been used clinically for the last four decades [99]. Inhibitors have been touted as a solution to antibiotic resistance, enabling antibiotics, that would be otherwise ineffective, to have a second lease of life [97]. However, there has been little attention paid to the effects of such combined therapies on the emergence of resistance to both antibiotic and inhibitor.

There are indications that adjuvants can promote antibiotic resistance. One reason for this complexity is that interactions between the microbes can be central to how antibiotic resistance evolves and the potential effects of inhibitors ([45], Chapter 3). A recent study [45] combined experiments and modelling to highlight how the spread of cooperative mechanisms, of antibiotic resistance, can potentially be enhanced, by adjuvants. However, resistance mechanisms vary greatly in their potential for cooperativity among cells. Moreover, it is commonly assumed that

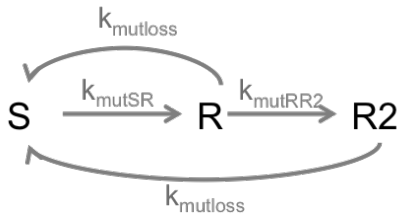


Figure 4.1: Diagram showing possible mutational pathways. The susceptible strain, S, can mutate into the antibiotic resistant strain, R, by horizontal gene transfer at rate, k_{mutSR}. R can then acquire *de novo* resistance to the inhibitor at rate k_{mutRR2}, becoming strain $R2$. Either R or $R2$ may lose the horizontally acquired element, carrying resistance, and become S, at rate $k_{mutloss}$.

adjuvants can also prevent resistance but this conclusion is not backed up by formal analysis ([97]). Our goal, therefore, was to develop new models, that capture both drug interactions and cell interactions, to evaluate when adjuvants will promote or prevent, resistance evolution (see Table 4.1 for examples of how different resistance mechanisms can affect microbial interactions).

We developed a model of resistance evolution (Figure 4.1), in which a susceptible strain may evolve single resistance to an antibiotic and from there become doubly resistant to both the antibiotic and an adjuvant. We find that giving an antibiotic with an inhibitor, before resistance emerges, has the potential to block the evolutionary pathway to antibiotic-inhibitor dual resistance, by minimising selection for the singly resistant strain. Next, we use a stochastic model to explore the effect of rare random mutation events in this system. Modelling cells discretely in this way, reinforces the result of the deterministic model - inhibiting resistance to the antibiotic alone can suppress the emergence of resistance to the combined treatment. In summary, our results suggest that antibiotic adjuvants not only have a biochemical basis for reducing the impact of resistant strains, but can be used as prophylactic evolutionary tools, to suppress the emergence of resistance, if used with sufficiently high doses of antibiotic.

Table 4.1: The social effect of different mechanisms of resistance, as potential adjuvant targets for inhibition.

Mechanism	Social Effect on Microbial Interactions	Inhibition
β-lactamase Production	Cooperative/Social ([23, 24, 41])	Clinically available β-lactamase inhibitors, Clavulanic acid, Sulbactam and Tazobactam. May inhibit cheating and cause selection for β-lactam resistant strains at a lower effective antibiotic concentration (Chapter 3 and [45]).
Intracellular antibiotic inactivation	Depending on level of breakdown can be social or asocial. Inactivation of Chloramphenicol antibiotics internally to resistant cells has been shown to protect susceptible cells in mice [72]. However, the Chapter 2 experiments with aminoglycoside resistance found no cross-protective effect.	No current clinical inhibitors.
Efflux Pumps	Asocial with potential to raise relative antibiotic concentration outside the cell and thus adversely affect susceptible strains [44].	Research into possible clinical inhibitors is ongoing [112].

Programmed Cell Death	Altruistic. Antibiotic can cause *E. coli* to release the Shiga toxin by lysing, damaging eurkaryotic cells [113].	Bacterial virulence was reduced in mice immunized with autolysin, inhibiting autolysis [114].
Biofilm Formation	Social/cooperative. Extracellular Polysaccharides (EPS) are produced, providing protection to neighbouring bacteria and increasing antibiotic resistance and tolerance [13].	Production of the EPS matrix can be inhibited and research into inhibitors is ongoing [115].
Quorum Sensing (QS)	Social/cooperative. QS strains produce signalling molecules which delay the initiation of costly cooperative traits, such as biofilm production and virulence, until bacteria are at a high enough density.	This is inhibited by some antibiotics, such as Ciprofloxacin. In one study Ciprofloxacin was found to reduce virulence in the short term but to promote it in the long term, as cheating, non-producing strains did not survive to outcompete the more virulent QS producers [116].
Indole Production	Social/cooperative. Resistant *E. coli* strains have been found to upregulate the signalling molecule, indole, allowing susceptible non-producers to survive [117].	No current clinical inhibitors.

4.3 Methods and Materials

4.3.1 The Deterministic Model

Model Overview

We want to understand the effect of inhibiting social and asocial mechanisms of drug resistance on selection for resistance. We consider a group of susceptible cells growing in an isolated infected area, such as an abscess, with constantly infused drug exposure. Cells grow and divide, depending on nutrient concentration, according to the logistic equation. Susceptible cells may transition to become resistant to the antibiotic, which is assumed costly to the producing cell. In addition, resistant cells possess the ability to detoxify the environment. This may confer a benefit to nearby susceptible strains, which do not pay the cost of carrying resistance. This capacity, for resistant cells to protect others, depends upon a parameter, which defines the rate at which they break down antibiotic externally to the cell. Varying this parameter is the equivalent of resistant bacteria degrading antibiotic at different rates. Antibiotic resistant cells may transition to become doubly resistant to both antibiotic and inhibitor. We assume that this double resistance incurs a greater fitness cost and reduces resistance to the antibiotic alone. For the analyses shown, we also assume the rate at which susceptible cells acquire resistance to the single antibiotic therapy is greater than the rate at which singly resistant cells become resistant to the dual antibiotic-inhibitor therapy. This would be the case, for example, if single resistance was acquired on a horizontally acquired gene [111] and subsequent *de novo* mutation was necessary to transform this into dual-resistance. Resistance may be lost at anytime, rendering a singly resistant or doubly resistant cell susceptible.

We model these processes as a system of ordinary differential equations (ODEs). The biochemical and pharmacodynamic properties, of these antibiotic and inhibitor systems, have been extensively explored in the literature [33, 99], allowing us to generate an explicit and physiologically realistic model. We then combine these approaches with evolutionary and ecological theory, to understand the effect of these drugs on the emergence of resistance.

Strain dynamics

We build on previous models [118–120] and consider a patch of susceptible cells in an infected area, growing in close enough proximity to be affected by the production of enzymes, by neighbouring cells, and to experience a common average concentration of antibiotic and inhibitor. Susceptible cells, S, grow according to the logistic growth equation, at rate σ_S, with a carrying capacity of K. This carrying capacity represents limitations to growth in this patch, such as nutrient limitation, which is characteristic of many infections [121]. S cells die depending on the concentration of antibiotic, AB, relative to their sensitivity to antibiotic, as denoted by their EC_{50S}. This is the concentration of AB at which the death rate reaches half of its maximum value, E_{max}. E_{max} models have been widely used to model antibiotic treatment [118]. S cells acquire resistance at rate k_{mutSR}, and become resistant cells, R (Figure 4.1). R cells grow in an analogous way to S cells, however, the cost of resistance is expressed as a reduced growth rate, σ_R. The increased resistance of the R strain is reflected in a higher EC_{50_R} than the S strain. In the presence of the inhibitor, I, R cells are no longer able to degrade the antibiotic. This is represented in the model by lowering the EC_{50_R} to equal that of the susceptible strain. This is modelled as a Hill function, with a switch point at $I = 1.5$ ng. R cells may acquire a mutation in their resistant enzyme, causing them to become inhibitor resistant (IR), at per capita rate, k_{mutRR2} (Figure 4.1). This rate is much lower than the rate at which single resistance occurred, k_{mutSR}. These doubly resistant cells, $R2$, again grow analogously to the S and R strains. $R2$ mutants have a greater fitness cost than R, reflected in an even lower growth rate, σ_{R2}. The IR enzyme is less effective at breaking down antibiotic, this is reflected in a lower $EC_{50_{R2}}$ than for the R strain. Both resistant strains may lose resistance at rate, $k_{mutloss}$, becoming susceptible and returning to the S strain. In all cases the rates of mutation have been made proportional to the total number of cells present. This treatment has been widely used in the literature [122], however, we recognise this is a simplification and it is likely rates of *de novo* resistance, plasmid

loss, for example through partitioning, and HGT will be affected by the number of dividing cells, as has been explored in the literature [123].

Antibiotic and Inhibitor dynamics

The antibiotic, AB, enters the growth compartment at a constant rate, α_{in}, and is removed from the compartment in a concentration dependent manner, at rate α_{out}. This parameter embodies various processes of antibiotic removal, including metabolism and excretion. This form of modelling antibiotic influx/efflux in the compartment is as if it is buffered by a much larger external compartment. R cells degrade AB at a maximum rate of k_{deg1}. The extent to which this maximum rate is reached is mediated by the concentration of inhibitor, I, relative to the IC_{50}. This is the concentration of I at which the rate of degradation is diminished to half its maximum value. The doubly resistant strain, $R2$, is not affected by the concentration of I, and degrades the antibiotic at rate k_{deg2}. Finally the inhibitor, I, enters the cells in much the same way as the antibiotic, at a constant rate, ρ_{in}, and is removed from the compartment in a concentration dependent manner at rate ρ_{out}. In the case of β-lactamase enzymes, the most common clinically used inhibitors are suicide inhibitors that irreversibly bind the β-lactamase enzyme [33]. This is modelled here as a mass action term, with R binding I at rate, k_{inhib}.

Our models are motivated by, but not restricted to, the case of β-lactamase inhibitors. In these specific systems, resistance in gram-positive and gram-negative bacteria is acquired almost exclusively by the HGT of genetic elements encoding β-lactamase enzymes [60]. β-lactamase inhibitors bind irreversibly into the active site of the β-lactamase enzyme, [99] and prevent further antibiotic break down. IR enzymes often break down antibiotic more slowly than the enzymes they are derived from [99] and are likely to impose a greater fitness burden on the resistant cell, for example when resistance involves the upregulation of the resistant enzyme [99]. The IR β-lactamase enzyme is often less effective at breaking down β-lactam antibiotics [99].

This model can be described by the following set of five ODEs (Parameterisation and definitions are shown in the Appendix (C.1), as is a model validation C.3).

$$\frac{dS}{dt} = S\left(\overbrace{\sigma_S\left(1-\frac{N}{K}\right)}^{\text{logistic growth}} - \overbrace{E_{max}\frac{\frac{AB}{EC_{50S}}}{1+\frac{AB}{EC_{50S}}}}^{\text{antibiotic death}} - \overbrace{k_{mutSR}}^{S\to R}\right) + \overbrace{(R+R2)\,k_{mutloss}}^{R,\,R2\to S} \tag{4.1}$$

$$\frac{dR}{dt} = R\left(\sigma_R\left(1-\frac{N}{K}\right) - E_{max}\frac{\frac{AB}{EC_{50R}}}{1+\frac{AB}{EC_{50R}}} - k_{mutRR2} - k_{mutloss}\right) + Sk_{mutSR} \tag{4.2}$$

$$\frac{dR2}{dt} = R2\left(\sigma_{R2}\left(1-\frac{N}{K}\right) - E_{max}\frac{\frac{AB}{EC_{50R2}}}{1+\frac{AB}{EC_{50R2}}} - k_{mutloss}\right) + Rk_{mutRR2} \tag{4.3}$$

$$\frac{dAB}{dt} = \alpha_{in} - AB\alpha_{out} - RABk_{deg1}\left(1-\frac{\frac{I}{IC_{50}}}{1+\frac{I}{IC_{50}}}\right) - k_{deg2}R2AB \tag{4.4}$$

$$\frac{dI}{dt} = \rho_{in} - I\rho_{out} - k_{inhib}RI \tag{4.5}$$

4.3.2 Non-dimensionalised Equations

Non-dimensionalisation is the process of removing physical units of measure from an equation by substitution. This improves computational accuracy and efficiency. In addition, this process allows us to see how variables in the model interact and to sweep a broader, generalised parameter space. We can use the dimensionless substitutions described in Table C.3 to rewrite eqs. (4.1) to (4.5) in a form that reduces the number of parameters and improves computational efficiency (see Appendix (C) for derivation). All variables and parameters are rescaled according to the substitutions outlined in Table C.4 eqs. (C.62) to (C.66) to reach the final set of non-dimensional equations eqs. (4.6) to (4.10). All equations were simulated

using MATLAB's in-built solver, ode45 [124]. (The parametrisation and definitions are shown in the Appendix (C.1.3)).

$$\frac{d\bar{S}}{d\bar{t}} = \bar{S}\left(\left(1-\bar{N}\right) - a\left(\frac{\overline{AB}}{1+\overline{AB}}\right) - b\right) + \left(\bar{R}+\overline{R2}\right)c \tag{4.6}$$

$$\frac{d\bar{R}}{d\bar{t}} = \bar{R}\left(\alpha_R\left(1-\bar{N}\right) - a\left(\frac{\gamma_R\overline{AB}}{1+\gamma_R\overline{AB}}\right) - c - d\right) + \bar{S}b \tag{4.7}$$

$$\frac{d\overline{R2}}{d\bar{t}} = \overline{R2}\left(\alpha_{R2}\left(1-\bar{N}\right) - a\left(\frac{\gamma_{R2}\overline{AB}}{1+\gamma_{R2}\overline{AB}}\right) - c\right) + \bar{R}d \tag{4.8}$$

$$\frac{d\overline{AB}}{d\bar{t}} = e - \overline{AB}f - \bar{R}\overline{AB}g\left(1-\frac{\bar{I}}{1+\bar{I}}\right) - \overline{R2AB}h \tag{4.9}$$

$$\frac{d\bar{I}}{d\bar{t}} = i - j\bar{I} - k\bar{I}\bar{R} \tag{4.10}$$

4.3.3 The Stochastic Model

The deterministic model allowed us to gain an intuitive understanding of the effect of multiple microbial and chemical processes interacting with one another on the evolutionary trajectory of this system. However, to understand better the role of rare mutation events, we next modelled these deterministic equations stochastically using the Gillespie Stochastic Simulation Algorithm (GillespieSSA) [125] in RStudio [102]. The SSA is composed of a set of reactions which describe how individuals (cells or reactants in our system) in a finite population interact and change over time. Each reaction is described by a state change vector (Table 4.3) and a propensity function (Table 4.2). The state change vector defines how the population will change with the probability contained in the propensity function. Gillespie's original SSA is exact, however it is too slow for most applications. For computational efficiency we use the approximate SSA method of Explicit Tau-Leaping (ETL) which independently samples the number of firings for each reaction over the time step, tau, from a Poisson distribution. From this we calculate an approximate stochastic trajectory for the system.

The original set of eqs. (4.1) to (4.5) can be converted into a set of propensity functions, containing a list of the rate of different events occurring in the system (Table 4.2), and a state change matrix (Table 4.3), defining the reactions that would occur with the stated propensity. The logistic growth equation, used in the deterministic model, has been re-written in terms of births and deaths [126]. In this way it can be split into two reactions, a_1, birth, with propensity $S\left(b_S - \frac{(b_S-d)N}{K}\right)$ and a_2, death, with propensity Sd. For continuity with the continuous model we define $\sigma_S = b_s - d$ where d is some common death rate of the bacterial strain and b_S is the birth rate of S. The GSSA model was parameterised as described in Tables C.1 and C.2, with equivalent parameters to the non-dimensionalised parameters used in the deterministic model.

Table 4.2: Propensity Functions

Identity	Reaction	Propensity Function	
a_1	S birth	$S\left(b_S - \frac{(b_S - d)\,N}{K}\right)$	(4.11)
a_2	S death	Sd	(4.12)
a_3	S death by antibiotic	$SE_{max}\frac{\frac{AB}{EC_{50S}}}{1+\frac{AB}{EC_{50S}}}$	(4.13)
a_4	S mutates to R	Sk_{mutSR}	(4.14)
a_5	R birth	$a_R R\left(b - \frac{(b - d)\,N}{K}\right)$	(4.15)
a_6	R death	$a_R Rd$	(4.16)
a_7	R death by antibiotic	$RE_{max}\frac{\frac{AB}{EC_{50R}}}{1+\frac{AB}{EC_{50R}}}$	(4.17)
a_8	R mutates to $R2$	Rk_{mutRR2}	(4.18)

a_9	R mutates to S	$Rk_{mutloss}$	(4.19)
a_{10}	$R2$ birth	$\kappa_{R2}R2\left(b-\frac{(b-d)\,N}{K}\right)$	(4.20)
a_{11}	$R2$ death	$\kappa_{R2}R2d$	(4.21)
a_{12}	$R2$ death by antibiotic	$R2E_{max}\frac{\frac{AB}{EC_{50R2}}}{1+\frac{AB}{EC_{50R2}}}$	(4.22)
a_{13}	$R2$ mutates to S	$R2k_{mutloss}$	(4.23)
a_{14}	AB enters the compartment	α_{in}	(4.24)
a_{15}	AB exits the compartment	$AB\alpha_{out}$	(4.25)
a_{16}	AB degraded by R	$RABk_{deg1}\left(1-\frac{\frac{I}{IC_{50}}}{1+\frac{I}{IC_{50}}}\right)$	(4.26)
a_{17}	AB degraded by $R2$	$k_{deg2}R2AB$	(4.27)
a_{18}	I enters the compartment	ρ_{in}	(4.28)
a_{19}	I exits the compartment	$I\rho_{out}$	(4.29)
a_{20}	I inhibits R	RIk_{inhib}	(4.30)

Table 4.3: State Change Matrix

	a_1	a_2	a_3	a_4	a_5	a_6	a_7	a_8	a_9	a_{10}	a_{11}	a_{12}	a_{13}	a_{14}	a_{15}	a_{16}	a_{17}	a_{18}	a_{19}	a_{20}
S	+1	-1	-1	-1	0	0	0	0	+1	0	0	0	+1	0	0	0	0	0	0	0
R	0	0	0	+1	+1	-1	-1	-1	-1	0	0	0	0	0	0	0	0	0	0	0
$R2$	0	0	0	0	0	0	0	+1	0	+1	-1	-1	-1	0	0	0	0	0	0	0
AB	0	0	0	0	0	0	0	0	0	0	0	0	0	+1	-1	-1	-1	0	0	0
I	0	0	0	0	0	0	0	0	0	0	0	0	0	0	0	0	0	+1	-1	-1

4.4 Results

4.4.1 Resistance evolution without inhibitor

We begin with the most basic case, modelling the effect of antibiotic on non-cooperating resistant and susceptible strains, competing in the absence of the inhibitor (Figure 4.2A, first column). When no antibiotic is present, the susceptible stain dominates, as it has the highest growth rate, due to the cost of resistance imposed on the other strains. On intermediate and high doses of antibiotic, the resistant strain rapidly outcompetes the susceptible strain, as we would expect. Next, we turn to the social case, in which the resistant strain degrades the antibiotic externally to cells (expressed by the term g in our non-dimensionalised model). In contrast to the asocial case, at intermediate doses of antibiotic, the resistant strain takes longer to outcompete the susceptible strain. Furthermore, as the resistant strain emerges, the susceptible strain initially also increases, due to cross-protection from the effect of the antibiotic (Figure 4.2B, first column). This result recapitulates evidence of cross-protection seen by us and others ([41] and Chapter 2). We see a benefit to the social resistant strain, at the higher concentration of antibiotic, where its external degradation of the antibiotic allows it to survive, outcompete the susceptible strain, and be maintained, at a much higher density.

4.4.2 The inhibitor can suppress antibiotic resistance

In both the social and asocial cases, when no antibiotic is present, the susceptible strain outcompetes the resistant strain. This is because, without antibiotic, resistance incurs a growth cost and carries no benefit (Figure 4.2A and B, first column, first row). The addition of inhibitor without antibiotic, has no effect (Figure 4.2A and B, second column, first row). At intermediate concentrations of antibiotic, the addition of inhibitor eventually causes the doubly resistant strain to emerge. In the case of an asocial resistance mechanism, this represents an increase in the amount of time the susceptible strain is selected for and a slight decrease in the total bacterial load (Figure 4.2A, first and second columns). In the cooperative social

case, the addition of inhibitor causes resistance to emerge earlier than growth on antibiotic alone. However, the bacterial load is relatively reduced by the inhibitor (Figure 4.2B, first and second columns). At high doses of antibiotic, the addition of inhibitor suppresses the emergence of either resistant strain, over the timecourses considered here. By using a high dose of antibiotic, the pool of susceptible strains capable of becoming resistant, is decreased. Double resistance is only able to emerge via the resistant strain, in this system (Figure 4.1). In the presence of the inhibitor, the resistant strain carries a fitness cost and is unable to breakdown the antibiotic. Hence, there is never selection for the resistant strain and thus the mutational pathway, to the doubly resistant strain, is inhibited.

The effect of the inhibitor is summarized in Figure 4.2C. During growth on the antibiotic alone, increasing the rate at which the resistant strain degrades antibiotic externally (represented in the dimensionless model as $g = \frac{k_{deg1}K}{\sigma_S EC_{50S}}$), causes resistance to emerge more slowly. This is because resistance is costly to the producing strain and the greater the extent of cooperative antibiotic degradation, the more the susceptible strain can benefit, without paying the associated cost. With the addition of inhibitor (Figure 4.2C, bottom panels), this effect of cooperative resistance is removed. The susceptible strain outcompetes the resistant strain for longer, however, eventually the doubly resistant strain is selected. The only exception to this occurs at the highest concentrations of antibiotic. In this case, the pool of susceptible cells is so greatly reduced that the doubly resistant strain does not emerge.

4.4.3 Modelling partial inhibition

So far, we have assumed that the inhibitor completely strips resistant cells of antibiotic resistance, such that they behave like the susceptible cells (Figure 4.2). Specifically, we capture this with the EC_{50R}, which is included in the dimensionless parameter,γ_R. The EC_{50R} is the concentration of antibiotic at which the death rate of R, due to antibiotic, reaches half its maximum. The value of 2.5 is taken for γ_R when no inhibitor is present. This will vary between strains, however, in one example, the change in resistance to ceftazidime, in *Pseudomonas aeruginosa*

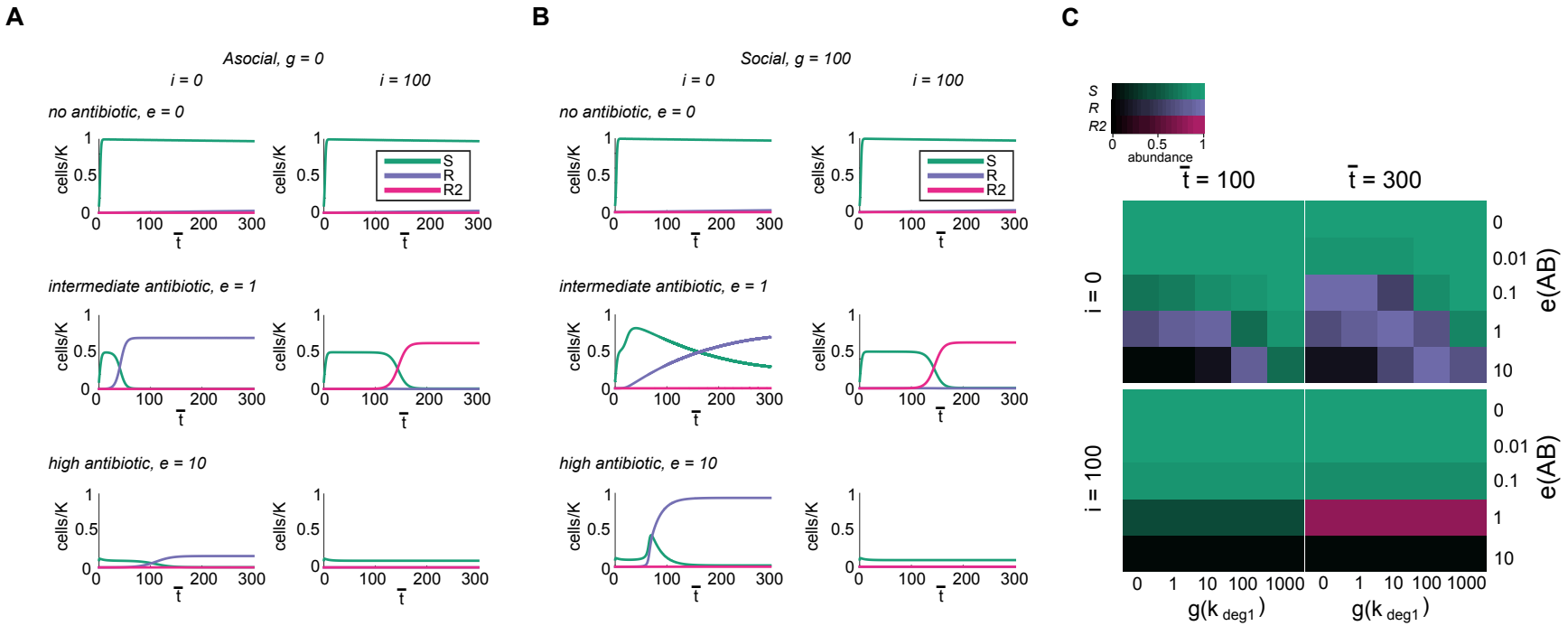


Figure 4.2: The use of an inhibitor can suppress the emergence of resistant strains. Timecourses are shown of the Susceptible strain, S, inoculated at $\bar{S}$=0.1. The first column in **A** shows the asocial case, in which there is no external breakdown of antibiotic by R (g = 0), on no inhibitor ($i = 0$), exposed to increasing concentrations of antibiotic (non-dimensionalised parameter, e). The second column shows the same conditions, with the addition of inhibitor ($i = 100$). In **B**, conditions are the same, with the exception that the resistant strain R is now able to cooperatively degrade antibiotic externally to the cell. **C** summarizes these results. Panels are coloured by the winning strain at the time points $\bar{t} = 100$ and $\bar{t} = 300$. The effects of an increasing dose of antibiotic, e, is shown on the y axis. Across the x axis the level of cooperative external degradation (represented by dimensionless parameter, g) increases.

isolates from Cystic Fibrosis patients, went from 0.4 ng/μl in susceptible strains to 1.4 ng/μl in some resistant strains [127], making this a reasonable estimate. γ_R is the relative susceptibility of the resistant strain, relative to the susceptible strain.

$$\gamma_R = \frac{EC_{50R}}{EC_{50S}} \tag{4.31}$$

As just discussed, so far we have assumed the susceptibility to antibiotic of S and R strains, in the absence of the inhibitor, is the same.

$$\gamma_R = \begin{cases} 1, & \bar{I} > 0.01 \\ 2.5, & \bar{I} \leq 0.01 \end{cases}$$

However, in reality, there is the potential for a resistant strain, to retain higher resistance to the antibiotic than the susceptible strain, even if, in the presence of the inhibitor, it is relatively reduced (Chapter 3). We wished to find out if this would affect the conclusion, that the addition of inhibitor can suppress the emergence of the doubly resistant strain. We therefore studied the case where the resistant strain sensitivity to the antibiotic is decreased by the presence of the inhibitor, but not to the same level as the susceptible strain, as follows.

$$\gamma_R = \begin{cases} 1.5, & \bar{I} > 0.01 \\ 2.5, & \bar{I} \leq 0.01 \end{cases}$$

This would occur, for example, if the majority of a degradation were to be retained, by the resistant cell, in the periplasmic space, with some extracellular leakage, capable of providing a benefit to a nearby susceptible strain. This is often the case in β-lactamase production. This change to the model only affects the treatment regime in the presence of the inhibitor and so we only show these deterministic outcomes in Figure 4.3. At high doses of antibiotic and inhibitor, resistance is suppressed (Figure 4.3A and B, bottom row). This is the same as the previous case. This happens because, at high doses, the doubly resistant strain can only emerge from the susceptible strain and the susceptible strain is strongly repressed. However, at intermediate concentrations of antibiotic, first the singly resistance strain emerges and this is then overtaken, by the doubly resistant strain (Figure 4.3A and B, middle

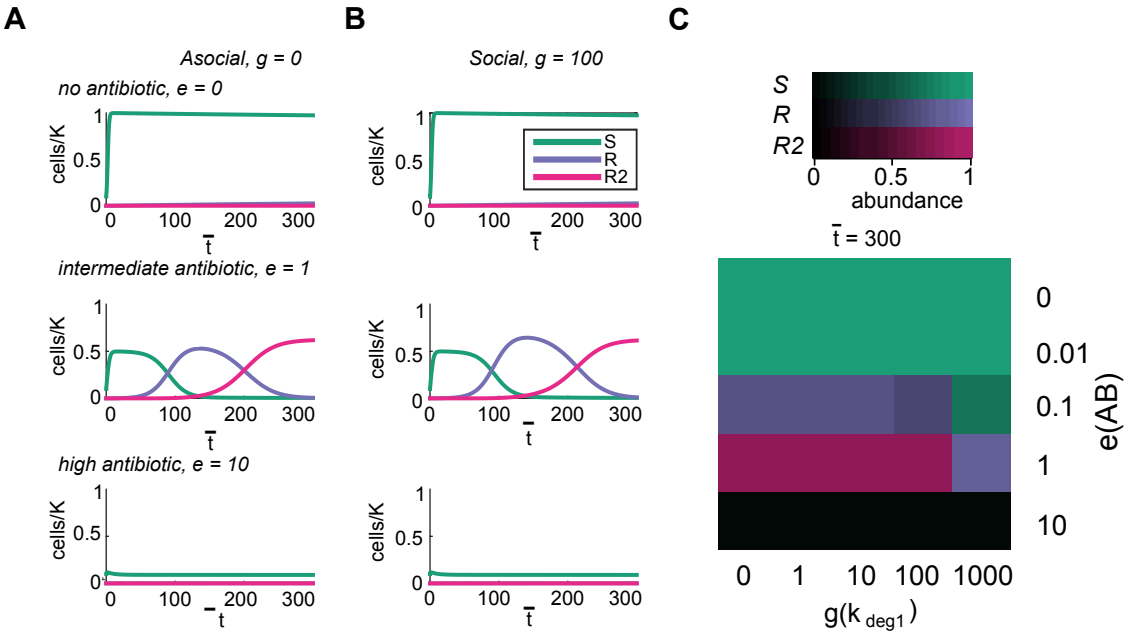


Figure 4.3: Antibiotic alongside inhibitor suppresses the emergence of resistant strains, even when resistant cells maintain a growth advantage. Timecourses are shown of the Susceptible strain, S, inoculated at $\bar{S}$=0.1. The first column in **A** shows the asocial case, in which there is no external breakdown of antibiotic ($g = 0$) by R, in the presence of inhibitor ($i = 100$), exposed to increasing concentrations of antibiotic (non-dimensionalised parameter, e). In **B**, conditions are the same, with the exception that the resistant strain R is now able to cooperatively degrade antibiotic externally to the cell. **C** summarizes these results. Panels are coloured by the winning strain at $\bar{t} = 300$. The effects of an increasing dose of antibiotic, e, is shown on the y axis. Across the x axis the level of cooperative external degradation (represented by dimensionless parameter, g) increases.

row). This causes the doubly resistant strain to take longer to emerge. However, as in the previous case (Figure 4.2A and B, middle row), the doubly resistant strain does eventually emerge. The more the resistant strain breaks down the antibiotic externally (higher k_{deg1}), the longer it takes for the doubly resistant strain to emerge (Figure 4.3C, x axis). In short, we find that the addition of an inhibitor can suppress resistance in both cases, whether EC_{50R} becomes the same as EC_{50S}, or not. Moving forward we focus on the simpler case, in which inhibition is complete and the EC_{50} of both strains becomes the same with the addition of inhibitor.

4.4.4 Stochastic modelling underlines the power of adjuvants to prevent resistance

The deterministic model suggests strategies that will remove a doubly resistant strain before it arises. These function by using both antibiotic and inhibitor in combination, to shut off the route to double resistance, via the singly resistant strain. However, the deterministic model does not capture the stochastic nature of resistance evolution. The emergence of resistance relies on a single rare event - the mutation of a susceptible strain into a resistant one. This rare event can change the course of evolution, depending at what point it emerges. This characteristic, so important in real-life disease progression and treatment outcome, cannot be captured by the deterministic model, in which all species are present from the beginning, albeit at very low levels. To address this limitation, we next implemented our system stochastically, using the Gillespie Stochastic Simulation Algorithm (GSSA) [125] (Figure 4.4). We focus here on the case of cooperative antibiotic resistance but we show in the Appendix (Figures C.2 and C.3) that the same effects occur in the asocial case.

Over the course of 100 simulations of a susceptible strain growing on no antibiotic we see, as expected, that all populations remain largely susceptible (Figure 4.4A) and the evolutionary trajectory of the deterministic model is similar to a representative simulation (Figure 4.4D and G respectively). We then considered what happens with an intermediate dose of antibiotic. After 200 hours, the majority of simulations have a similar outcome to the deterministic model and are largely composed of singly resistant cells (Figure 4.4B, E and H). However, when the susceptible strain grew on the combined antibiotic and inhibitor, for 200 hours, the bacterial density remained much lower than the other treatment regimes and the double resistant strain did not emerge (Figure 4.4C). Importantly, we chose here an antibiotic concentration, at which the deterministic model (Figure 4.4F) predicts that resistant strains will arise, in the face of resistance inhibition. The stochastic model, therefore, only strengthens the conclusion, that adjuvants have the potential to inhibit resistance evolution. The difference to the deterministic model comes about because the earlier

model is forced to always have the doubly resistant strain present at some very low density, available for selection to act upon. However, in the stochastic model, populations are finite, as they are in real infections, and the doubly resistant strain can only occur if it evolves from the singly resistant strain. Under these conditions, the combined therapy never selects for the singly resistant strain and so, even if it briefly emerges, the probability of it gaining double resistance is low. In sum, the stochastic model supports the result of the deterministic model, that combining antibiotic and inhibitor can suppress the emergence of the doubly resistant strain, by cutting off its evolutionary route of emergence.

4.4.5 The later inhibitor is added the more likely double resistance is to emerge

After seeing that the use of an inhibitor alongside an antibiotic could have such strong effects on resistance evolution, we wished to ask; would the timing, at which the inhibitor was given, have further effects?

We saw in the Figure 4.4 that adding inhibitor, with the antibiotic, at the start of treatment, prevents the emergence of resistance and reduces the overall disease burden, experienced over the course of the infection. This is because, by selecting against the intermediate step, in the evolution of double resistance, its emergence may be suppressed. This implies that the timing at which an inhibitor is given may have an effect on selection for resistance and, ultimately, treatment success or failure. In Figure 4.5 the inhibitor has been added at different time points, calculated based on when R outcompetes the S strain in the deterministic model at an intermediate dose of the antibiotic alone (Figure 4.2). First we add the inhibitor at $t = 20$ hours, before resistance would have overtaken the susceptible strain (Figure 4.5A). The outcome, after 200 hours, is the same, as if the inhibitor had been added at the same time as the antibiotic (Figure 4.4C). However, after this time point, the later the inhibitor is added, the more often the doubly resistant strain, $R2$ emerges and takes over (Figure 4.5B-D). This is because the antibiotic alone selects for the singly resistant strain, R, creating a pool of cells from which

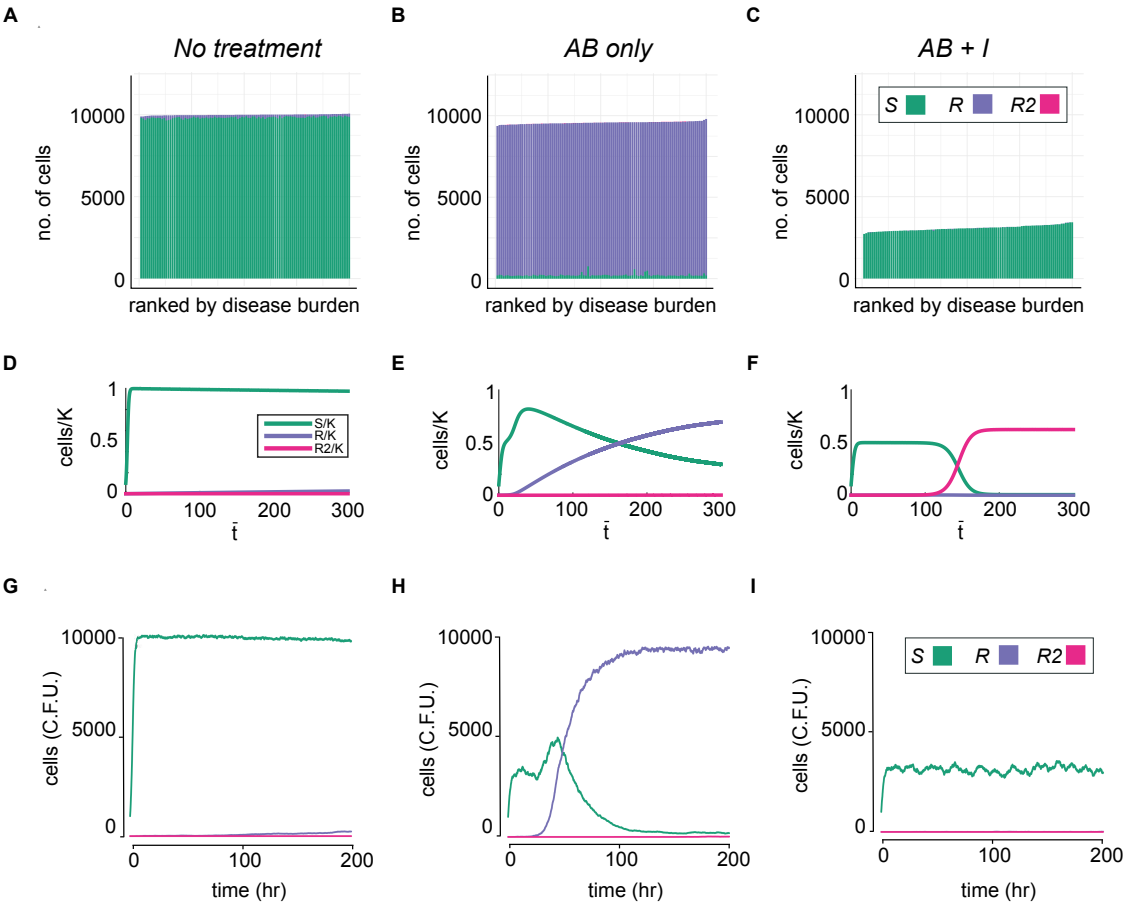


Figure 4.4: Stochastic modelling reveals inhibitors suppress the emergence of resistance, even at intermediate doses of antibiotic. The growth of a starting population of 1000 susceptible cells was modelled stochastically, using the GSSA, growing without treatment (**A**), on antibiotic ($\alpha_{in} = 50$, $\alpha_{out} = 0.45$) (**B**) and on antibiotic combined with inhibitor ($\alpha_{in} = 50$, $\alpha_{out} = 0.45$, $\rho_{in} = 15000$, $\rho_{out} = 0.1$) (**C**). These graphs show the result after 200 hours, of 100 simulations, ranked by disease burden. This means they are ordered by the number of bacteria contributing to the infection at the final time point. The same conditions were simulated deterministically (**D, E, F**). Representative individual time courses are also shown (**G, H, I**).

double resistance can be selected, as we can see at $t = 50$ hours (Figure 4.5B-D). We can also see, from the sample stochastic time courses (Figure 4.5K and L), that when the resistant strain emerges before inhibitor is added, this provides a pool of resistant cells capable of acquiring double resistant mutations.

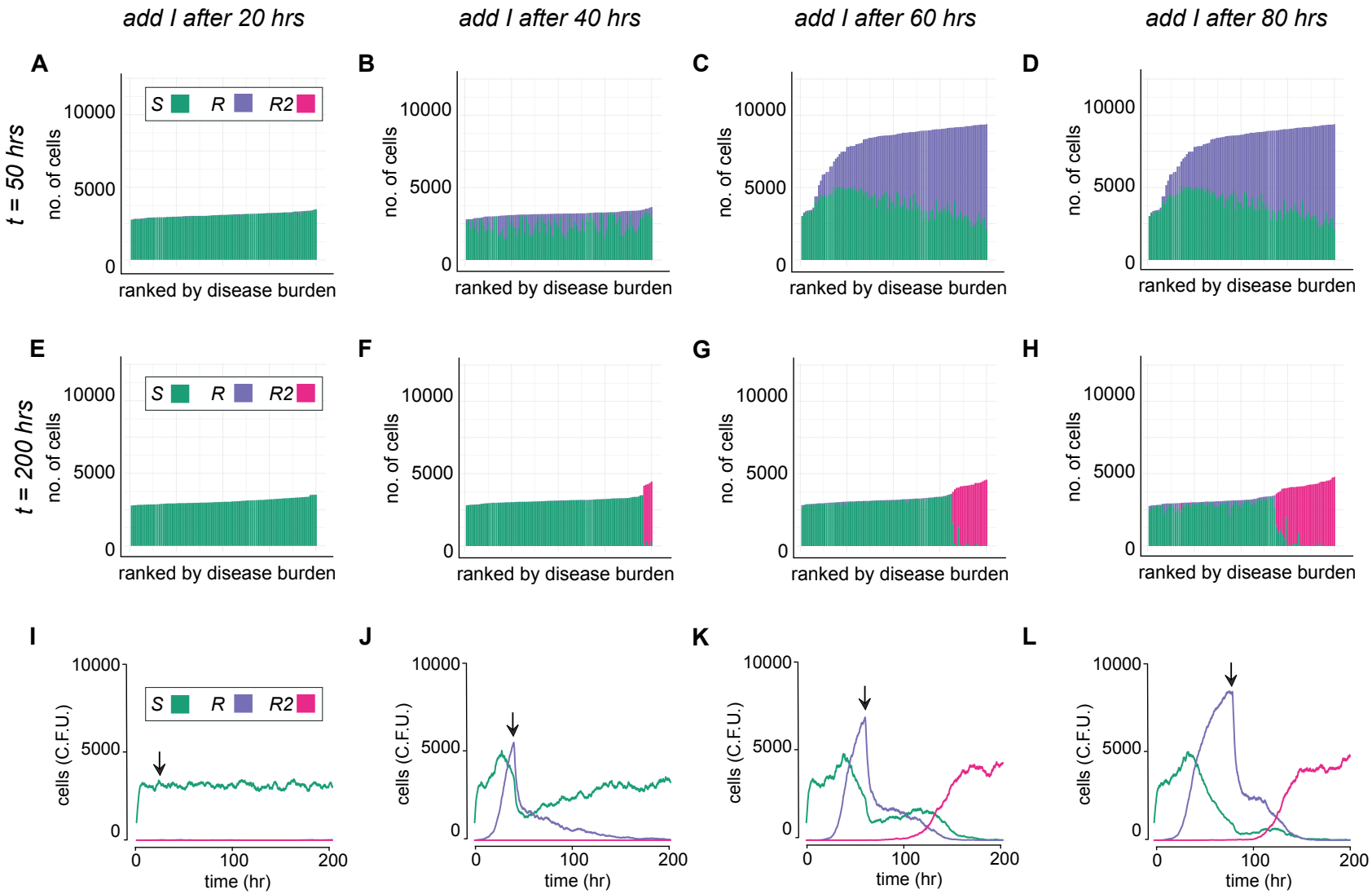


Figure 4.5: The later inhibitor is added the more likely double resistance is to emerge. 1000 cells of the susceptible strain were inoculated on antibiotic and inhibitor was added after 20 hours (**A**), 40 hours (**B**), 60 hours (**C**) or 80 hours (**D**). Moving down the panels, the outcome of 100 simulations, ranked by disease burden, is shown after 50 hours, and 200 hours. Below this, sample stochastic simulation time courses are shown for each condition (**I-L**), an arrow indicates the time at which inhibitor was added.

4.5 Discussion

Antibiotic resistance has become an increasingly worrisome concern for global health security with the shrinking arsenal of effective antibiotics at a doctor's disposal [96]. Inhibitory adjuvants have been a fruitful avenue of research, with clinical success [99]. Here, we show that inhibitors can be used, not only to combat resistance once it has emerged, by suppressing antibiotic resistant strains, as inhibitors were intended [98], but to delay the evolution of resistance to combined antibiotic-inhibitor therapies. We see that inhibitors can be used to block the evolutionary pathway to double resistance and, therefore, can be considered as a form of evolutionary prophylaxis. This occurs because inhibiting the resistance mechanism of the singly resistant strain removes the benefits of resistance, but leaves the fitness cost. Hence, the combined antibiotic and inhibitor can select against a singly resistant mutant. As this mutant is at an intermediate stage on the route to double resistance, preventing its emergence also suppresses evolution of the doubly resistant strain. We can infer that a further benefit of this treatment regime will be to reduce the transmission of resistant infection, by lowering the total bacterial load and removing the resistant fraction (Figure 4.4). This makes the use of inhibitors a strategy that could also be beneficial from a public health perspective.

Our results caution against the logic of using adjuvants only once an infection has been found to contain strains resistant to an antibiotic [128]. If the evolutionary pathway to inhibitor resistance is via resistance to the antibiotic alone, this is likely to select for double resistance. Once such doubly resistant mutants are created they may be transmitted in the community. We recognise that, in reality the trade-off often grappled with by clinicians is that resistance to an antibiotic-inhibitor combination can only emerge if that combination is used. Our results agree with this policy to save the most effective antibiotics as weapons of last resort to prevent resistance emerging - in our model double resistance never emerges if the inhibitor is never used. However, in cases where resistance to the antibiotics is high there may be a window of time in which use of an inhibitor actually slows down the emergence of double resistance. On the other hand, we and others have seen scenarios where

low doses of antibiotic, in combination with inhibitor, can select for the singly resistant strain, in the short term. Our model also recapitulates this when the susceptibility of the resistant strain is only partially lowered by the presence of the inhibitor (Figure 4.3A and B, middle row). Further complications may also arise if different concentrations of the inhibitor are used or in cases where the inhibitor is cleared from the host at a different rate to the antibiotic.

This model provides further evidence for the clinical paradigm of hitting hard and early with antibiotics [129]. It is most effective to use a high dose in order to reduce the microbial population before is has the chance to evolve resistance (Figure 4.2A, bottom left). This has been seen in *in vivo* experiments, in which, the early treatment of *E. coli* infected mice has been shown to reduce mortality compared to treatment regimes which start later [130].

Our results also suggest the treatment course should be as short as possible, to limit the time for which pathogens are under selection for resistance. For example, if antibiotic treatment had been discontinued after 80 hours, on the highest dose of antibiotic, in Figure 4.2A (bottom left), treatment could have been discontinued, once the susceptible strain was repressed, but the R strain had not yet emerged. This is in line with a recent review by Llewelyn *et al.* [131], who suggest the antibiotic course has 'had its day' and patients should stop taking antibiotics when they feel better to prevent selection for resistance.

This model explores the system outlined in Figure 4.1, in which, susceptible cells must go through an intermediate stage of being singly resistant to the antibiotic and susceptible to the inhibitor in order to become resistant. A common example of this would be to acquire resistance, from the environment, through HGT, and then for resistant cells to undergo *de novo* mutation, to become doubly resistant. This has been seen, in the specific case of resistance to β-lactams and β-lactamase inhibitors, for which β-lactamase enzymes are almost exclusively acquired through HGT [60]. Next, *de novo* point mutations can occur, in the active site of the β-lactamase gene, such that the inhibitor is no longer able to bind [99]. If such doubly resistant strains become prevalent in the population, they too may be

transferred horizontally, such that susceptible strains could become doubly resistant directly. Under these conditions, both inhibitor and antibiotic would have lost their effectiveness and so we have focused here on modeling the earlier stages of evolution and how this worst-case scenario can be avoided.

Our modelling underlines the potential complexities associated with the use of antibiotic adjuvants, that can arise from a combination of drug and strain interactions. Evolutionary modelling is a powerful way to break down this complexity and evaluate the possible effects of applying drugs and drug combinations on resistance evolution. Our work suggests that adjuvants, if correctly used, are a powerful way, not only to treat infection, but also to suppress resistance evolution.

4.6 Acknowledgements

Thanks to Jessica Hedge for help with Linux and using the computer server. Further thanks are due to William P. J. Smith for comments on the maths and Daniel Unterweger for proofreading this chapter.

[Mesdames et] 'Messieurs, c'est les microbes qui auront le dernier mot.'

[Ladies and] 'Gentlemen, it is the microbes who will have the last word.'

— Louis Pasteur (1822-1895)

5 Conclusion

Antimicrobial resistance is increasingly being recognised as one of the key challenges confronting twenty first century medicine [96]. To maintain the effectiveness of the antibacterial drugs we currently have, and those we have yet to discover, it will be vital to understand the evolutionary forces driving selection for antibiotic resistance. Bacteria are commonly studied as free-swimmers in planktonic culture, where interactions between neighbouring cells can be rare and fleeting. However, in reality, bacteria commonly grow in surface-associated communities, where the effect one cell exerts on its neighbour may have profound consequences for their relative fitness and ultimately their evolutionary survival or demise. The aim of this thesis has been to explore the consequences of growth, in these kinds of spatially-structured environments, for the evolution of antibiotic resistance.

During biofilm growth, bacteria are densely packed and the products secreted by one microbe can have a direct impact on the fitness of their neighbours. I have shown that growth in such environments allows significant cross-protection, for a resistant mechanism that does not show cross-protection in liquid culture. Specifically, I found that in colonies, susceptible strains benefit from the local detoxification of carbenicillin, without paying the cost of carrying a resistant plasmid, and thereby they can outcompete resistant strains. The same cross protection was not seen for

the aminoglycoside, streptomycin, which is inactivated internally. I also considered the effect of physically mixing strains as they grow by daily disruption of the colony with an innoculation loop. This simple spatial disruption increased cross-protection by putting susceptible cells next to resistant ones and amplified the conditions under which resistant strains were outcompeted.

In the words of Feynman, 'it is very easy to answer many of these fundamental biological questions; you just look at the thing!' Perhaps nowhere is this more true than in microbiology and the study of cell-cell interactions. In Chapter 2, I used confocal microscopy to reveal a further effect of living in closely packed, dense communities of cells. Susceptible cells, under stress from β-lactam antibiotic, elongate, forming filaments. This shape effect can have a strong impact on their relative fitness. Filamentous susceptible cells are able to overtake resistant cells and cut them off from gaining an optimal position at the colony edge, where they have preferential access to space and nutrients. This effect was confirmed by simulations of cells with differing lengths, using individual based modelling. Filamentation of the susceptible cell in response to antibiotic has been traditionally thought of as a phenotype of stress and sickness [132] - a result of the combined assault of antibiotic on the cell wall synthesis machinery and the initiation of the SOS response. However, here we see this stress-associated phenotype increase the fitness of the susceptible strain, with the result that, counter-intuitively, low doses of antibiotic select for the susceptible strain to a greater extent than no antibiotic at all.

My work, therefore, shows that the rise of strains resistant to β-lactam antibiotics is far from guaranteed. It is interesting then to note that β-lactam antibiotics are ancient and widely used in nature [133], despite the fact that β-lactamase enzymes are one of the most commonly found resistance mechanisms on the planet [134]. Perhaps β-lactam antibiotics have continued to be beneficial to producers for so long because they encourage cooperative resistance mechanisms, that are themselves evolutionarily fragile. These antibiotics attack the cell wall and therefore must be neutralised before they reach it. In many cases this forces bacteria to evolve resistance mechanisms to protect themselves from outside the cell, mechanisms

that can be exploited by susceptible bacteria. Under certain conditions susceptible strains will outcompete resistant strains and thereby the potency of antimicrobials, which attack the cell wall, may be maintained.

In his Nobel acceptance speech, Alexander Fleming warned 'if you use penicillin use enough,' fearing low doses of antibiotic would promote the *de novo* emergence of resistance. The clinical norm is to use the highest dose of antibiotic achievable without toxicity, however my work suggests that, for cooperative mechanisms, it may be wiser to use lower doses, which allow susceptible cells to remain in the bacterial population via cross-protection. Indeed, it has been suggested an intermediate dose may reduce the total burden of infection whilst maintaining competition between susceptible and resistant strains, giving the immune system the opportunity to clear the infection [91]. In the treatment of some cancers, an intermediate dosing strategy has been shown to slow down the rate at which resistance evolves and thereby prolong the effective life of a drug, by maintaining competition between susceptible and resistant cancer lines within a tumour [135].

As antibiotics increasingly fail to treat a mounting number of infections, researchers have turned to adjuvant drugs, which can be given alongside an antibiotic. Adjuvants increase the antibiotic efficacy without having an antibacterial effect in their own right, for example, by inhibiting common mechanisms of resistance. However, my experimental work cautions that the effects on resistance evolution may not always be beneficial (Chapter 3). Adjuvants can increase selection for resistance in dense communities of cells. Conversely, during growth in liquid culture, an inhibitor removed the advantage of resistant strains, under a comparable level of antibiotic-induced stress. Such experiments show the effect of inhibitors on resistance evolution is complex.

The literature is lacking theory to understand the evolutionary and ecological consequences of inhibiting different mechanisms of resistance. The biochemistry of such systems, however, is well understood. This allowed us to create a model which united existing evolutionary theory with the biochemical mechanism of inhibition, to unpick the role of interacting cellular and chemical processes. Our

findings support using a high dose of antibiotic and adjuvant as early as possible to prevent the emergence of resistance. We find there are conditions under which inhibitors select for single resistance to the antibiotic to a greater extent than the antibiotic alone. In particular, when cooperative resistant strains retain a greater relative resistance to the antibiotic in the presence of the inhibitor than susceptible strains. However, our results also suggest that the use of an antibiotic alongside an inhibitor can suppress the emergence of the doubly resistant strain. Inhibitors can act, therefore, as a form of evolutionary prophylaxis, by creating conditions under which the singly resistant strain is never favoured and thereby cutting off the evolutionary route to combined antibiotic-inhibitor resistance. This supports the conclusion that inhibitors can suppress resistance not only in a biochemical sense [97] but also in an evolutionary sense.

The dilemma, often faced by doctors prescribing antibiotics, is to hold back selected, effective antibiotics as weapons, of last resort. In the simplest sense, my model is in agreement with this - if inhibitor-antibiotic combinations are never used, resistance to them does not emerge. However, as resistance to antibiotic mono-therapies becomes more common, dosing early with an antibiotic-inhibitor combination may suppress resistance evolution. This regimen maintains a lower bacterial load, composed of a greater fraction of susceptible cells. This is also likely to be a benefit from a public health perspective, by reducing the transmission of resistant bacteria. Lower transmission of resistance will lead to infections which are treatable. Treatable infections which are well managed will lead to fewer transmissions. This creates a beneficial cycle of reduced antibiotic usage, due to fewer infections, and thereby reduced selection for resistance.

My results suggest caution using inhibitors after antibiotic mono-therapy has selected for resistance. While it may improve treatment outcome, it will strongly select for resistance to the combined antibiotic inhibitor therapy, by forcing susceptible cells down the evolutionary pathway to combined resistance. These results suggest either hitting hard and early with antibiotic-inhibitor combinations or using a different class of antibiotic, if the original class of antibiotic has failed to treat the

infection. Ceasing antibiotic treatment early, when resistance has emerged and is no longer effective, will reduce the time window in which resistance is selected, ensure patients are treated effectively and reduce the transmission of resistant infections. This is in agreement with recent clinical advice [131], although it remains to be seen how effectively patients can make use of this advice in practice.

Further Work

At the turn of the twentieth century Ehrlich spoke of the prospect of 'magic bullet' therapies - a brief course of treatment capable of providing a cure. Cancer treatment and antimicrobial therapies have both had successful 'magic bullet' treatments. Such treatments have fundamentally changed the nature of modern medicine and the expectations of patients. The next great hurdle is that such specifically targeted therapies, the essence of what makes them so effective, is also their achilles heel, as by so effectively killing their target cells they exert a strong selection pressure for the resistance that ultimately renders them ineffective. The evolution of resistance, in response to the high selection pressure imposed on bacteria, by the mounting use of antibiotics, is inevitable. However, there is some hope that it might be directed and controlled to maintain the efficacy of these essential treatments and to direct research into 'evolution-proof' treatment strategies [136]. More work is needed in this growing field [60], despite extensive theoretical work on the use of antibiotics and the evolution of resistance in the literature, we have advanced little in terms of being able to advise a doctor, confronted with an infected patient, on the best course of antibiotics to use [137]. Studies following the outcome for patients on different treatment courses of antibiotics are needed, in addition to experimental work, both *in vivo* and *in vitro*, to unpick the key mechanisms at play.

Evolutionary biology is currently being applied to the problem of drug resistance in a number of ways. It has been widely recognised in the case of malaria, TB, HIV and leprosy that combinatorial therapies are more effective and delay the emergence of resistance [91]. Similar ideas are beginning to take hold elsewhere too, [138] mention investigate synergistic and antagonistic drug interactions in combination

therapy. In addition, anti-virulence strategies, such as the Trojan Horse are being investigated [139]. Such investigations show that evolutionary biology can be both a powerful force for the emergence of novel threats from disease and an insightful tool for the study and treatment of infection. More research in this area is set to enhance our ability to understand and predict what is likely to occur in terms of treatment outcome and resistance evolution.

5.1 Concluding Remarks

My thesis has shown that social evolution can provide insights into how competing bacteria behave as they are exposed to selection pressure from antibiotics. We have seen that not all antibiotics are created equal in terms of selection for resistance and this can be explained in part by the fitness effect exerted by a cell on its neighbour. As resistant infections become more common, our knowledge of how microbes cooperate and compete will be fundamental to understanding and overcoming resistance.

Appendices

A

Appendix to Chapter 2: Cooperation, Competition and Antibiotic Resistance in Bacterial Colonies

A.1 Supplementary Materials and Methods

Bacterial strains

We transformed YFP and DsRed labelled [140] strains of *P. aeruginosa* strain PA01 with plasmid Rms149 [74] by electroporation [141] using a Gene Pulser apparatus (Bio-Rad). Transformants were selected on Luria-Bertani (LB) (Fisher Scientific, NJ, USA) agar plates containing 200 µg/ml streptomycin. Plasmid transformation was confirmed by PCR (see Supplementary Experimental Procedures) using GoTaq green Mastermix (Promega, Madison, WI, USA) and by plasmid extraction using QIAprep Spin Miniprep (Qiagen, Inc., Chatworth, California, USA). Minimum inhibitory concentration (MIC) assays were performed in triplicate by agar dilution [100] (Table S1).

Liquid competitions

To test for cross-protection we investigated whether susceptible plasmid-free strains had a higher survival rate in the presence of resistant plasmid-bearing strains than

alone. Strains were competed in increasing concentrations of antibiotic. Pre-cultures of the strains were incubated at 37 °C with 250 RPM shaking overnight in 3 ml of LB broth (Fisher Scientific, NJ, USA). Pre-cultures were diluted in 3 ml of fresh LB broth to an OD_{600} of 0.05 and incubated at the same conditions for 2 hours. Cultures of the strains were then mixed at a ratio of 1:1 in phosphate buffered saline (PBS) with an OD_{600} of 0.3. This was diluted 10-fold in PBS and 1 µl was added per well in a 96 well plate, in triplicate. Wells contained a final total volume of 200 µl LB broth with the following antibiotic concentrations: streptomycin; 1, 2, 4, 8 µg/ml and carbenicillin; 3, 6, 12, 24 µg/ml, which were chosen as sub-MIC values, and a no-antibiotic control for every competition. Competitions were run for 12 hours overnight at the ambient temperature of the lab (20 °C) at 250 RPM. Competitions were diluted 10^5-fold and 50 µl of each was added to a plate using glass beads to count colony forming units (C.F.U.), using fluorescence to differentiate cells labelled with YFP. The number of cells in the inoculum was also measured in the same way.

Liquid competitions were also performed over 16 hours and set up in the same way without antibiotic. In order to most accurately measure the cost of the plasmid, cells from these competitions were counted using flow cytometry [142].

Competitions on agar

To investigate the conditions required for protection of the susceptible strain by a β-lactamase producing strain we performed the same competitions on solid agar plates. These were set up in the same way as liquid competitions. The resulting 1:1 mixtures were diluted by a tenth in PBS. 1 µl of this mixture was added per agar plate in a single central drop. Plates contained 25 ml 1 x LB Miller agar (40 g/l; 15 g/l of which is agar) and the following antibiotic concentrations: streptomycin; 2, 4, 8 µg/ml and carbenicillin; 6, 12, 24 µg/ml which were chosen as sub-MIC values in addition to a no antibiotic control for every competition. Initial ratios were calculated by plating 50 µl of a 10^{-6} dilution of the inocula on LB agar plates. These were incubated overnight at 37 °C so C.F.U. could be counted. Competition plates were left at 20 °C and imaged on a stereoscope daily for 6 days. On day 7 the colonies

were scraped from the agar and suspended in 1 ml PBS, diluted 10^6 and 10^5-fold and plated out to count C.F.U, using fluorescence to differentiate cells labelled with YFP.

The fitness was determined using the following formula [101]:

$$\text{susceptible fitness} = \frac{ln\left(\frac{N_{\text{suceptible,final}}}{N_{\text{susceptible,initial}}}\right)}{ln\left(\frac{N_{\text{resistant,final}}}{N_{\text{resistant,initial}}}\right)} \tag{A.1}$$

Where $N_{\text{suceptible,initial}}$ and $N_{\text{suceptible,final}}$ are the numbers of susceptible cells before and after the competition and $N_{\text{resistant,initial}}$ and $N_{\text{resistant,final}}$ are the numbers of resistant cells before and after the competition.

Manipulating spatial structure with inoculum density

We wished to determine the role of increasing spatial structure in colonies on susceptible fitness. To do this, structuring was created in the colony by varying the number of cells in the initial inoculum [84]. The strains were set up as described above and then this 1:1 mixture was diluted 10-fold, 100-fold, and 1000-fold in PBS. Each of these dilutions was used to inoculate colonies by adding 1 μl to plates containing either no antibiotic or 12 μg/ml carbenicillin. A 10^5-fold dilution of the initial mixture was plated out so initial ratios could be calculated from C.F.U. Plates were left at 20 °C and imaged on an Axio Zoom. V16 microscope (Zeiss) daily for 6 days. Half of the plates were mixed daily after imaging, using an inoculation loop [69]. On the seventh day the colonies were scraped and suspended in 1 ml PBS, diluted 10^6-fold and 50 μl was plated out with glass beads to count C.F.U.

Microscopy

The Axio Zoom.V16 microscope (Zeiss) under the PlanApo Z 0.5X objective and the associated Zen Blue software was used to carry out fluorescence microscopy imaging. These colonies were imaged while still growing on the agar plate and these images were taken at 3.5X. For confocal imaging colonies were cut out of the agar plate and placed on a slide. Confocal laser scanning microscopy (CLSM) imaging was carried out with the LSM 700 laser scanning microscope (Zeiss) under the 50X objective using Zen Black software.

Aspect Ratio Experiments

We suspected cell length was driving the increase in fitness on carbenicillin. To investigate this further, susceptible and resistant cells were competed on no antibiotic and on 12 μg/ml carbenicillin, this being the concentration at which we had previously seen a cross-protective effect. Colonies were set up as previously described, as competitions on agar plates, and imaged destructively, at 40X using confocal microscopy, in triplicate, on days 0, 1, 2, 3 and 4. 1 μl of PBS was added to the edge of the colony to disperse cells so they could be counted by analysis of the image with open source FIJI software [143]. The aspect ratio was assessed using the cell counting function.

Time-lapse microscopy

Colonies were inoculated in the same way as solid competitions. Cultures were allowed to grow for 10 hours at 20 °C. Then the colony and surrounding agar were cut out of the plate and mounted on a glass-bottomed petri dish for fluorescence imaging, using a 64X objective under oil emersion.

Statistical Analysis

Statistical analyses were carried out in R [102]. An ANOVA was used unless otherwise stated; please see the Supplementary Experimental Procedures for further details. Error bars show standard error. Solid and liquid competition experiments were performed using all colour combinations to allow for different costs associated with the colour markers. For these experiments (Figures 2.1 and 2.2) the mean and standard error of two experiments, each with n = 6 for co-cultures and n = 3 for monocultures, are shown. The differences between colour markers were not significant in the solid competition experiments, hence later experiments were performed using just one colour combination and show the mean and standard deviation of two experiments with n = 3 (Figure 2.4).

Individual-based modelling of cell interactions at the colony edge

We ran colony growth simulations to help understand the role of cell shape in the enrichment of antibiotic-susceptible (S) cells at the colony edge during growth in the presence of the resistant strain (R), on carbenicillin. We used an individual-based computer model, based on the open source software, CellModeller 4 [144, 145], which is described in more detail later in this Appendix (Figure A.6).

In our model, sections of the colony edge are represented using collections of bacterial cells (Figures 2.6 and A.6). Each cell is a rigid, capsule (spherocylinder) with unique index i, fixed radius r, variable segment length l_i, position $p_i = (p_x, p_y, p_z)_i^\top$ and orientation $\hat{a_i} = (a_x, a_y, a_z)_i^\top$. Capsules increase in volume V_i exponentially by elongating along their principal axes, dividing lengthways into two identical daughter cells once they double in volume. The range of aspect ratios $AR = 1 + l/2r$ adopted during the cell cycle is controlled by changing the cell birth volume V_0. *R*- and *S*-type capsules are set to have mean aspect ratios of 3.3 and 6.1 respectively; these parameters are drawn directly from the cell aspect ratio measurements described in this study (Figure 2.5A).

To represent resource competition, each cell's intrinsic growth rate is determined by the local concentration u of two non-interacting solutes, Oxygen (O) and another nutrient (N), e.g. a limiting carbon source. A cell's volume V_i increases in time t according to the equation

$$\frac{dV_i}{dt} = \mu_{max}\left(\frac{u_O(p_i)}{u_O(p_i)+K_O}\right)\left(\frac{u_N(p_i)}{u_N(p_i)+K_N}\right)V_i \tag{A.2}$$

, where K_O and K_N are saturation constants for Oxygen and nutrient uptake respectively, and μ_{max} represents the maximum solute uptake rate. All cells share the same μ_{max}, irrespective of their morphology. $u_O\ (p_i)$ and $u_N\ (p_i)$ correspond to local Oxygen and nutrient concentrations, evaluated at the cell's centroid p_i; the fields u_O and u_N are approximated using the reaction-diffusion equations

$$D_O\nabla^2 u_O = \rho\gamma_O\mu_{max}\left(\frac{u_O}{(u_O+K_O)}\right)\left(\frac{u_N}{u_N+K_N}\right)\psi(p_1 \ldots p_n), \tag{A.3}$$

$$D_N \nabla^2 u_N = \rho \gamma_N \mu_{max} \left(\frac{u_O}{u_O + K_O} \right) \left(\frac{u_N}{u_N + K_N} \right) \psi(p_1 \dots p_n), \tag{A.4}$$

where D_O, D_N and γ_O, γ_N represent solute diffusivities and substrate biomass yields for the two solutes respectively, and ρ corresponds to the cell biomass density. The scalar field $\psi(p_1 \dots p_n)$, describes the spatial variation in cell volume fraction, computed from the cell configuration $p_1 \dots p_n$. Each simulation timestep, solute fields are computed by solving this equation in non-dimensional form using the FEniCS finite element library. Oxygen and nutrient diffuse into the domain from above and below respectively (Figure S6). Following the cell growth phase, cell configurations are returned to mechanical equilibrium using an energy minimisation algorithm [144]. For simplicity, active cell motility is not included, such that only growth and cell-cell collisions cause cell movement. Mechanical boundaries at the sides and base of the domain are imposed to represent repulsive forces from the cells around and behind the edge section, and from the agar surface below it.

We used our model to grow 100 μm sections of the colony edge from 1:1 mixtures of R and S cells. Simulations were initiated by randomly placing 20 cells of each type in the area defined by $0<x\leq5$ μm, $0<x\leq100$ μm, representing the leading edge of the colony as it enters the simulation domain. Cells were then allowed to grow and divide so that the colony edge propagated in the radial (x) direction, reaching an average colony volume of 1.043 x 103 μm^3 (approximately 6,500 cells) after 56h. A summary of the variables and coefficients used in our model is available later in the Supplementary Experimental Procedures.

Individual-based modelling of growth in colony and planktonic environments

We used a modified version of our individual-based modelling framework to explore the effect of growing in colony and planktonic environments on fitness. Here, as with previous models [17, 146], cells are all approximately spherical instead of rod-shaped, and cellular growth is controlled by a single limiting solute. Vertical 2D colony slices were grown from 1:1 mixtures of labelled capsule cells (denoted A and B), placed randomly on the base of a 300 μm-wide box. Cells of type A

were programmed to grow exponentially at rate μ_A, whereas cells of type B grew faster at rate $\mu_B > \mu_A$, representing intrinsic differences in cell growth rate. Both cell types were given the same shape, with a birth aspect ratio of 1.1. To simplify the description of cell-solute interactions, we omitted the nutrient field from the model (corresponding to the limit $u_N >> K_N$), so that cell growth was made dependent on the concentration of oxygen only:

$$\frac{dV_X}{dt} = \mu_X \left(\frac{u_O}{u_O + K_O} \right) V_X, \qquad X = A, B, \tag{A.5}$$

$$D_u \nabla^2 u_O = \rho\gamma \left(\frac{u_O}{u_O + K_O} \right) [\mu_A \phi_A + \mu_B \phi_B], \tag{A.6}$$

where $\phi_A \phi_B$ represent the local volume fractions of type A and B cells respectively; other model variables have the same meanings and values as before. We carried out simulations using values of μ_A equal to 95 or 90% of μ_B, equal to μ_O as before. In each case, the colony was fed with either a plentiful ($u_{(O,0)}$= 500x10^{-3} kgm^{-3}) or a poor Oxygen supply ($u_{(O,0)}$= 5x10^{-3} kgm^{-3}), representing the perfusion conditions present in liquid or solid cultures respectively. In each case, simulations were terminated once the total cell population reached a maximum value of approximately 7.5 x 10^3 cells. In Figure S4B, we quantify this effect using boxplots of the relative cell fitness

$$\frac{\omega_B}{\omega_A} = \frac{log\left(\frac{N_{B,\text{final}}}{N_{B,\text{initial}}}\right)}{log\left(\frac{N_{A,\text{final}}}{N_{A,\text{initial}}}\right)} \tag{A.7}$$

for each case, where $N_{(X,\text{initial})}$ and $N_{(X,\text{final})}$ correspond to the initial and final populations of each cell type $X = A, B$.

A.2 Supplementary Figures

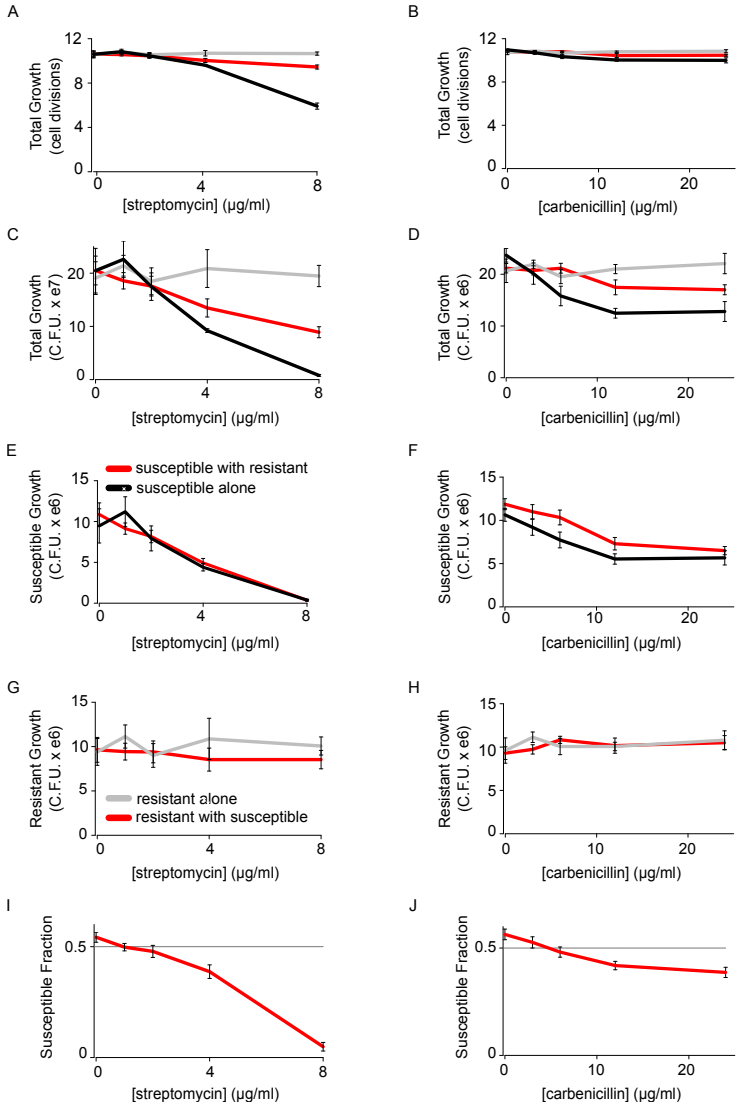


Figure A.1: Cell count data from the liquid culture experiment to supplement Figure 2.1, where we present these data in terms of cell divisions and fitness. Susceptible and resistant strains were competed in liquid culture overnight, with either carbenicillin (extracellular resistance) or streptomycin (intracellular resistance). At all concentrations tested, there is never an increase in selection for the susceptible strain, in the presence of the antibiotic. Final susceptible, resistant and total cell counts and total growth rates are shown for streptomycin (A, C, E, G) and carbenicillin (B, D, F, H). The final susceptible fraction has also been calculated in streptomycin (I) and carbenicillin (J). The mean and standard error of two experiments, each with n = 6 for co-cultures and n = 3 for monocultures, are shown.

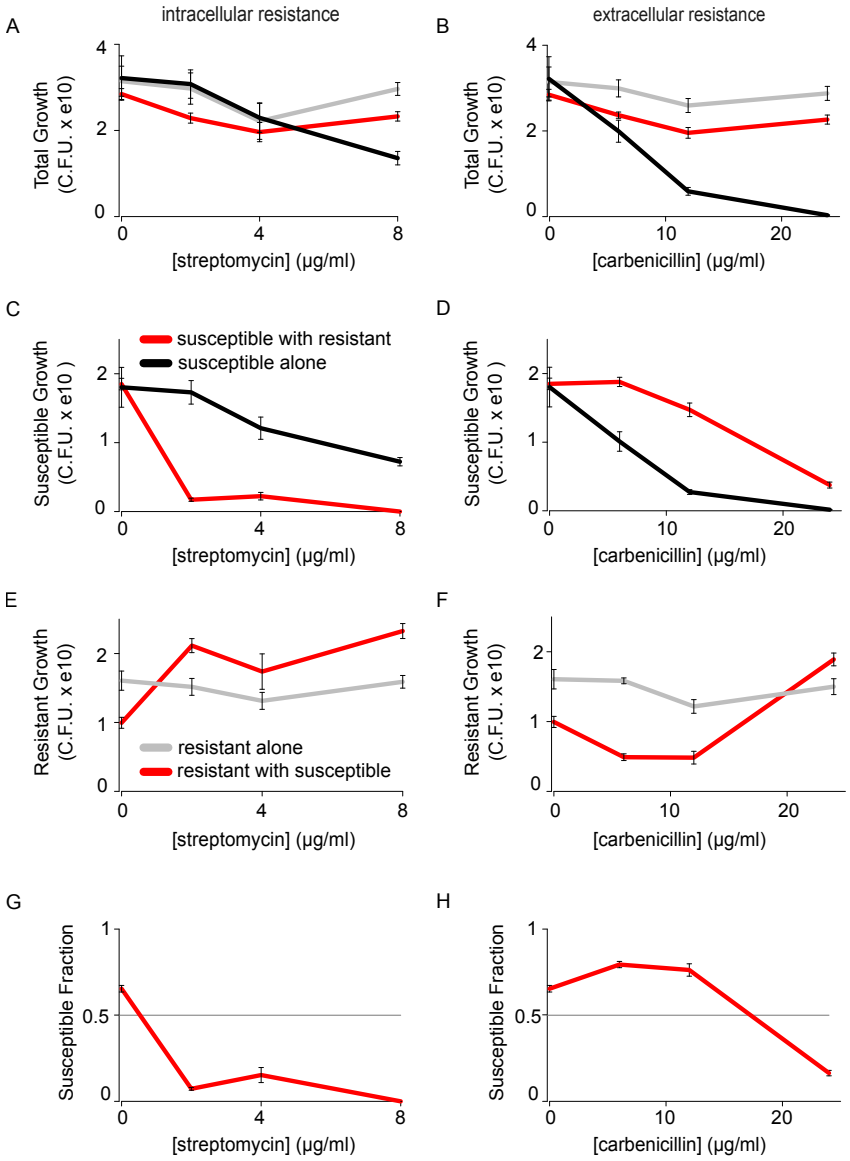


Figure A.2: Cell count data from growth on agar experiment to supplement Figure 2.2, where we present these data in terms of cell divisions and fitness. During growth on agar, in the presence of streptomycin (intracellular resistance) there is always selection for the resistant strain (A, C, E, G). However, when the resistance mechanism is extracellular, as is the case for carbenicillin, there is selection for the susceptible strain (B, D, F, H). The mean and standard error of two experiments, each with n = 6 for co-cultures and n = 3 for monocultures, are shown.

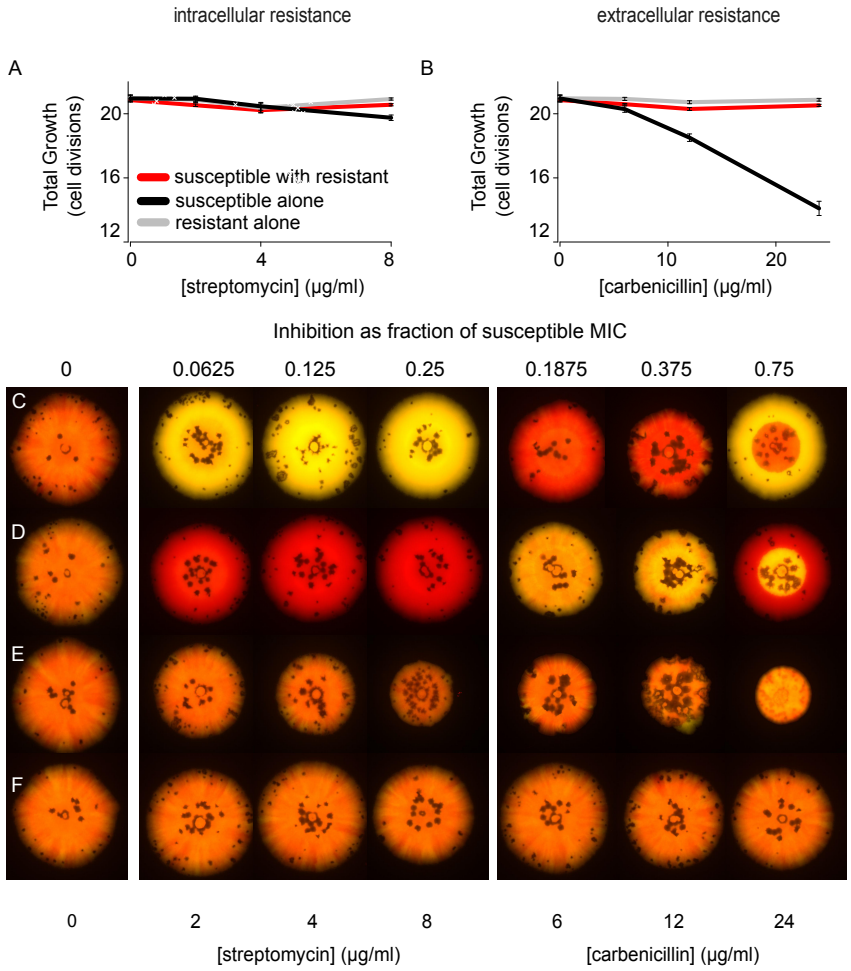


Figure A.3: Total growth rate and accompanying colony images of competitions on agar to supplement Figure 2.2, where we present these data in terms of susceptible and resistant growth and show only the colony images for competitions between susceptible and resistant strains. During growth on agar in the presence of streptomycin (intracellular resistance) there is always selection for the resistant strain. However, when the resistance mechanism is extracellular, as is the case for carbenicillin, there is selection for the susceptible strain at intermediate concentrations. Total growth rates are shown on streptomycin (A) and carbenicillin (B). Images of the following competitions after 6 days of growth are shown: yellow resistant and red susceptible (C), yellow susceptible and red resistant (D), both colour susceptible (E) and both colours resistant (F). The mean and standard error of two experiments, each with n = 6 for co-cultures and n = 3 for monocultures, are shown.

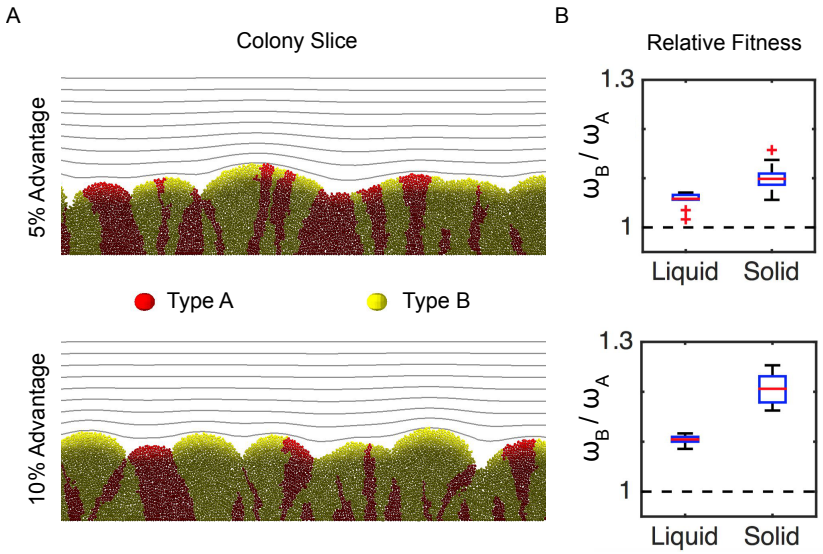


Figure A.4: Individual-based modelling demonstrates that solid culture conditions can amplify cell growth advantages. We modelled competitions between identical cell shapes A and B (pictured centre), conferring B cells with either a 5% (top row) or 10% (bottom row) growth rate advantage over A-type cells. Representative screenshots (A) show 2D colony sections grown under solid culture conditions, where rapid cell growth is limited to a thin layer at the top of the colony. Cells are coloured by type and by growth rate as previously (Figure 2.6), so that fast-growing cells appear brightly-coloured. Contours correspond to Oxygen concentration isoclines in increments of 10% of $u_{(O,0)}$; snapshots show the central 200 µm section of the simulation domain. Plots of relative cell fitness $\frac{\omega_B}{\omega_A}$, show that the type-B cell growth rate advantage is increased approximately 2-fold, under solid culture conditions relative to liquid culture controls, in which the entire colony receives sufficient perfusion for rapid growth (B). 10 simulation replicates were sampled per case.

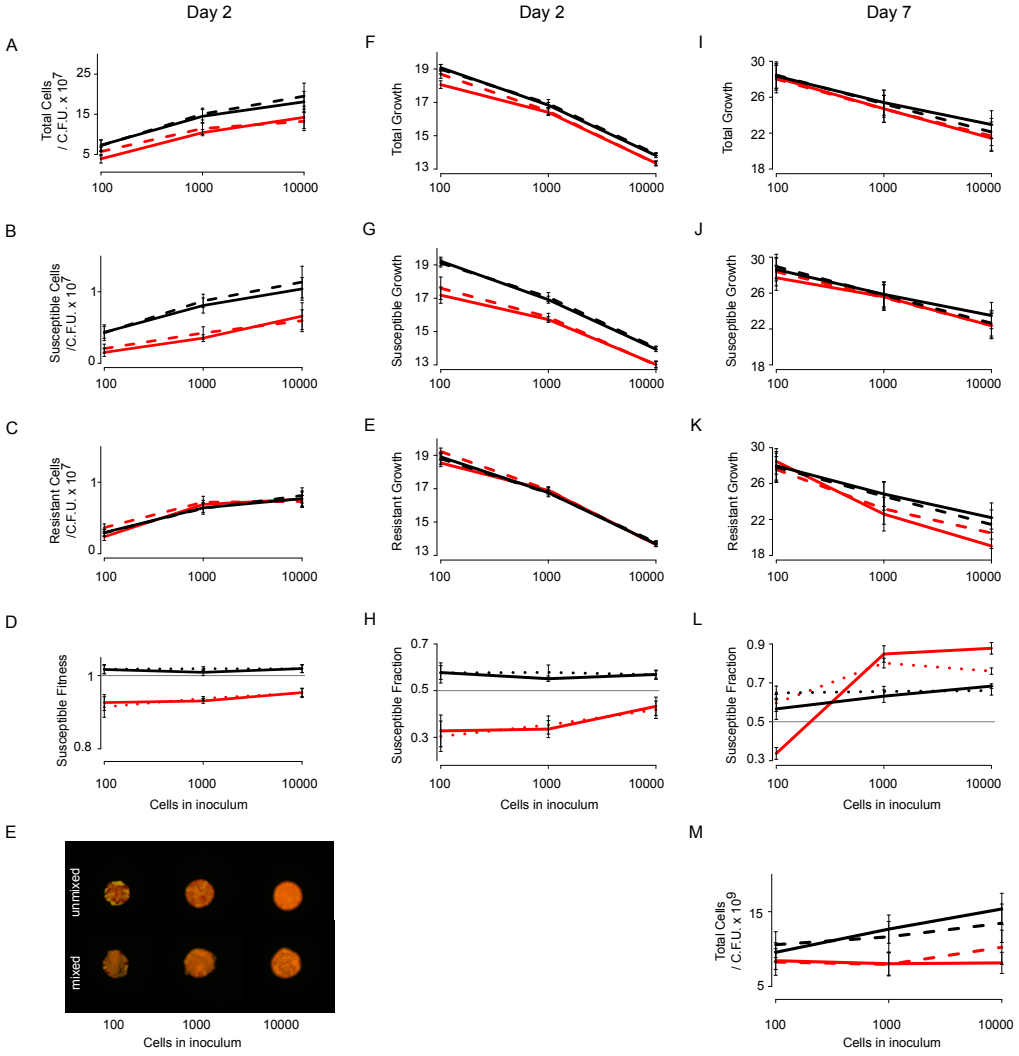


Figure A.5: 2 day and 7 day growth with increasing inoculum density to supplement Figure 2.4, where we present only the 7 day growth in terms of cell divisions and fitness. Susceptible and resistant strains were co-inoculated onto plates containing either no antibiotic (black line) or 12 µg/ml carbenicillin (red line). The dotted line shows a mixing treatment used to disrupt any emergent spatial structure. After two days, before colonies are confluent, mixing has no effect on growth (A, B, C, D, E, G, F, G, H). However after 7 days, when spatial structure has been allowed to develop, mixing restores selection for susceptible strains in the most highly structured (lowest inoculum) density colonies (I, J, K, L, M). This is not the case when there is no antibiotic present. The mean and standard error of two experiments, each with n = 3, are shown.

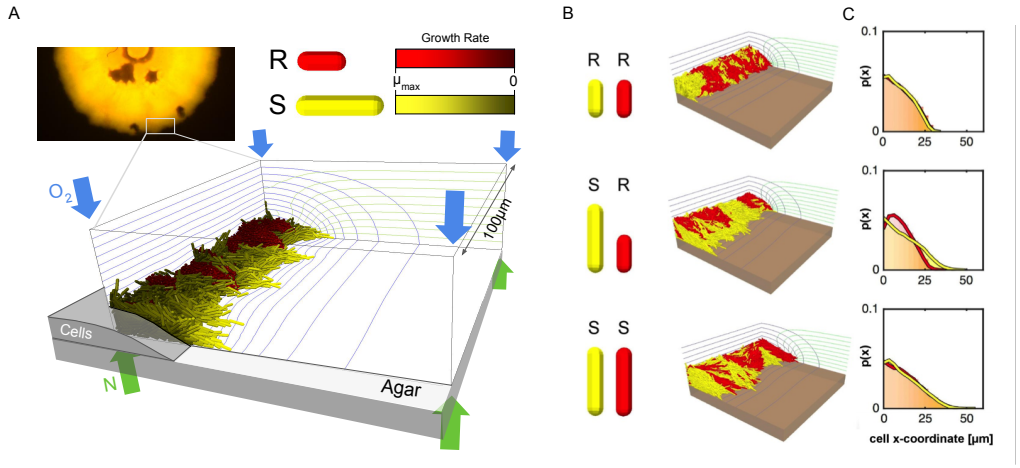


Figure A.6: Simulating growth at the colony edge using a 3D hybrid individual-based model shows cell morphology drives the fitness advantage of susceptible cells. This is a supplement to Figure 2.6, where we present the results of this model. We use a hybrid modelling framework (A) to simulate resource competition between different cell shapes. A 100 µm section of the colony edge is modelled using a walled cuboidal domain, containing both discrete cells and continuous chemical fields. Resistant (R) or susceptible (S) cells are represented using short or long capsules, respectively. Cells elongate according to the local concentration of Oxygen (O2, blue contours) and Nutrient (N, green contours), which diffuse into the colony from above and below as indicated. Each cell is coloured by its individual growth rate: both resources are required for growth such that only cells on the outer edge of the colony are able to proliferate. Repulsive elastic forces between growing capsules lead to expansion of the colony edge along the agar surface. Contours mark isoclines in each field in increments of 10%. The 3D colony edge simulations produced by this model show cell morphology drives the fitness advantage of antibiotic-susceptible (S) cells (B, C). Mixtures of cells with short resistant (R) and long susceptible (S) aspect ratios (SR) behave differently to control simulations where both strains have the same shape (RR, SS) (B). The S cell is more sensitive to branching, leading to enrichment at the colony edge when grown alongside R cells. This does not occur in the RR case, in which neither strain branches, nor the SS case, in which both strains branch. Histograms of cell x-coordinate quantify the enrichment of S cells at the colony edge in the SR case only (C). The spatial structure produces a growth rate advantage for S cells in SR mixtures, but not otherwise. All data were taken after 56 hours of growth, using a merged sample of 10 colonies.

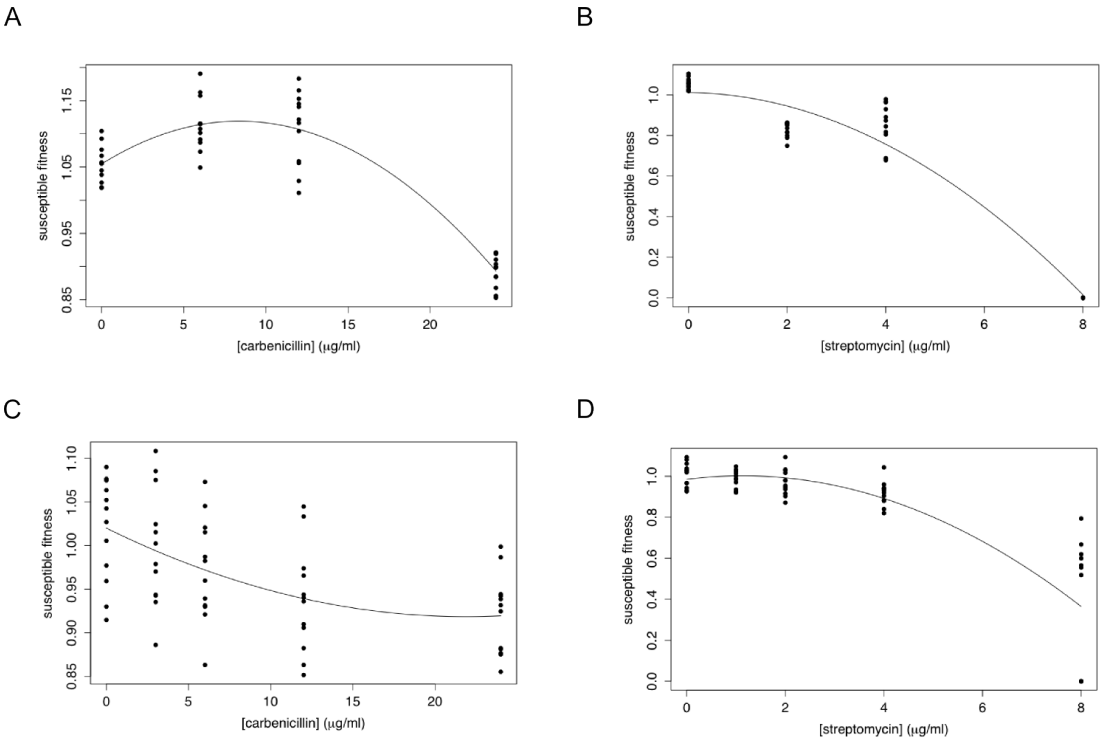


Figure A.7: MSC calculation. To estimate the minimum selective concentration (MSC) (Table A.2) quadratic models (tables A.6 and A.7) were fitted to the fitness of the susceptible strain relative to the resistant strain in the four cases of colony growth on carbenicillin (A) or streptomycin (B) and liquid growth on carbenicillin (C) or streptomycin (D). The coefficients from these models are outlined below.

A.3 Supplementary Tables

Table A.1: Minimum inhibitory concentration (MIC) of streptomycin and carbenicillin to plasmid-(Rms149) bearing resistant strain and plasmid-free susceptible strain, when grown on solid and liquid LB media.

	Carbenicillin (µg/ml)		Streptomycin (µg/ml)	
Strain	LB broth	LB agar	LB broth	LB agar
Resistant	8192	8192	2048	2048
Susceptible	32	32	16	32

Table A.2: Minimum Selective Concentration (MSC) was calculated by fitting susceptible fitness data from competition experiments to a quadratic model. These calculations are described in greater detail in the Supplementary Experimental Procedures.

	MSC (µg/ml) as fraction of susceptible MIC	
Antibiotic	Agar	Broth
Carbenicillin	20 (0.62 MIC)	2.3 (0.071 MIC)
Streptomycin	0.78 (0.024 MIC)	1.6 (0.097 MIC)

Table A.3: Primers used in this study [142].

Rms149-F	GCCGTATTTCATCAACAT
Rms149-R	ACGAAGCTGAAGATTTAC

Table A.4: A quadratic model was fitted to the fitness of the susceptible strain growing as a colony on carbenicillin. Multiple R-squared: 0.8508, Adjusted R-squared: 0.8442 P-value: < 2.2e-16

Coefficients	Estimate	Std. Error	Pr(>|t|)
(Intercept)	1.055e+00	1.064e-02	<2e-16 ***
concentration	1.543e-02	2.252e-03	1.69e-08 ***
concentration^2	-9.232e-04	8.703e-05	7.94e-14 ***

Table A.5: A quadratic model was fitted to the fitness of the susceptible strain growing in liquid containing carbencillin. Multiple R-squared: 0.2904, Adjusted R-squared: 0.2655 P-value: 5.669e-05

Coefficients	Estimate	Std. Error	Pr(>|t|)
(Intercept)	1.0200949	0.0143083	<2e-16 ***
concentration	-0.0092886	0.0033783	0.00798 **
concentration^2	0.0002121	0.0001317	0.11279

Table A.6: A quadratic model was fitted to the fitness of the susceptible strain growing as a colony on streptomycin. Multiple R-squared: 0.9455, Adjusted R-squared: 0.9431 P-value: < 2.2e-16

Coefficients	Estimate	Std. Error	Pr(>|t|)
(Intercept)	1.011371	0.027196	<2e-16 ***
concentration	-0.002723	0.017261	0.875
concentration^2	-0.015237	0.002001	1.26e-09 ***

Table A.7: A quadratic model was fitted to the fitness of the susceptible strain growing in liquid containing streptomycin. Multiple R-squared: 0.73, Adjusted R-squared: 0.7205 P-value: < 2.2e-16

Coefficients	Estimate	Std. Error	Pr(>|t|)
(Intercept)	0.984739	0.037451	<2e-16 ***
concentration	0.030807	0.026527	0.25
concentration^2	-0.013542	0.003103	5.42e-05 ***

Table A.8: Variables used in this study.

Variable	Symbol	Units
Cartesian coordinates	x,y,z	m
Cell volume fraction field	$\psi(p_1 \dots p_n)$,	-
Oxygen field	u_O	kg m^{-3}
Nutrient field	u_N	kg m^{-3}
For each cell i:		
position vector	$p_i = (p_x, p_y, p_z)_i^\top$	m
orientation unit vector	$\hat{a_i} = (a_x, a_y, a_z)_i^\top$	
-		
segment length	l_i	m
volume	$V_i = 4/3\pi R_i^3 + \pi l_i R_i^2$	m^3
local Oxygen concentration	$u_O p_i$	kg m−3
local nutrient concentration	$u_N p_i$	kg m−3
specific growth rate	$\mu_{max} \left(\frac{u_O(p_i)}{u_O(p_i)+K_O)}\right) \left(\frac{u_N(p_i)}{u_N(p_i)+K_N}\right)$	s^{-1}

Table A.9: Model parameters used in this study. Units and sources listed apply to all parameters in groups (indicated with indentation in column 1), unless specified otherwise.

Parameter	Symbol	Value	Units	Source
Domain size:			m	[146]
width	L_x	0.1 x 10^{-3}		
depth	L_y	0.1 x 10^{-3}		
height	L_z	$max(p_x) + \delta$		
Cell radius	r	0.5 x 10^{-6}	m	[144]
Cell birth aspect ratio:	AR_0		-	This study
R-type		2.5		
S-type		4.5		
Boundary height	δ	20.0 x 10^{-3}	m	[88]
Solute diffusivity:			$m^2 s^{-1}$	
Oxygen	D_O	2.0 x 10^{-9}		[146]
Nutrient	D_N	1.0 x 10^{-9}		
Bulk concentrations:			kg m^{-3}	
Oxygen	$u_{(O,\text{bulk})}$	0.5 x 10^{-3}		[146]
Nutrient	$u_{(N,\text{bulk})}$	0.25 x 10^{-3}		Assumed
Cell biomass density	ρ	290	kg m^{-3}	[146]
Max. specific uptake rate	μ_{max}	15.2 x 10^{-3}	$s^{-}1$	[146]
Saturation constant:			kg m^{-3}	
Oxygen	K_O	0.17 x 10^{-3}		[88]
Nutrient	K_N	0.85 x 10^{-3}		Assumed
Biomass yield:			-	
Oxygen	γ_O	22.22		[146]
Nutrient	γ_N	55.55		Assumed
FEniCS solver tolerance	ϵ_F	1.0 x 10^{-6}	-	[88]
Mesh element length	h_F	5.0 x 10^{-6}	m	[88]
Division axis noise	η_{ax}	9	%	[144]
Division volume noise	η_{ax}	0.2	%	[144]
Regularisation weight	α	0.04	-	[144]
CM solver tolerance	ϵ_{CM}	1.0 x 10^{-3}	-	(11)
Number of substeps	N_{sub}	10	-	[144]
Max. contact iterations	N_{iter}	8	-	[144]
Cell grid element length	h_{CM}	10.0 x 10^{-6}	m	[144]
Time step	δt	2.0	h	This study

Table A.10: Solute PDE boundary conditions used in this study. $\hat{n}$ refers to the unit vector tangential to a given domain boundary.

Solute	Boundary	Condition	Description
Oxygen (O)	Top	$u_O = u_{(O,\text{bulk})}$	Supply from bulk fluid
	Base	$\nabla u_O \hat{n} = 0$	Zero flux through agar
	Sides	$\nabla u_O \hat{n} = 0$	Zero flux through sides
Nutrient (N)	Top	$u_N = 0$	Removal by bulk fluid
	Base	$u_N = u_{(N,\text{bulk})}$	Supply from agar

B

Appendix to Chapter 3: Antibiotic adjuvants and bacterial competition

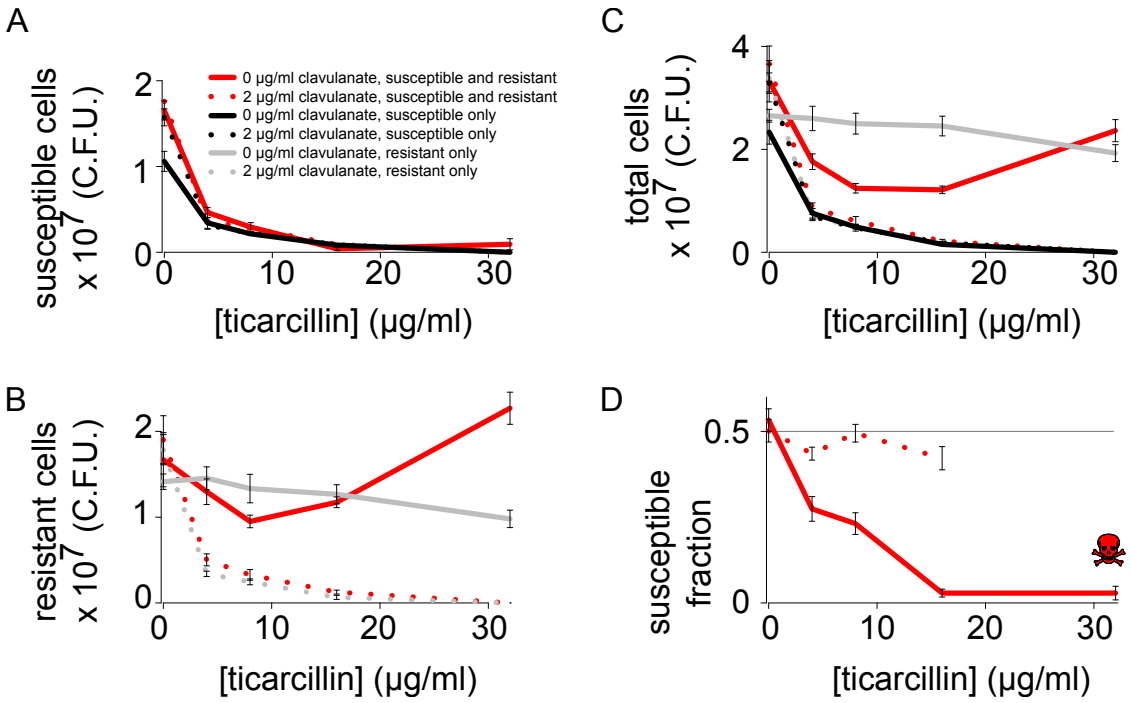


Figure B.1: Selection for antibiotic resistance in liquid culture as supplement to Figure 3.1. Susceptible and resistant strains were competed in liquid culture supplemented with ticarcillin or ticarcillin with a β-lactamase inhibitor, 2 μg/ml clavulanic acid. Both conditions suppressed the growth of the susceptible strain (A). In contrast, the growth of the resistant strain was only suppressed by ticarcillin in the presence of the β-lactamase inhibitor (B). As a result the relative selection for the resistant strain was weaker in the presence of the β-lactamase, however, the susceptible fraction of cells was never above 0.5 under any condition with antibiotic (D). The skull denotes none of either strain was counted. The mean and standard error of two experiments, each with n = 6 for co-cultures and n = 3 for monocultures, are shown.

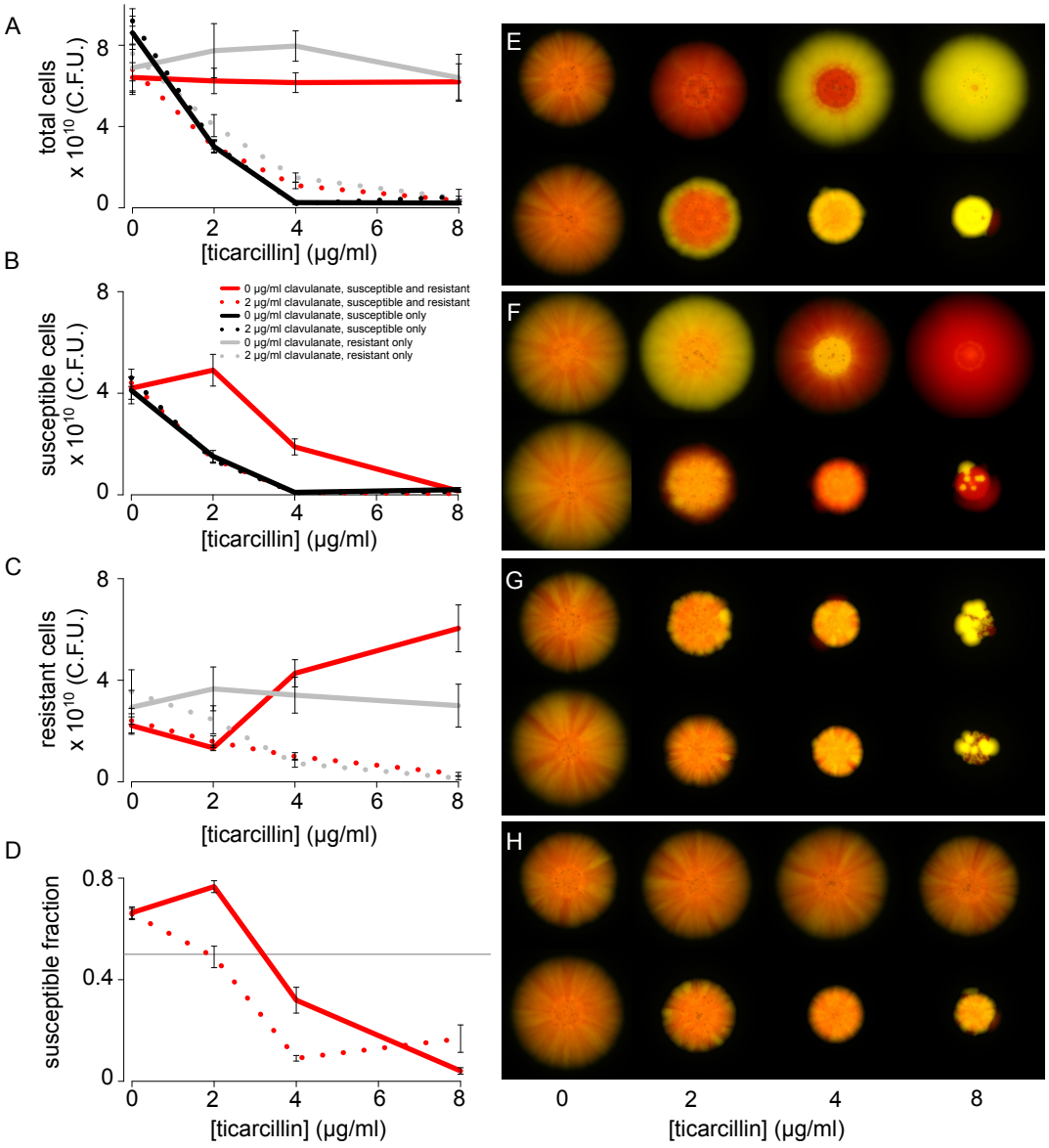


Figure B.2: Antibiotic resistance evolution in bacterial colonies as a supplement to Figure 3.2. Susceptible and resistant strains were competed on increasing concentrations of ticarcillin, with and without the β-lactamase inhibitor, 2 μg/ml clavulanic acid. Total growth of susceptible colonies was repressed by the antibiotic with and without the inhibitor, however, the growth of colonies containing the resistant strain was only repressed in the presence of an inhibitor (A). Without the inhibitor, growth of the susceptible strain was less suppressed in the presence of the resistant strain than alone, suggesting the resistant strain had a cross protective effect (B). Resistant growth was only affected by the antibiotic when the inhibitor was present (C). At some sub-inhibitory concentrations of ticarcillin the susceptible fraction was above 0.5, however, this fraction dropped with the addition of the β-lactamase inhibitor (D). Representative images of these colonies after 6 days, in which the susceptible is in red and the resistant strain yellow (E), the opposite colour combination (F), susceptible only (G) and resistant only (H), are also shown. The top row of each set of images were grown without clavulanic acid and the bottom row were grown in the presence of 2 μg/ml clavulanic acid. The mean and standard error of two experiments, each with n = 6 for co-cultures and n = 3 for monocultures, are shown.

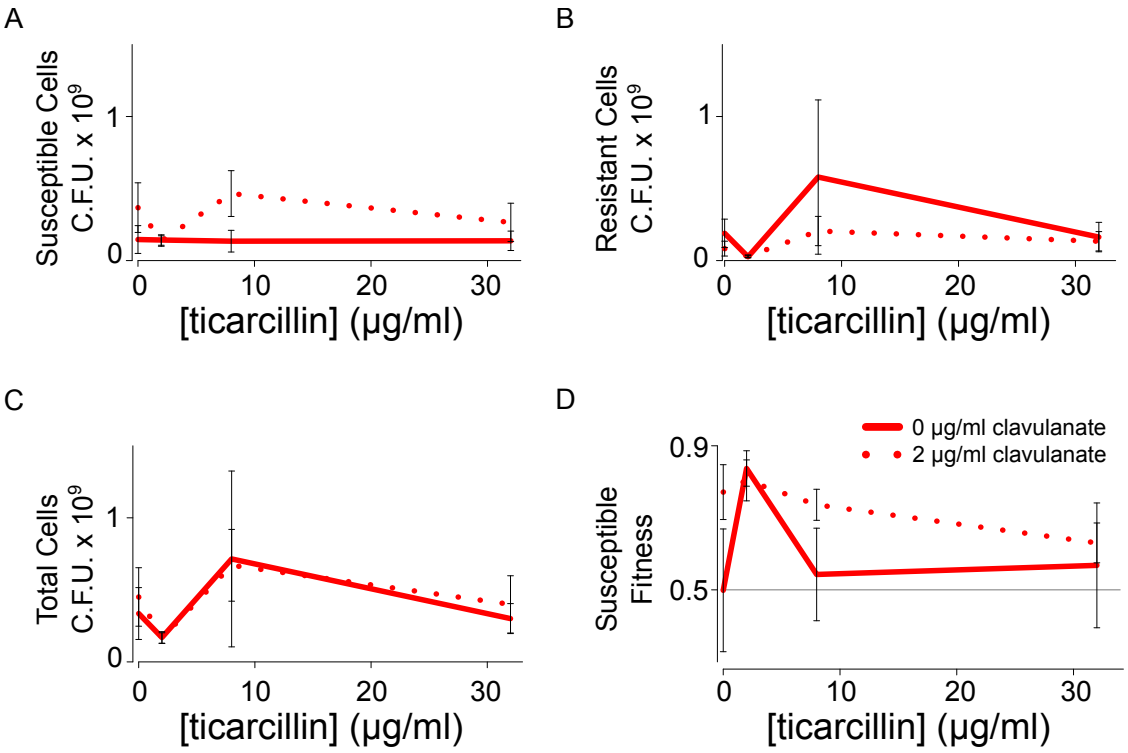


Figure B.3: ***In vivo*** **effects of using a β-lactam inhibitor as supplement to Figure 3.4.** Susceptible and resistant strains were competed in a mouse wound model supplemented with ticarcillin (solid line) or ticarcillin with a β-lactamase inhibitor, 2 μg/ml clavulanic acid (dotted line). The susceptible strain final C.F.U. are shown in (A). The resistant C.F.U. are shown in (B). Total C.F.U. combined of both strains is not highly affected by the antibiotic in this model at these concentrations (C). The final susceptible fraction is shown in (D). The mean and standard error of two experiments, each with n = 3, unless one of the mice did not survive, are shown.

C

Appendix to Chapter 4: Antibiotic adjuvants and the evolution of antibiotic resistance.

C.1 Parametrization

C.1.1 State Variables (Populations)

Variable	Description	Units	GSSA Value
S	Susceptible cell population.	cells	1000 (Infectious dose for an *E. Coli* outbreak was 700 cells [147].)
R	Antibiotic resistant cell population.	cells	0
$R2$	Antibiotic and inhibitor resistant cell population.	cells	0
AB	Antibiotic	ng	0
I	Inhibitor	ng	0

Table C.1: State Variables (Populations)

C.1.2 Model Parameters

Variable	Description	Units	GSSA Value	Reference
b_S	Susceptible birth rate.	doublings hr^{-1}	1.1	Approximated from experimental data (Chapter 1). This is approximately in line with the birth rate of *E. coli* [148].
d	Cell death rate.	doublings hr^{-1}	0.1	Death rate per generation increases from 0 to 2.7% over 180 generations in *E. coli* (i.e. it depends on the age of the cell however this is beyond the scope of this study. Here we round down from the mean of 1.35%) [148].
σ_S	Susceptible growth rate.	doublings hr^{-1}	1	$b_S - d$
κ_R	R maximum growth rate modifier, $\sigma_R = \kappa_R \sigma_S$ due to fitness cost of resistance.	NA	0.95	The fitness cost of resistance has been found to vary from 0 to 50% [8].
κ_{R2}	$R2$ maximum growth rate modifier, $\sigma_{R2} = \kappa_{R2} \sigma_S$ due to fitness cost of double resistance.	NA	0.9	[8]
K	Population carrying capacity.	cells	10000	Total bacterial load in dental abscesses has been reported to range from 10^4 to 10^9 cells [149]

E_{max}	Maximum death rate due to antibiotic.	cells	1	*In vivo* maximum killing effect of β-lactam antibiotics on generation rate constant in *E. coli* ATCC 25922 is 1.38 hr^{-1} [150].
EC_{50S}	Concentration of antibiotic at which the death rate of the susceptible strain is at half of its maximum.	ng	50	0.4 ng μl^{-1} ceftazidime in susceptible *Pseudomonas aeruginosa* isolates from Cystic Fibrosis lung patients [127]
EC_{50R}	Concentration of antibiotic at which the death rate of the resistant strain is at half of its maximum.	ng	$\begin{cases} 50, & I > 1.5 \\ 125, & I \leq 1.5 \end{cases}$	1.2 ng μl^{-1} resistant *Pseudomonas aeruginosa* isolates from Cystic Fibrosis lung patients [127]. MICs can increase up to two orders of magnitude with inhibitor resistance [151].
EC_{50R2}	Concentration of antibiotic at which the death rate of the doubly resistant strain is at half of its maximum.	ng	100	See above.
k_{mutSR}	Rate of mutation of S into R, for example by HGT.	cells hr^{-1}	10^{-4}	Estimates vary from 10^{-4} to 10^{-6} [152].
k_{mutRR2}	Rate of mutation of R into $R2$, for example by *de novo* mutation.	cells hr^{-1}	10^{-5}	Lower probability than plasmid acquisition. TEM-1 β-lactamase can become inhibitor resistant by multiple routes from single or multiple point mutations [153].

$k_{mutloss}$	Rate of mutation of $R2$ and R into S, for example by plasmid loss.	cells hr^{-1}	10^{-3}	A range of plasmid loss rates have been recorded from $5x10^{-2}$ to $1.5x10^{-3}$ [123].
k_{deg1}	Rate of antibiotic degradation by R.	ng hr^{-1}	10^{-3} if social, 0 if asocial	Established by parameter sweep (Figure C.1).
k_{deg2}	Rate of antibiotic degradation by $R2$.	ng hr^{-1}	$5x10^{-6}$	$k_{deg2} < k_{deg1}$ k_{cat}/K_m of IR TEM-1 mutants is 10-50%of the size for amoxicillin and up to 1% of the size for ticarcillin [153].
k_{inhib}	Rate at which I inhibits antibiotic degradation by R.	ng hr^{-1}	10^{-6}	The dissociation constant K_i, determined from fit to experimental data is 4.56 ng tazobactam ml^{-1} for TEM-1 in *E. coli* [45].
IC_{50}	Concentration of I at which the degradation of AB by I is at half its maximum, k_{deg1}.	ng	150	IC_{50} for TEM-1 in *E. coli* is 0.08 μM clavulanic acid, 0.1 μM tazobactam or 6.1 μM sulbactam [153]. [154] provides a range of IC_{50} values for IR enzymes, however, here we assume this to be higher than the clinically administered range and the $R2$ strain is unaffected by I.
α_{in}	Rate of entry of AB into the compartment.	ng hr^{-1}	500 or 0.	Varies by treatment regime.
α_{out}	Rate of exit of AB from the compartment.	ng hr^{-1}	0.45 or 0.	Varies by treatment regime.

ρ_{in}	Rate of entry of I into the compartment.	ng hr^{-1}	15000 or 0.	Varies by treatment regime.
ρ_{out}	Rate of exit of I from the compartment.	ng hr^{-1}	0.1 or 0.	Varies by treatment regime.

Table C.2: Model Parameters

C.1.3 Dimensionless Variables

Dimensionless Variable		Significance	Range	Initial Value
$\bar{S} = \frac{S}{K}$	(C.1)	The Susceptible bacterial cell density relative to the total possible cell population, i.e. the carrying capacity, K.	0 - 1	0.1
$\bar{R} = \frac{R}{K}$	(C.2)	The Resistant bacterial cell density relative to the total possible cell population, i.e. the carrying capacity, K.	0 - 1	0
$\overline{R2} = \frac{R2}{K}$	(C.3)	The doubly Resistant bacterial cell density relative to the total possible cell population, i.e. the carrying capacity, K.	0 - 1	0
$\overline{AB} = \frac{AB}{EC_{50Sus}}$	(C.4)	Antibiotic concentration relative to the EC_{50} of the Susceptible strain.	0 - γ_R (currently max 2.5).	0
$\bar{I} = \frac{I}{IC_{50}}$	(C.5)	Inhibitor concentration relative to the IC_{50} of the Resistant strain.	0 - ∞.	0
$\bar{t} = t\sigma_S$	(C.6)	Time now relative to amount of susceptible growth that could have occurred in a time step.	0 - ∞.	0

Table C.3: Dimensionless Variables

C.1.4 Dimensionless Parameters

Parameter	Variables	Significance	Default Value
$a = \frac{E_{max}}{\sigma_S}$ (C.7)	S, R, $R2$	Maximum growth inhibition due to antibiotic relative to susceptible growth rate.	1
$b = \frac{k_{mutSR}}{\sigma_S}$ (C.8)	S, R	Rate of plasmid acquisition, $S \rightarrow R$, relative to susceptible growth rate.	$k_{mutSR} << \sigma_S$ $c > b >> d$ $b = 10^{-4}$
$c = \frac{k_{mutloss}}{\sigma_S}$ (C.9)	R, $R2$	Rate of plasmid loss, $R \rightarrow S$ and $R2 \rightarrow S$, relative to the maximum susceptible growth rate.	$k_{mutloss} << \sigma_S$ $c > b >> d$ $c = 10^{-3}$
$d = \frac{k_{mutRR2}}{\sigma_S}$ (C.10)	R, $R2$	$R \rightarrow R2$ mutation rate relative to susceptible growth rate.	$k_{mutRR2} << \sigma_S$ $c > b >> d$ $d = 10^{-5}$
$e = \frac{\rho_{in}}{\sigma_S EC_{50Sus}}$ (C.11)	AB	Rate of antibiotic entry into the compartment relative to the EC_{50Sus} and the maximum susceptible growth rate, i.e. the entry of $\overline{AB}$ relative to the susceptible growth rate.	0 or 10
$f = \frac{\rho_{out}}{\sigma_S}$ (C.12)	AB	Rate of antibiotic flow out the compartment relative to the EC_{50Sus} and the maximum susceptible growth rate, i.e. the exit of $\overline{AB}$ relative to the susceptible growth rate.	0 or 0.45

$g = \frac{k_{deg1}K}{\sigma_S}$	(C.13)	AB	Total capacity for antibiotic degradation, if all cells were R, relative to the susceptible growth rate.	100 in social case, 0 in asocial case.
$h = \frac{k_{deg2}K}{\sigma_S}$	(C.14)	AB	Total capacity for antibiotic degradation, if all cells were $R2$, relative to the susceptible growth rate.	0.5
$i = \frac{\beta_{in}}{\sigma_S IC_{50}}$	(C.15)	I	Rate of inhibitor entry into the compartment relative to the IC_{50} and the maximum susceptible growth rate, i.e. the entry of $\bar{I}$ relative to the susceptible growth rate.	0 or 100
$j = \frac{\beta_{out}}{\sigma_S}$	(C.16)	I	Rate of inhibitor flux out of the compartment relative to the IC_{50} and the maximum susceptible growth rate, i.e. the exit of $\bar{I}$ relative to the susceptible growth rate.	0 or 0.1
$k = \frac{k_{inhib}K}{\sigma_S}$	(C.17)	I	Total capacity for enzyme inhibition, if all cells were R, relative to the susceptible growth rate.	0.1
$\alpha_R = \frac{\lambda_R}{\lambda_S}$	(C.18)	R	Growth cost of resistance.	0.95
$\alpha_{R2} = \frac{\lambda_{R2}}{\lambda_S}$	(C.19)	$R2$	Growth cost of resistance.	0.9

$\gamma_R = \frac{EC_{50R}}{EC_{50Sus}}$ (C.20)	R	Relative growth inhibition by antibiotic.	$\gamma_R = \begin{cases} 1, & \bar{I} > 0.01 \\ 2.5, & \bar{I} \leq 0.01 \end{cases}$
$\gamma_{R2} = \frac{EC_{50R2}}{EC_{50Sus}}$ (C.21)	$R2$	Relative growth inhibition by antibiotic.	2

Table C.4: Dimensionless Parameters

C.1.5 Default Dimensionless Parameter Settings

Parameter		Value
$a = \frac{E_{max}}{\sigma_S}$	(C.22)	1
$b = \frac{k_{mutSR}}{\sigma_S}$	(C.23)	10^{-4}
$c = \frac{k_{mutloss}}{\sigma_S}$	(C.24)	10^{-3}
$d = \frac{k_{mutRR2}}{\sigma_S}$	(C.25)	10^{-5}
$e = \frac{\rho_{in}}{\sigma_S EC_{50Sus}}$	(C.26)	1

$f = \frac{\rho_{out}}{\sigma_S}$	(C.27)	0.5
$g = \frac{k_{deg1}K}{\sigma_S}$	(C.28)	0.1
$h = \frac{k_{deg2}K}{\sigma_S}$	(C.29)	0.05
$i = \frac{\beta_{in}}{\sigma_S IC_{50}}$	(C.30)	1
$j = \frac{\beta_{out}}{\sigma_S}$	(C.31)	0.5
$k = \frac{k_{inhib}K}{\sigma_S}$	(C.32)	0.1
$\alpha_R = \frac{\lambda_R}{\lambda_S}$	(C.33)	0.95
$\alpha_{R2} = \frac{\lambda_{R2}}{\lambda_S}$	(C.34)	0.9
$\gamma_R = \frac{EC_{50R}}{EC_{50Sus}}$	(C.35)	$\gamma_R = \begin{cases} 1.5, & \bar{I} > 0.01 \\ 2.5, & \bar{I} \leq 0.01 \end{cases}$
$\gamma_{R2} = \frac{EC_{50R2}}{EC_{50Sus}}$	(C.36)	2

C.2 Derivation of Dimensionless ODEs

C.2.1 Susceptible Growth

The original differential equation for Susceptible growth is as follows:

$$\frac{dS}{dt} = S\left(\lambda_S - d_s - k_{mutSR}\right) + \left(R + R2\right)k_{mutloss} \tag{4.1}$$

We can substitute the dimensionless measure of S relative to the maximum population of cells, K, in the form $\bar{S} = \frac{S}{K}$, and, similarly, $\bar{R} = \frac{R}{K}$ and $\bar{R2} = \frac{R2}{K}$. These rearrange to $S = \bar{S}K$, $R = \bar{R}K$ and $R2 = \overline{R2}K$, giving

$$\frac{d\bar{S}}{dt}K = \bar{S}K\left(\lambda_S - d_s - k_{mutSR}\right) + K\left(\bar{R} + \overline{R2}\right)k_{mutloss}. \tag{C.37}$$

Dividing through by K gives

$$\frac{d\bar{S}}{dt} = \bar{S}\left(\lambda_S - d_s - k_{mutSR}\right) + \left(\bar{R} + \overline{R2}\right)k_{mutloss}. \tag{C.38}$$

Given

$$\lambda_S = \sigma_S\left(1 - \frac{N}{K}\right) \tag{??}$$

where $N = S + R + R2$, this can be rewritten using $\overline{N} = \frac{N}{K}$,

$$\lambda_S = \sigma_S\left(1 - \overline{N}\right). \tag{C.39}$$

As can the death rate due to antibiotic,

$$d_S = E_{max}\frac{\frac{AB}{EC_{50S}}}{1 + \frac{AB}{EC_{50S}}} \tag{??}$$

using $\overline{AB} = \frac{AB}{EC_{50S}}$,

$$d_S = E_{max}\frac{\overline{AB}}{1 + \overline{AB}}. \tag{C.40}$$

eqs. (C.39) and (C.40) can be substituted back into C.38 to give

$$\frac{d\bar{S}}{dt} = \bar{S}\left(\sigma_S\left(1 - \overline{N}\right) - E_{max}\frac{\overline{AB}}{1 + \overline{AB}} - k_{mutSR}\right) + \left(\bar{R} + \overline{R2}\right)k_{mutloss}. \tag{C.41}$$

Finally, the substitution $\bar{t} = t\sigma_S$ leads to

$$\frac{d\bar{S}}{d\bar{t}}\sigma_S = \bar{S}\left(\sigma_S\left(1-\overline{N}\right) - E_{max}\frac{\overline{AB}}{1+\overline{AB}} - k_{mutSR}\right) + \left(\bar{R}+\overline{R2}\right)k_{mutloss}. \quad \text{(C.42)}$$

From where we divide through by σ_S, giving rise to

$$\boxed{\frac{d\bar{S}}{d\bar{t}} = \bar{S}\left(\left(1-\overline{N}\right) - \frac{E_{max}}{\sigma_S}\frac{\overline{AB}}{1+\overline{AB}} - \frac{k_{mutSR}}{\sigma_S}\right) + \left(\bar{R}+\overline{R2}\right)\frac{k_{mutloss}}{\sigma_S}.} \quad \text{(C.62)}$$

C.2.2 Resistant Growth

The original differential equations for Resistant growth is as follows:

$$\frac{dR}{dt} = R\left(\lambda_R - d_R - k_{mutRR2} - k_{mutloss}\right) + Sk_{mutSR} \quad (4.2)$$

As before, we can substitute the dimensionless measure of R relative to the maximum population of cells, K, in the form $\bar{R} = \frac{R}{K}$, and, similarly, $\bar{S} = \frac{S}{K}$ and $\bar{R2} = \frac{R2}{K}$, giving

$$\frac{d\bar{R}}{dt}K = \bar{R}K\left(\lambda_R - d_R - k_{mutloss} - k_{mutRR2}\right) + K\bar{S}k_{mutSR}. \quad \text{(C.43)}$$

Dividing through by K gives

$$\frac{d\bar{R}}{dt} = \bar{R}\left(\lambda_R - d_R - k_{mutloss} - k_{mutRR2}\right) + \bar{S}k_{mutSR}. \quad \text{(C.44)}$$

Given

$$\lambda_R = \sigma_R\left(1-\frac{N}{K}\right) \quad \text{(??)}$$

where $N = S + R + R2$, this can be rewritten using $\overline{N} = \frac{N}{K}$ and $\sigma_R = \kappa_R\sigma_S$ (given κ_R is the resistant cost to growth rate adjustment),

$$\lambda_R = \kappa_R\sigma_S\left(1-\overline{N}\right). \quad \text{(C.45)}$$

As can the death rate due to antibiotic,

$$d_R = E_{max}\frac{\frac{AB}{EC_{50R}}}{1+\frac{AB}{EC_{50R}}} \quad \text{(??)}$$

using $\overline{AB} = \frac{AB}{EC_{50S}}$, where $EC_{50R} = \gamma_R EC_{50S}$,

$$d_R = E_{max}\frac{\gamma_R\overline{AB}}{1+\gamma_R\overline{AB}}. \tag{C.46}$$

eqs. (C.45) and (C.46) can be substituted back into C.44 to give

$$\frac{d\bar{R}}{dt} = \bar{R}\left(\kappa_R\sigma_S\left(1-\overline{N}\right) - E_{max}\frac{\gamma_R\overline{AB}}{1+\gamma_R\overline{AB}} - k_{mutloss} - k_{mutRR2}\right) + \bar{S}k_{mutSR}. \tag{C.47}$$

Finally, the substitution $\bar{t} = t\sigma_S$ leads to

$$\frac{d\bar{R}}{d\bar{t}}\sigma_S = \bar{R}\left(\kappa_R\sigma_S\left(1-\overline{N}\right) - E_{max}\frac{\gamma_R\overline{AB}}{1+\gamma_R\overline{AB}} - k_{mutloss} - k_{mutRR2}\right) + \bar{S}k_{mutSR}. \tag{C.48}$$

From where we divide through by σ_S, giving rise to

$$\boxed{\frac{d\bar{R}}{d\bar{t}} = \bar{R}\left(\kappa_R\left(1-\overline{N}\right) - \frac{E_{max}}{\sigma_S}\frac{\gamma_R\overline{AB}}{1+\gamma_R\overline{AB}} - \frac{k_{mutloss}+k_{mutRR2}}{\sigma_S}\right) + \bar{S}\frac{k_{mutSR}}{\sigma_S}.} \tag{C.63}$$

C.2.3 Doubly Resistant Growth

The original differential equations for doubly Resistant growth is as follows:

$$\frac{dR2}{dt} = R2\left(\lambda_{R2} - d_{R2} - k_{mutloss}\right) + Rk_{mutRR2} \tag{4.3}$$

As previously, we can substitute the dimensionless measure of $R2$ relative to the maximum population of cells, K, in the form $\overline{R2} = \frac{R2}{K}$, and, similarly, $\bar{R} = \frac{R}{K}$ and $\bar{S} = \frac{S}{K}$, giving

$$\frac{d\overline{R2}}{dt}K = \overline{R2}K\left(\lambda_{R2} - d_{R2} - k_{mutloss}\right) + K\bar{R}k_{mutRR2}. \tag{C.49}$$

Dividing through by K gives

$$\frac{d\overline{R2}}{dt} = \overline{R2}\left(\lambda_{R2} - d_{R2} - k_{mutloss}\right) + \bar{R}k_{mutRR2}. \tag{C.50}$$

Given

$$\lambda_{R2} = \sigma_{R2}\left(1-\frac{N}{K}\right) \tag{??}$$

where $N = S + R + R2$, this can be rewritten using $\overline{N} = \frac{N}{K}$ and $\sigma_{R2} = \kappa_{R2}\sigma_S$ (given κ_{R2} is the resistant cost to growth rate adjustment),

$$\lambda_{R2} = \kappa_{R2}\sigma_S\left(1 - \overline{N}\right). \tag{C.51}$$

As can the death rate due to antibiotic,

$$d_{R2} = E_{max}\frac{\frac{AB}{EC_{50R2}}}{1 + \frac{AB}{EC_{50R2}}} \tag{??}$$

using $\overline{AB} = \frac{AB}{EC_{50S}}$, where $EC_{50R2} = \gamma_{R2}EC_{50S}$,

$$d_{R2} = E_{max}\frac{\gamma_{R2}\overline{AB}}{1 + \gamma_{R2}\overline{AB}}. \tag{C.52}$$

eqs. (C.51) and (C.52) can be substituted back into (C.50) to give

$$\frac{d\bar{R}2}{dt} = \bar{R}2\left(\kappa_{R2}\sigma_S\left(1 - \overline{N}\right) - E_{max}\frac{\gamma_{R2}\overline{AB}}{1 + \gamma_{R2}\overline{AB}} - k_{mutloss}\right) + \bar{R}k_{mutRR2}. \tag{C.53}$$

Finally, the substitution $\bar{t} = t\sigma_S$ leads to

$$\frac{d\bar{R}2}{d\bar{t}}\sigma_S = \bar{R}2\left(\kappa_{R2}\sigma_S\left(1 - \overline{N}\right) - E_{max}\frac{\gamma_{R2}\overline{AB}}{1 + \gamma_{R2}\overline{AB}} - k_{mutloss}\right) + \bar{R}k_{mutRR2}. \tag{C.54}$$

From where we divide through by σ_S, giving rise to

$$\boxed{\frac{d\bar{R}2}{d\bar{t}} = \bar{R}2\left(\kappa_{R2}\left(1 - \overline{N}\right) - \frac{E_{max}}{\sigma_S}\frac{\gamma_{R2}\overline{AB}}{1 + \gamma_{R2}\overline{AB}} - \frac{k_{mutloss}}{\sigma_S}\right) + \bar{R}\frac{k_{mutRR2}}{\sigma_S}.} \tag{C.64}$$

C.2.4 Antibiotic Dynamics

The original differential equation for antibiotic dynamics is as follows:

$$\frac{dAB}{dt} = \alpha_{in} - AB\alpha_{out} - RABk_{deg1}\left(1 - \frac{\frac{I}{IC_{50}}}{1 + \frac{I}{IC_{50}}}\right) - k_{deg2}R2AB. \tag{4.4}$$

We can substitute the dimensionless measure of AB relative to the susceptible EC_{50S}, $\overline{AB} = \frac{AB}{EC_{50S}}$, giving

$$\frac{d\overline{AB}}{dt}EC_{50S} = \alpha_{in} - EC_{50S}\overline{AB}\alpha_{out} - EC_{50S}R\overline{AB}k_{deg1}\left(1 - \frac{\frac{I}{IC_{50}}}{1 + \frac{I}{IC_{50}}}\right) - k_{deg2}EC_{50S}R2\overline{AB}. \tag{C.55}$$

This can then be divided through by EC_{50S} to arrive at

$$\frac{d\overline{AB}}{dt} = \frac{\alpha_{in}}{EC_{50S}} - \overline{AB}\alpha_{out} - R\overline{AB}k_{deg1}\left(1 - \frac{\frac{I}{IC_{50}}}{1+\frac{I}{IC_{50}}}\right) - k_{deg2}R2\overline{AB}. \quad \text{(C.56)}$$

Next we can substitute in the dimensionless measures of the resistant bacteria strains, $\overline{R2} = \frac{R2}{K}$ and $\bar{R} = \frac{R}{K}$, and the inhibitor, $\bar{I} = \frac{I}{IC_{50}}$,

$$\frac{d\overline{AB}}{dt} = \frac{\alpha_{in}}{EC_{50S}} - \overline{AB}\alpha_{out} - K\bar{R}\overline{AB}k_{deg1}\left(1 - \frac{\bar{I}}{1+\bar{I}}\right) - Kk_{deg2}\overline{R2AB}. \quad \text{(C.57)}$$

Finally we can substitute t for the dimensionless, $\bar{t} = t\sigma_S$, as follows

$$\boxed{\frac{d\overline{AB}}{d\bar{t}} = \frac{\rho_{in}}{\sigma_S EC_{50S}} - \frac{\overline{AB}\rho_{out}}{\sigma_S} - \bar{R}\overline{AB}\frac{k_{deg1}K}{\sigma_S}\left(1 - \frac{\bar{I}}{1+\bar{I}}\right) - \overline{R2AB}\frac{k_{deg2}K}{\sigma_S}} \quad \text{(C.65)}$$

C.2.5 Inhibitor Dynamics

The original equation governing the concentration of inhibitor is

$$\frac{dI}{dt} = \rho_{in} - I\rho_{out} - k_{inhib}RI. \quad (4.5)$$

We first substitute the dimensionless measure of inhibitor, $\bar{I} = \frac{I}{IC_{50}}$,

$$\frac{d\bar{I}}{dt}IC_{50} = \rho_{in} - IC_{50}\bar{I}\rho_{out} - k_{inhib}IC_{50}R\bar{I}. \quad \text{(C.58)}$$

We then divide through by IC_{50} to give

$$\frac{d\bar{I}}{dt} = \frac{\rho_{in}}{IC_{50}} - \bar{I}\rho_{out} - k_{inhib}R\bar{I}. \quad \text{(C.59)}$$

Next we replace R with its dimensionless counterpart, $\bar{R} = \frac{R}{K}$,

$$\frac{d\bar{I}}{dt} = \frac{\rho_{in}}{IC_{50}} - \bar{I}\rho_{out} - k_{inhib}K\bar{R}\bar{I}. \quad \text{(C.60)}$$

And we can make time dimensionless by making it relative to the susceptible growth rate, $\bar{t} = t\sigma_S$, as follows,

$$\frac{d\bar{I}}{d\bar{t}}\sigma_S = \frac{\rho_{in}}{IC_{50}} - \bar{I}\rho_{out} - k_{inhib}K\bar{R}\bar{I}. \quad \text{(C.61)}$$

This rearranges to

$$\boxed{\frac{d\bar{I}}{d\bar{t}} = \frac{\rho_{in}}{IC_{50}\sigma_S} - \bar{I}\frac{\rho_{out}}{\sigma_S} - \frac{k_{inhib}K}{\sigma_S}\bar{R}\bar{I}.} \tag{C.66}$$

In summary, the final set of non-dimensionalised equations is the following:

$$\frac{d\bar{S}}{dt} = \bar{S}\left(\left(1-\bar{N}\right) - \frac{E_{max}}{\sigma_S}\left(\frac{\overline{AB}}{1+\overline{AB}}\right) - \frac{k_{mutSR}}{\sigma_S}\right) + \left(\bar{R}+\overline{R2}\right)\left(\frac{k_{mutloss}}{\sigma_S}\right) \tag{C.62}$$

$$\frac{d\bar{R}}{d\bar{t}} = \bar{R}\left(\kappa_R\left(1-\bar{N}\right) - \frac{E_{max}}{\sigma_S}\left(\frac{\gamma_R\overline{AB}}{1+\gamma_R\overline{AB}}\right) - \frac{k_{mutloss}+k_{RR2}}{\sigma_S}\right) + \bar{S}\left(\frac{k_{mutSR}}{\sigma_S}\right) \tag{C.63}$$

$$\frac{d\overline{R2}}{d\bar{t}} = \overline{R2}\left(\kappa_{R2}\left(1-\bar{N}\right) - \frac{E_{max}}{\sigma_S}\left(\frac{\gamma_{R2}\overline{AB}}{1+\gamma_{R2}\overline{AB}}\right) - \frac{k_{mutloss}}{\sigma_S}\right) + \bar{R}\left(\frac{k_{mutRR2}}{\sigma_S}\right) \tag{C.64}$$

$$\frac{d\overline{AB}}{d\bar{t}} = \frac{\rho_{in}}{\sigma_S EC_{50Sus}} - \frac{\overline{AB}\rho_{out}}{\sigma_S} - \bar{R}\overline{AB}\frac{k_{deg1}K}{\sigma_S}\left(1-\frac{\bar{I}}{1+\bar{I}}\right) - \overline{R2AB}\frac{k_{deg2}K}{\sigma_S} \tag{C.65}$$

$$\frac{d\bar{I}}{d\bar{t}} = \frac{\beta_{in}}{\sigma_S IC_{50}} - \frac{\bar{I}\beta_{out}}{\sigma_S} - \bar{I}\bar{R}\frac{k_{inhib}K}{\sigma_S} \tag{C.66}$$

C.3 Model Validation

To validate the model, first we looked for cross protection in the simplest case; a co-culture of S and R, in which there was no mutation (Figure C.1A and B). The first panel shows only the fate of the susceptible strain after 300 susceptible growth cycles. Antibiotic concentration is embodied in the non-dimensional model by the parameter e (C.11). We see that as the concentration of antibiotic increases, moving vertically down the panel, the susceptible strain fares less well against the resistant strain. Moving horizontally across the panel, we increase the sociality parameter, g C.13). This parameter is the dimensionless representation of the rate at which the singly

resistant strain, R, degrades the antibiotic. As this parameter is increased, moving horizontally across the panel, the susceptible strain is better able to outcompete the resistant strain and the concentration of antibiotic at which there is selection for R decreases. Figure C.1B shows the evolutionary trajectory over time of the two strains. We see in the top graph that when there is no antibiotic degradation by the resistant strain the susceptible strain is immediately outcompeted by the resistant strain. However when the resistant strain produces antibiotic-degrading enzyme, the susceptible strain is able to outcompete the resistant strain, even on the same concentration of antibiotic.

After replicating our experimental findings in the simplest case, we introduced mutation into the system, in a co-culture of S and R (Figure C.1C and D). The result of introducing mutation into the system is similar to the mutation-free case, with the exception that susceptible strains are able to outcompete resistant strains at even higher concentrations of antibiotic when the rate of antibiotic degradation by the resistant strain is high (bottom right of far right central panel). This can be explained by considering that now resistant strains are able to lose resistance and mutate into the less costly, protected, susceptible strain.

As a final validation of this system we simulated the susceptible strain inoculated alone under the same conditions, able to mutate into the R and $R2$ strains (Figure C.1E and F). Here we consider the outcome of relatively short term competition experiments after $\bar{t} = 300$. Results at equilibrium will differ from those shown here, however in a patient it is unlikely infection will continue to equilibrium. At lower doses of antibiotic the susceptible strain fares better than in the previous cases as it does not have to compete for resources with the resistant strain. We see the extent of antibiotic degradation makes a significant difference to the total bacterial load experienced in Figure C.1G. In which the top graph shows the progression of disease with no external degradation and the panel below shows the progression of disease at the same antibiotic concentration. We see the level of degradation is higher, though the disease burden is also higher. Though a confounding factor, in interpreting

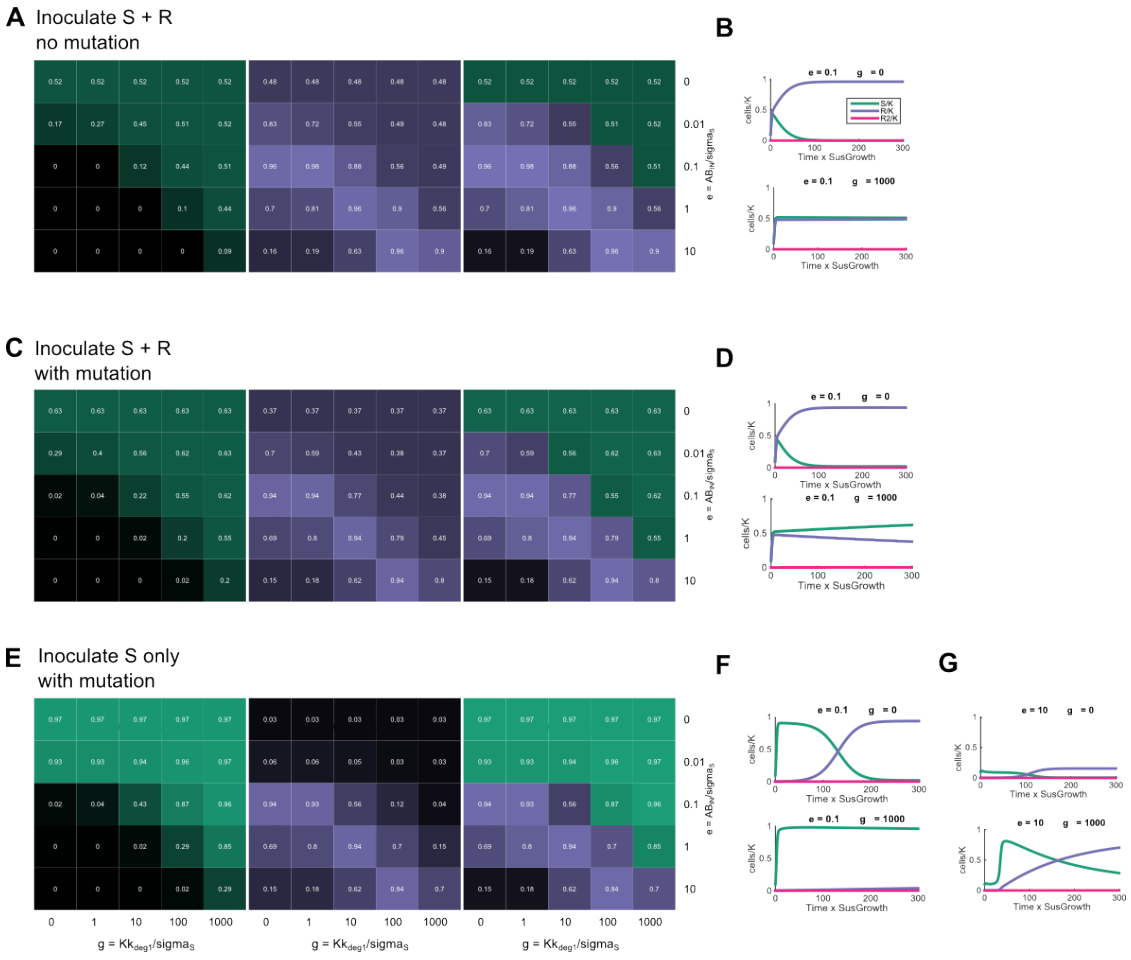


Figure C.1: Extent of external antibiotic degradation strongly affects the concentration of antibiotic selecting for resistance. Susceptible, S and resistant, R strains were first competed on varying concentrations of antibiotic (e, y axis), with varying the extent to which R broke down the antibiotic externally increasing across the x axis, g (**A**). Inocula of $\bar{S}$=0.1 and $\bar{R}$=0.1 were used. Moving from left to right the first panel shows the fate of S cells after $\bar{t} = 300$. The second panel shows R cells in the same competition and the final panel is coloured by the winner at that time point and shows the ratio of that winner in the centre of each square. Two sample evolutionary trajectories over the entire time course are shown for the asocial ($g = 0$) and highly social ($g = 1000$) cases on antibiotic ($e = 0.1$). **C** and **D** show the equivalent figures for the S and R strains grown together in the same way but this time with mutation. **E** and **F** show this for a competition inoculated with only the S strain at $\bar{S}$=0.1.

the effect of cross protection, is that the resistant strain is also affected at this concentration of antibiotic and so degradation rescues the resistant strain also.

C.4 The Stochastic Model shows the same effects of inhibitors for the asocial case.

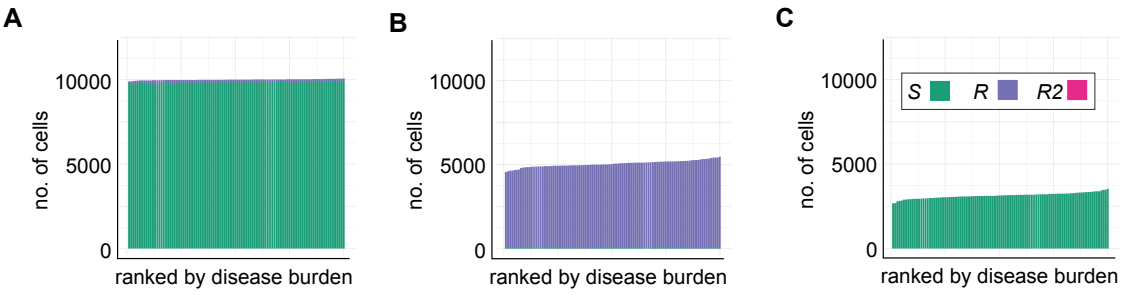


Figure C.2: Stochastic modelling reveals inhibitors suppress the emergence of resistance, even at intermediate doses of antibiotic. Complement to Figure 4.4. The growth of a starting population of 1000 susceptible cells was modelled stochastically, using the GSSA, growing without treatment (**A**), on antibiotic ($\alpha_{in} = 50$, $\alpha_{out} = 0.45$) (**B**) and on antibiotic combined with inhibitor ($\alpha_{in} = 50$, $\alpha_{out} = 0.45$, $\rho_{in} = 15000$, $\rho_{out} = 0.1$) (**C**). The mechanism for resistance in these simulations did not break down antibiotic externally to the cell. These graphs show the result after 200 hours, of 100 simulations, ranked by disease burden.

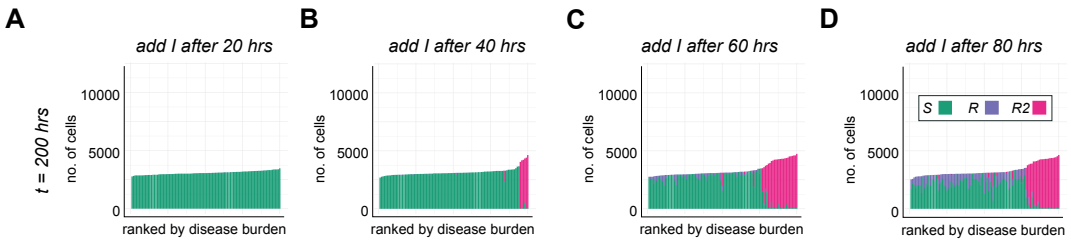


Figure C.3: The later inhibitor is added the more likely double resistance is to emerge. Complement to Figure 4.5. 1000 cells of the susceptible strain were inoculated on antibiotic and inhibitor was added after 20 hours (**A**), 40 hours (**B**), 60 hours (**C**) or 80 hours (**D**). Moving down the panels the outcome of 100 simulations, ranked by disease burden, is shown after 200 hours. The mechanism for resistance in these simulations did not break down antibiotic externally to the cell.

References

1. Barber, M. & Rozwadowska-dowzenko, M. Infection with penicillin-resistant staphylococci in hospital and general practice. *The Lancet* **2,** 641–644 (1948).
2. Kåhrström, C. T. Entering a post-antibiotic era? *Nature Reviews Microbiology* **11,** 146–146 (2013).
3. Ling, L. L. *et al.* A new antibiotic kills pathogens without detectable resistance. *Nature* **517,** 455—459 (2015).
4. Walker, D. & Fowler, T. Annual Report of the UK Chief Medical Officer (2011).
5. Welsh, F. *Antibiotics resistance 'as big a risk as terrorism' - medical chief* 2013. <http://www.bbc.co.uk/news/health-21737844>.
6. Levin, B. *et al.* The population genetics of antibiotic resistance. *Clinical infectious diseases* **24,** S9–S16 (1997).
7. Opatowski, L., Guillemot, D., Boelle, P. Y. & Temime, L. Contribution of mathematical modeling to the fight against bacterial antibiotic resistance. *Curr Opin Infect Dis* **24,** 279–287 (2011).
8. Vogwill, T. & MacLean, R. C. The genetic basis of the fitness costs of antimicrobial resistance: a meta-analysis approach. *Evolutionary Applications* **8,** 284–295 (2015).
9. MaLean, R. C., Fuentes-Hernandez, A., Greig, D., Hurst, L. D. & Gudelj, I. A mixture of "cheats" and "co-operators" can enable maximal group benefit. *PLoS biology* **8** (2010).
10. Costerton, J. W., Stewart, P. S. & Greenberg, E. P. Bacterial Bioflims : A Common Cause of Persistant Infections. *Science* **284,** 1318–1322 (1999).
11. Costerton, J. W., Lewandowski, Z., Caldwell, D. & Korber, D. Microbial Biofilms. *Annual review of microbiology* **49,** 711–745 (1995).
12. Høiby, N., Bjarnsholt, T., Givskov, M., Molin, S. & Ciofu, O. Antibiotic resistance of bacterial biofilms. *International journal of antimicrobial agents* **35,** 322–32 (2010).
13. Stewart, P. S. & Costerton, J. W. Antibiotic resistance of bacteria in biofilms. *Lancet* **358,** 135–8 (2001).
14. Stewart, P. S. Mechanisms of antibiotic resistance in bacterial biofilms. *International journal of medical microbiology : IJMM* **292,** 107–13 (2002).
15. West, S. a., Griffin, A. S., Gardner, A. & Diggle, S. P. Social evolution theory for microorganisms. *Nature reviews. Microbiology* **4,** 597–607 (2006).
16. Kreft, J.-U. Biofilms promote altruism. *Microbiology* **150,** 2751–60 (2004).

17. Nadell, C. D., Foster, K. R. & Xavier, J. B. Emergence of spatial structure in cell groups and the evolution of cooperation. *PLoS computational biology* **6,** e1000716 (2010).

18. West, S. a., Griffin, a. S. & Gardner, a. Social semantics: altruism, cooperation, mutualism, strong reciprocity and group selection. *Journal of evolutionary biology* **20,** 415–32 (2007).

19. Ghoul, M., Griffin, A. S. & West, S. a. Toward an Evolutionary Definition of Cheating. *Evolution; international journal of organic evolution,* 1–14 (2013).

20. Andersson, D. I. & Hughes, D. Antibiotic resistance and its cost: is it possible to reverse resistance? *Nature Reviews Microbiology* **8,** 260–71 (2010).

21. Crespi, B., Foster, K. & Ubeda, F. First principles of Hamiltonian medicine. *Philosophical Transactions of the Royal Society B: Biological Sciences* **369,** 20130366–20130366 (2014).

22. Foster, K. R. Biomedicine. Hamiltonian medicine: why the social lives of pathogens matter. *Science (New York, N.Y.)* **308,** 1269–1270 (2005).

23. Conlin, P. L., Chandler, J. R. & Kerr, B. Games of life and death: antibiotic resistance and production through the lens of evolutionary game theory. *Current opinion in microbiology* **21C,** 35–44 (2014).

24. Vega, N. M. & Gore, J. Collective antibiotic resistance: mechanisms and implications. *Current Opinion in Microbiology* **21,** 28–34 (2014).

25. Kelsic, E. D., Zhao, J., Vetsigian, K. & Kishony, R. Counteraction of antibiotic production and degradation stabilizes microbial communities. *Nature* (2015).

26. Currie, C. J. *et al.* Antibiotic treatment failure in four common infections in UK primary care 1991-2012: longitudinal analysis. *BMJ* **349,** g5493–g5493 (2014).

27. Goossens, H., Ferech, M., Vander Stichele, R. & Elseviers, M. Outpatient antibiotic use in Europe and association with resistance: a cross-national database study. *Lancet* **365,** 579–87 (2005).

28. Prescott, John Francis and Baggot, J. D. *Antimicrobial Therapy in Veterinary Medicine* 135 (1993).

29. Jacoby, G. a. & Munoz-price, L. S. The New β Lactamases. *The New England Journal of Medicine* **352,** 380–391 (2014).

30. Kohanski, M. a., Dwyer, D. J. & Collins, J. J. How antibiotics kill bacteria: from targets to networks. *Nature reviews. Microbiology* **8,** 423–35 (2010).

31. Brook, I. β-lactamase-producing bacteria in mixed infections. *Clinical Microbiology and Infection* **10,** 777–84 (2004).

32. Brook, I. The role of beta-lactamase-producing-bacteria in mixed infections. *BMC infectious diseases* **9,** 202 (2009).

33. Labia, R. & Peduzzi, J. Cinetique de l'inhibition de beta-lactamases par l'acide clavulanique. *BBA - Enzymology* **526,** 572–579 (1978).

34. Livermore, D. M. β-Lactamases in laboratory and clinical resistance. *Clinical microbiology reviews* **8,** 557–584 (1995).

35. Ciofu, O., Beveridge, T. J., Kadurugamuwa, J., Walther-rasmussen, J. & Høiby, N. Chromosomal beta-lactamase is packaged into membrane vesicles and secreted from Pseudomonas aeruginosa. *Journal of antimicrobial biology* **45,** 9–13 (2000).

36. Schaar, V., Nordström, T., Mörgelin, M. & Riesbeck, K. Moraxella catarrhalis outer membrane vesicles carry β-lactamase and promote survival of Streptococcus pneumoniae and Haemophilus influenzae by inactivating amoxicillin. *Antimicrobial agents and chemotherapy* **55,** 3845–53 (2011).

37. Schaar, V., Uddbäck, I., Nordström, T. & Riesbeck, K. Group A streptococci are protected from amoxicillin-mediated killing by vesicles containing β-lactamase derived from Haemophilus influenzae. *The Journal of antimicrobial chemotherapy* **69,** 117–20 (2014).

38. Tacking, R. Penicillinase-producing bacteria in mixed infections in rabbits treated with penicillin. *Acta Pathologica Microbiologica Scandinavica* **35,** 445–454 (1954).

39. Simon, H. J. & Sakai, W. Staphylococcal antagonism to penicillin-G therapy of hemolytic streptococcal pharyngeal infection. Effect of oxacillin. *Pediatrics* **31,** 463–9 (1963).

40. Brook, I. The role of beta-lactamase-producing bacteria in the persistence of streptococcal tonsillar infection. *Reviews of Infectious Diseases* **6,** 601–7 (1984).

41. Dugatkin, L. A., Perlin, M., Lucas, J. S. & Atlas, R. Group-beneficial traits, frequency-dependent selection and genotypic diversity: an antibiotic resistance paradigm. *Proceedings of the Royal Society B: Biological Sciences* **272,** 79–83 (2005).

42. Clark, D. *et al.* Evolution of altruists and cheaters in near-isogenic populations of Escherichia coli. *Frontiers in Bioscience* **14,** 4815–4824 (2009).

43. Dugatkin, L. A., Dugatkin, A. D., Atlas, R. M. & Perlin, M. H. Cheating on the edge. *PloS one* **3,** e2763 (2008).

44. Bottery, M. J., Wood, A. J. & Brockhurst, M. A. Selective conditions for a multidrug resistance plasmid depend on the sociality of antibiotic resistance. *Antimicrobial Agents and Chemotherapy* **60,** 2524–2527 (2016).

45. Yurtsev, E. A., Chao, H. X., Datta, M. S., Artemova, T. & Gore, J. Bacterial cheating drives the population dynamics of cooperative antibiotic resistance plasmids. *Molecular systems biology* **9,** 683 (2013).

46. Perlin, M. H. *et al.* Protection of Salmonella by ampicillin-resistant Escherichia coli in the presence of otherwise lethal drug concentrations. *Proceedings. Biological sciences / The Royal Society* **276,** 3759–68 (2009).

47. Perez, A. C. *et al.* Residence of Streptococcus pneumoniae and Moraxella catarrhalis within polymicrobial biofilm promotes antibiotic resistance and bacterial persistence in vivo. *Pathogens and disease* **70,** 280–8 (2014).

48. Connell, J. L., Ritschdorff, E. T., Whiteley, M. & Shear, J. B. 3D printing of microscopic bacterial communities. *Proceedings of the National Academy of Sciences* **110,** 18380–18385 | (2013).

49. Medaney, F., Dimitriu, T., Ellis, R. J. & Raymond, B. Live to cheat another day: bacterial dormancy facilitates the social exploitation of β-lactamases. *The ISME journal* **10,** 778 (2016).

50. Van Elsas, J. D. & Bailey, M. J. The ecolgy of transfer of mobile genetic elements. *FEMS Microb. Ecol.* **42,** 187–197 (2002).

51. Martínez, J. L., Baquero, F. & Andersson, D. I. Predicting antibiotic resistance. *Nature reviews. Microbiology* **5,** 958–65 (2007).

52. Andersson, D. I. & Hughes, D. Persistence of antibiotic resistance in bacterial populations. *FEMS Microbiology Reviews* **35,** 901–911 (2011).

53. Navon-Venezia, S., Ben-Ami, R. & Carmeli, Y. Update on Pseudomonas aeruginosa and Acinetobacter baumannii infections in the healthcare setting. *Current opinion in infectious diseases* **18,** 306–13 (2005).

54. Fitzgerald, M. & Ryan, D. Cystic fibrosis and anaesthesia. *Continuing Education in Anaesthesia, Critical Care & Pain* **11,** 204–209 (2011).

55. Lyczak, J. B., Cannon, C. L. & Pier, G. B. Lung Infections Associated with Cystic Fibrosis. *Clinical microbiology reviews* **15,** 194–222 (2002).

56. Lister, P. D., Wolter, D. J. & Hanson, N. D. Antibacterial-resistant Pseudomonas aeruginosa: clinical impact and complex regulation of chromosomally encoded resistance mechanisms. *Clinical microbiology reviews* **22,** 582–610 (2009).

57. Alekshun, M. N. & Levy, S. B. Molecular Mechanisms of Antibacterial Multidrug Resistance. *Cell* **128,** 1037–1050 (2007).

58. Howard, D. H., Scott, R. D., Packard, R. & Jones, D. The global impact of drug resistance. *Clinical infectious diseases : an official publication of the Infectious Diseases Society of America* **36,** S4–S10 (2003).

59. Baym, M., Stone, L. K. & Kishony, R. Multidrug evolutionary strategies to reverse antibiotic resistance. *Science* **351,** 3292–3292 (2016).

60. Hughes, D. & Andersson, D. I. Evolutionary consequences of drug resistance: shared principles across diverse targets and organisms. *Nature Reviews Genetics* **16,** 459–471 (2015).

61. Zur Wiesch, P. A., Kouyos, R., Engelstädter, J., Regoes, R. R. & Bonhoeffer, S. Population biological principles of drug-resistance evolution in infectious diseases. *The Lancet Infectious Diseases* **11,** 236–247 (2011).

62. Nadell, C. D., Xavier, J. B. & Foster, K. R. The sociobiology of biofilms. *FEMS Microbiology Reviews* **33,** 206–224 (2009).

63. Stacy, A., McNally, L., Darch, S. E., Brown, S. P. & Whiteley, M. The biogeography of polymicrobial infection. *Nature Reviews Microbiology* **14,** 93–105 (2016).

64. Hall-Stoodley, L., Costerton, J. W. & Stoodley, P. Bacterial biofilms: from the natural environment to infectious diseases. *Nature reviews. Microbiology* **2,** 95–108 (2004).

65. Vlamakis, H. & Kolter, R. Biofilms. *Cold Spring Harbor Perspectives in Biology* **2,** a000398 (2010).

66. Ceri, H. *et al.* The Calgary Biofilm Device : New Technology for Rapid Determination of Antibiotic Susceptibilities of Bacterial Biofilms. *Journal of Clinical Microbiology* **37,** 1771–1776 (1999).

67. Parsek, M. R. & Singh, P. K. Bacterial biofilms: an emerging link to disease pathogenesis. *Annual review of microbiology* **57,** 677–701 (2003).

68. Koch, G. *et al.* Evolution of resistance to a last-resort antibiotic in staphylococcus aureus via bacterial competition. *Cell* **158,** 1060–1071 (2014).

69. Kim, W., Racimo, F., Schluter, J., Levy, S. B. & Foster, K. R. Importance of positioning for microbial evolution. *PNAS* **111,** E1639–E1647 (2014).

70. Schluter, J., Nadell, C. D., Bassler, B. L. & Foster, K. R. Adhesion as a weapon in microbial competition. *The ISME journal* **9,** 139–49 (2015).

71. Griffin, A. S., West, S. A. & Buckling, A. Cooperation and competition in pathogenic bacteria. **430,** 2–5 (2004).

72. Sorg, R. A. *et al.* Collective Resistance in Microbial Communities by Intracellular Antibiotic Deactivation. *PLoS Biol* **14,** 1–19 (2016).

73. Iredell, J., Brown, J. & Tagg, K. Antibiotic resistance in Enterobacteriaceae: mechanisms and clinical implications. *BMJ* **352,** 6420 (2016).

74. Haines, A. S., Jones, K., Cheung, M. & Thomas, C. M. The IncP-6 plasmid Rms149 consists of a small mobilizable backbone with multiple large insertions. *Journal of Bacteriology* **187,** 4728–4738 (2005).

75. Mitri, S., Clarke, E. & Foster, K. R. Resource limitation drives spatial organization in microbial groups. *The ISME Journal* **10,** 1471–1482 (2015).

76. Mitri, S., Xavier, J. B. & Foster, K. R. Social evolution in multispecies biofilms. *Proceedings of the National Academy of Sciences* **108,** 10839–46 (2011).

77. Van Dyken, J. D., Müller, M. J. I., Mack, K. M. L. & Desai, M. M. Spatial population expansion promotes the evolution of cooperation in an experimental Prisoner's Dilemma. *Current biology : CB* **23,** 919–23 (2013).

78. Nadell, C., Drescher, K. & Foster, K. R. Spatial structure, cooperation, and competition in biofilms. *Nature Reviews Microbiology,* Accepted (2016).

79. Andersson, D. I. & Hughes, D. Microbiological effects of sublethal levels of antibiotics. *Nature Reviews Microbiology* **12,** 465–478 (2014).

80. Miller, C. *et al.* SOS Response Induction by β-Lactams and Bacterial Defense Against Antibiotic Lethality. **305,** 1629–1631 (2004).

81. Blázquez, J. *et al.* PBP3 inhibition elicits adaptive responses in Pseudomonas aeruginosa. *Molecular Microbiology* **62,** 84–99 (2006).

82. Oliveira, N. M., Niehus, R. & Foster, K. R. Evolutionary limits to cooperation in microbial communities. *Proceedings of the National Academy of Sciences* **111,** 17941–17946 (2014).

83. Xavier, J. B. & Foster, K. R. Cooperation and conflict in microbial biofilms. *Proceedings of the National Academy of Sciences* **104,** 876–881 (2007).

84. Van Gestel, J., Weissing, F. J., Kuipers, O. P. & Kovács, A. T. Density of founder cells affects spatial pattern formation and cooperation in Bacillus subtilis biofilms. *The ISME journal* **10,** 2069–2079 (2014).

85. Mitri, S., Clarke, E. & Foster, K. R. Resource limitation drives spatial organization in microbial groups. *The ISME Journal* **10,** 1471–1482 (2016).

86. Korolev, K. S., Xavier, J. B., Nelson, D. R. & Foster, K. R. A quantitative test of population genetics using spatiogenetic patterns in bacterial colonies. *The American naturalist* **178,** 538–52 (2011).

87. Van Ditmarsch, D. *et al.* Convergent evolution of hyperswarming leads to impaired biofilm formation in pathogenic bacteria. *Cell Reports* **4,** 697–708 (2013).

88. Smith, W. P. J. *et al.* Cell morphology drives spatial patterning in microbial communities. *PNAS* (2016).

89. Mitri, S. & Foster, K. R. The genotypic view of social interactions in microbial communities. *Annual review of genetics* **47,** 247–73 (2013).

90. Hallatschek, O. & Nelson, D. R. Life at the front of an expanding population. *Evolution; international journal of organic evolution* **64,** 193–206 (2010).

91. Read, A. F., Day, T. & Huijben, S. The evolution of drug resistance and the curious orthodoxy of aggressive chemotherapy. *Proceedings of the National Academy of Sciences* **108,** 10871–10877 (2011).

92. Kouyos, R. D. *et al.* The path of least resistance: aggressive or moderate treatment? *Proceedings. Biological sciences / The Royal Society* **281,** 20140566 (2014).

93. Drusano, G. L. Antimicrobial pharmacodynamics: critical interactions of 'bug and drug'. *Nature reviews. Microbiology* **2,** 289–300 (2004).

94. Walsh, F. *Antibiotic resistance: Cameron warns of medical 'dark ages'* 2014. <http://www.bbc.co.uk/news/health-28098838>.

95. On Antimicrobial Resistance, R. *Tackling drug-resistant infections globally: final report and recommendations* (Review on Antimicrobial Resistance, 2016).

96. World Health Organization. Global action plan on antimicrobial resistance. *WHO Press,* 1–28 (2015).

97. Wright, G. D. Antibiotic Adjuvants: Rescuing Antibiotics from Resistance. *Trends in Microbiology* **24,** 862–871 (2016).

98. Wright, G. D. Resisting resistance: New chemical strategies for battling superbugs. *Chemistry and Biology* **7,** 127–132 (2000).

99. Drawz, S. M. & Bonomo, R. A. Three decades of beta-lactamase inhibitors. *Clinical Microbiology Reviews* **23,** 160–201 (2010).

100. Wiegand, I., Hilpert, K. & Hancock, R. E. W. Agar and broth dilution methods to determine the minimal inhibitory concentration (MIC) of antimicrobial substances. *Nature protocols* **3,** 163–75 (2008).

101. Lenski, R. E., Rose, M. R., Simpson, S. C. & Tadler, S. C. Long-Term Experimental Evolution in Escherichia coli. I. Adaptation and Divergence During 2,000 Generations. *The American naturalist* **138,** 1315–1341 (1991).

102. RStudio. *RStudio* Boston, MA, 2012. <`http://www.rstudio.org/`>.

103. Nikaido, H. & Normark, S. Sensitivity of Escherichia coli to various beta-lactams is determined by the interplay of outer membrane permeability and degradation by periplasmic beta-lactamases: a quantitative predictive treatment. *Molecular Microbiology* **1,** 29–36 (1987).

104. White, A. *et al.* Augmentin(R) (amoxicillin/clavulanate) in the treatment of community-acquired respiratory tract infection: a review of the continuing development of an innovative antimicrobial agent. *Journal of Antimicrobial Chemotherapy* **53,** 3–20 (2004).

105. Farmer, T. H., Degnan, B. A. & Payne, D. J. Penetration of beta-lactamase inhibitors into the periplasm of gram-negative bacteria. *FEMS microbiology letters* **176,** 11–5 (1999).

106. Peace, N., Olubukola, O. & Moshood, A. Stability of Reconstituted Amoxicillin Clavulanate Potassium under Simulated In-home Storage Conditions. *Journal of Applied Pharmaceutical Science* **02,** 28–31 (2012).

107. Jungbluth, G. L., Cooper, D. L., Doyle, G. D., Chudzik, G. M. & Jusko, W. J. Pharmacokinetics of ticarcillin and clavulanic acid (timentin) in relation to renal function. *Antimicrobial Agents and Chemotherapy* **30,** 896–900 (1986).

108. Gullberg, E., Albrecht, L. M., Karlsson, C., Sandegren, L. & Andersson, D. I. Selection of a Multidrug Resistance Plasmid by Sublethal Levels of Antibiotics and Heavy Metals. *mBio* **5,** 19–23 (2014).

109. Bengtsson-Palme, J. & Larsson, D. G. J. Concentrations of antibiotics predicted to select for resistant bacteria: Proposed limits for environmental regulation. *Environment International* **86,** 140–149 (2016).

110. Day, T. & Read, A. F. Does High-Dose Antimicrobial Chemotherapy Prevent the Evolution of Resistance? *PLoS Computational Biology* **12,** 1–20 (2016).

111. Martínez, J. L., Coque, T. M. & Baquero, F. What is a resistance gene ? Ranking risk in resistomes. *Nature Publishing Group* **13,** 116–123 (2014).

112. Lomovskaya, O. & Bostian, K. A. Practical applications and feasibility of efflux pump inhibitors in the clinic - A vision for applied use. *Biochemical Pharmacology* **71,** 910–918 (2006).

113. Meredith, H. R., Srimani, J. K., Lee, A. J., Lopatkin, A. J. & You, L. Collective antibiotic tolerance: mechanisms, dynamics and intervention. *Nature Chemical Biology* **11,** 182–188 (2015).

114. Berry, A. M., Lock, R. A., Hansman, D. & Paton, J. C. Contribution of autolysin to virulence of Streptococcus pneumoniae. *Infection and Immunity* **57,** 2324–2330 (1989).

115. Donlan, R. & Costerton, J. Biofilms: survivalmechanisms of clinically relevant microorganisms. *Clin.Microbiol. Rev.* **15,** 167–19 (2002).

116. Diggle, S. P., Griffin, A. S., Campbell, G. S. & West, S. a. Cooperation and conflict in quorum-sensing bacterial populations. *Nature* **450,** 411–4 (2007).

117. Lee, H. H., Molla, M. N., Cantor, C. R. & Collins, J. J. Bacterial charity work leads to population-wide resistance. *Nature* **467,** 82–5 (2010).

118. Regoes, R. R. *et al.* Pharmacodynamic Functions : a Multiparameter Approach to the Design of Antibiotic Treatment Regimens Pharmacodynamic Functions : a Multiparameter Approach to the Design of Antibiotic Treatment Regimens. *Antimicrobial agents and chemotherapy* **48,** 3670–3676 (2004).

119. Levin, B. R. & Udekwu, K. I. Population dynamics of antibiotic treatment: a mathematical model and hypotheses for time-kill and continuous-culture experiments. *Antimicrobial Agents and Chemotherapy* **54,** 3414–3426 (2010).

120. Niehus, R., Picot, A., Oliveira, N. M., Mitri, S. & Foster, K. R. The evolution of siderophore production as a competitive trait. *Evolution* **71,** 1443–1455 (2017).

121. Ferguson, M. I., Scott, E. M. & Collier, P. S. Development of resistance to ciprofloxacin in nutrient-rich and nutrient-limited growth conditions in vitro by Pseudomonas aeruginosa isolates from patients with cystic fibrosis. *Antimicrobial Agents & Chemotherapy* **35,** 2649–2651 (1991).

122. Bergstrom, C. T., Lipsitch, M. & Levin, B. R. Natural Selection, Infectious Transfer and the Existence Conditions for Bacterial Plasmids. *Genetics* **155,** 1505–1519 (2000).

123. Billy, T. C. L., Malkus, P. & Paulsson, J. New quantitative methods for measuring plasmid loss rates reveal unexpected stability. *Plasmid* **70,** 353–361 (2013).

124. Mathworks. MATLAB.

125. Pineda-Krch, M. GillespieSSA: a stochastic simulation package for R. <`http://pineda-krch.com/gillespiessa`> (2010).

126. Pineda-Krch, M., J. Blok, H., Dieckmann, U. & Doebeli, M. A tale of two cycles - Distinguishing quasi-cycles and limit cycles in finite predator-prey populations. *Oikos* **116,** 53–64 (2007).

127. Manduru, M. *et al.* In vitro pharmacodynamics of ceftazidime against Pseudomonas aeruginosa isolates from cystic fibrosis patients . In Vitro Pharmacodynamics of Ceftazidime against Pseudomonas aeruginosa Isolates from Cystic Fibrosis Patients. **41,** 2053–2056 (1997).

128. Scottish Dental & Clinical Effectiveness Programme. *Drug Prescribing For Dentistry Dental Clinical Guidance* **January,** 96 (2016).

129. Ehrlich, P. Address in Pathology, ON CHEMIOTHERAPY: Delivered before the Seventeenth International Congress of Medicine. *British medical journal* **2,** 353–9 (1913).

130. Kurioka, T., Yunou, Y., Harada, H. & Kita, E. Efficacy of Antibiotic Therapy for Infection with Shiga-Like Toxin-Producing Escherichia coli O157 : H7 in Mice with Protein-Calorie Malnutrition. *Eur J Clin Microbiol Infect Dis,* 561–571 (1999).

131. Llewelyn, M. *et al.* The antibiotic course has had its day. **3418,** 1–5 (2017).

132. Justice, S. S., Hunstad, D. a., Cegelski, L. & Hultgren, S. J. Morphological plasticity as a bacterial survival strategy. *Nature reviews. Microbiology* **6,** 162–168 (2008).

133. Wright, G. D. & Poinar, H. Antibiotic resistance is ancient: implications for drug discovery. *Trends in microbiology* **20,** 157–9 (2012).

134. Forsberg, K. J. *et al.* Bacterial phylogeny structures soil resistomes across habitats. *Nature* **509,** 612–616 (2014).

135. Gatenby, R. a. A change of strategy in the war on cancer. *Nature* **459,** 508–509 (2009).

136. Allen, R. C., Popat, R., Diggle, S. P. & Brown, S. P. Targeting virulence: can we make evolution-proof drugs? *Nature Reviews Microbiology* **12,** 300–308 (2014).

137. Woods, R. J. & Read, A. F. Clinical management of resistance evolution in a bacterial infection: A case study. *Evolution, medicine, and public health* **2015,** 281–8 (2015).

138. Palmer, A. C. & Kishony, R. Understanding, predicting and manipulating the genotypic evolution of antibiotic resistance. *Nature reviews. Genetics* **14,** 243–8 (2013).

139. Brown, S. P., West, S. a., Diggle, S. P. & Griffin, A. S. Social evolution in micro-organisms and a Trojan horse approach to medical intervention strategies. *Philosophical transactions of the Royal Society of London. Series B, Biological sciences* **364,** 3157–68 (2009).

140. Suh, S.-J., Silo-Suh, L. a. & Ohman, D. E. Development of tools for the genetic manipulation of Pseudomonas aeruginosa. *Journal of microbiological methods* **58,** 203–12 (2004).

141. Choi, K.-H. & Schweizer, H. P. Mini-Tn7 insertion in bacteria with single attTn7 sites: example Pseudomonas aeruginosa. *Nature protocols* **1,** 153–61 (2006).

142. San Millan, A., Heilbron, K. & MacLean, R. C. Positive epistasis between co-infecting plasmids promotes plasmid survival in bacterial populations. *The ISME journal* **8,** 601–12 (2014).

143. Schindelin, J. *et al.* Fiji: an open-source platform for biological-image analysis. *Nature methods* **9,** 676–82 (2012).

144. Rudge, T. J., Steiner, P. J., Phillips, A. & Haseloff, J. Computational modeling of synthetic microbial biofilms. *ACS Synthetic Biology* **1,** 345–352 (2012).

145. Rudge, T. J., Federici, F., Steiner, P. J., Kan, A. & Haseloff, J. Cell polarity-driven instability generates self-organized, fractal patterning of cell layers. *ACS Synthetic Biology* **2,** 705–714 (2013).

146. Picioreanu, C., Van Loosdrecht, M. C. M. & Heijnen, J. J. Mathematical modeling of biofilm structure with a hybrid differential- discrete cellular automaton approach. *Biotechnology and Bioengineering* **58,** 101–116 (1998).

147. Tuttle, J. *et al.* Lessons from a large outbreak of Escherichia coli O157:H7 infections: insights into the infectious dose and method of widespread contamination of hamburger patties. *Epidemiology and infection* **122,** 185–192 (1999).

148. Wang, P. *et al.* Robust growth of escherichia coli. *Current Biology* **20,** 1099–1103 (2010).

149. Siqueira, J. F. & Rôças, I. N. Microbiology and treatment of acute apical abscesses. *Clinical Microbiology Reviews* **26,** 255–273 (2013).

150. De Araujo, B. V. *et al.* PK-PD modeling of β-lactam antibiotics: In vitro or in vivo models? *The Journal of antibiotics* **64,** 439–446 (2011).

151. Kuck, N. a., Jacobus, N. V., Petersen, P. J., Weiss, W. J. & Testa, R. T. Comparative in vitro and in vivo activities of piperacillin combined with the β-lactamase inhibitors tazobactam, clavulanic acid, and sulbactam. *Antimicrobial agents and chemotherapy* **33,** 1964–1969 (1989).

152. Niehus, R., Mitri, S., Fletcher, A. G. & Foster, K. R. Migration and horizontal gene transfer divide microbial genomes into multiple niches. *Nature communications* **6,** 8924 (2015).

153. Chaibi, E. B., Sirot, D., Paul, G. & Labia, R. Inhibitor-resistant TEM beta-lactamases: phenotypic, genetic and biochemical characteristics. *Journal of Antimicrobial Chemotherapy* **43,** 447–458 (1999).

154. Nicolas-Chanoine, M. H. Inhibitor resistant beta-lactamases. *Journal of Antimicrobial Chemotherapy* **40,** 1–3 (1997).